USING ATMOSPHERIC MODELS TO ESTIMATE GLOBAL AIR POLLUTION MORTALITY

Susan Casper Anenberg

A dissertation submitted to the faculty of the University of North Carolina at Chapel Hill in partial fulfillment of the requirements for the degree of Doctor of Philosophy in the Department of Environmental Sciences and Engineering.

Chapel Hill
2011

Approved by:

J. Jason West

David Leith

Will Vizuete

Karin Yeatts

Bryan Hubbell

ABSTRACT

SUSAN CASPER ANENBERG: Using Atmospheric Models to Estimate Global Air Pollution Mortality

(Under the direction of J. Jason West)

Ground-level ozone and fine particulate matter ($PM_{2.5}$) are associated with premature mortality and can influence air quality on global scales. This work examines the global health impacts of ozone and $PM_{2.5}$ using concentrations simulated by global chemical transport models (CTMs), which allow full spatial coverage and analysis of hypothetical changes in emissions. Here, previous methods using global models are improved by using cause-specific and country-specific baseline mortality rates, and by using area-weighted average rates where gridcells overlap multiple countries.

Using these methods, we estimate 0.7 ± 0.3 and 3.7 ± 1.0 million global premature deaths annually due to anthropogenic ozone and $PM_{2.5}$, found as the difference between simulations with and without anthropogenic emissions. $PM_{2.5}$ mortality estimates are ~50% higher than previous measurement-based estimates based on common assumptions, mainly because rural populations are included, suggesting higher estimates, although the coarsely resolved global atmospheric model may underestimate urban $PM_{2.5}$ exposures. Estimating the mortality impacts of intercontinental transport of ozone shows that for North America, East Asia, South Asia, and Europe, foreign ozone precursor emission reductions contribute ~30%, 30%, 20%, and >50% of the deaths avoided by

reducing emissions in all regions together. For North America and Europe, reducing precursor emissions avoids more deaths outside the source region than within, due mainly to larger foreign populations. Finally, using the MOZART-4 global CTM, we estimate that halving global anthropogenic black carbon (BC) emissions reduces population-weighted average $PM_{2.5}$ by 542 ng/m^3 (1.8%) and avoids 157,000 (95% confidence interval, 120,000-194,000) annual premature deaths globally, with the vast majority occurring within the source region. Over 80% of these deaths occur in Asia, with 50% greater mortality impacts per unit BC emitted for South Asian versus East Asian emissions. Globally, the contribution of residential, industrial, and transportation BC emissions to BC-related mortality is 1.3, 1.2, and 0.6 times each sector's contribution to anthropogenic BC emissions, owing to the degree of co-location with population.

Future research should improve upon the many sources of uncertainty, incorporate shifting demographics, and examine the health impacts of realistic emission control technologies, which would affect emissions of multiple species simultaneously.

ACKNOWLEDGEMENTS

I am very grateful to my advisor, Jason West, for continuous guidance, advice, and mentorship.

To the members of my committee, thank you for your support along the way and for providing helpful insights and suggestions that enhanced this body of work.

I thank the many individuals at the US Environmental Protection Agency and the National Academy of Sciences for support through several fellowships and for invaluable lessons in the confluence of science and policy.

To my family, friends, and especially my husband who navigated this process with me, thank you for your unyielding support and encouragement. I am grateful to each and every one of you.

TABLE OF CONTENTS

LIST OF TABLES

LIST OF FIGURES

ABBREVIATIONS

ACS	American Cancer Society
AF	Attributable fraction
AF/ME	Africa/Middle East
BC	Black carbon
CASTNET	Clean Air Status and Trends Network
CH_4	Methane
CI	Confidence interval
CO	Carbon monoxide
CRF	Concentration response factor
CTM	Chemical transport model
EA	East Asia (China)
EANET	Acid Deposition Monitoring Network in East Asia
EC	Elemental carbon
EMEP	European Monitoring and Evaluation Programme
EPA	Environmental Protection Agency
EU	Europe
GFED-2	Global Fire Emissions Database version 2
HCT	High concentration threshold
HIA	Health impact assessment
HIS	Health import sensitivity
HIF	Health impact function
IMPROVE	Interagency Monitoring of Protected Visual Environments

IN	South Asia (India)
IPCC	Intergovernmental Panel on Climate Change
LCT	Low concentration threshold
MOZART-2	Model of Ozone and Related Tracers, version 2
MOZART-4	Model of Ozone and Related Tracers, version 4
NA	North America
NAAQS	National Ambient Air Quality Standards
NH	Northern Hemisphere
NMVOC	Non-methane volatile organic compound
NO_3	Nitrate aerosol
NOAA	National Oceanic and Atmospheric Administration
NO_x	Nitrogen oxides
O_3	Ozone
OC	Organic carbon
OH	Hydroxyl radical
OM	Organic matter
PI	Posterior interval
PM	Particulate matter
$PM_{2.5}$	Fine particulate matter
PM_{10}	Coarse particulate matter
POET	Precursors of Ozone and their Effects in the Troposphere
ppb	Part per billion
ppm	Part per million

REAS	Regional Emissions Inventory in Asia
RR	Relative risk
SA	South America
SA	South Asia
SD	Standard deviation
SE/AU	Southeast Asia/Australia
SOA	Secondary organic aerosol
SO_4	Sulfate aerosol
TF HTAP	Task Force on Hemispheric Transport of Air Pollution
US	United States
VOC	Volatile organic compound
WHO	World Health Organization
YLL	Years of life lost

Chapter 1. Introduction

Tropospheric (ground-level) ozone (O_3) and fine particulate matter ($PM_{2.5}$) are associated with deleterious health impacts, including premature mortality (e.g. Jerrett et al. 2009; Krewski et al. 2009). Concentrations of these pollutants have increased substantially since preindustrial times as a result of human activity (Volz and Kley 1988; Staehelin et al. 2001; Ginoux et al. 2006; Horowitz 2006; Schultz et al. 2006). In some countries, regulation has successfully improved air quality over recent decades (e.g. US EPA 2008b). However, air pollution continues to be a serious detriment to public health, particularly in rapidly developing countries where emissions continue to rise (Cohen et al. 2004; Lamarque et al. 2010; TF HTAP 2010).

Recent studies show that air pollution emissions from one region can influence air quality in other regions, with far-reaching impacts on health and the environment (e.g. National Academy of Sciences 2009; TF HTAP 2010). Air pollution is thus increasingly viewed as a global problem requiring international solutions (Holloway et al. 2003; Keating et al. 2004; Global Atmospheric Pollution Forum 2010; TF HTAP 2010). Furthermore, air pollution and climate are interrelated, and consideration of both health and climate impacts of air pollution can lead to identification of policies that benefit both simultaneously (e.g. Jacobson 2002; Bond and Sun 2005; Ramanathan and Carmichael 2008; Kopp and Mauzerall 2010).

Multi-national cooperation in air pollution mitigation will require tools to assess the health benefits of alternative mitigation strategies. This dissertation is aimed at assessing the impacts of global air pollution and its mitigation on global public health, and in doing so, identifying limitations and uncertainties that should be addressed to improve the utility of global health impact assessment in informing policy decisions.

1.1. Air pollution and its health impacts

Air pollution is a heterogeneous mixture of gaseous and particulate components. O_3 and $PM_{2.5}$ are two of the most ubiquitous air pollutants that have both been demonstrated to cause negative health impacts, including premature mortality. O_3 is not emitted directly, but is formed through photochemical reaction of precursor species, nitrogen oxides (NO_x) and volatile organic compounds (VOCs). O_3 precursors are produced both naturally by vegetation and soil, and anthropogenically through fuel combustion and industrial processes. Particulate matter (PM) is both emitted directly and formed indirectly through reaction in the atmosphere. Coarse PM (PM_{10}), between 2.5 and 10 μm in diameter, is largely transferred to the atmosphere by natural physical processes, such as wind-produced dust and sea salt. Conversely, fine PM ($PM_{2.5}$), ≤2.5 μm in diameter, is emitted by anthropogenic sources or produced by reaction of gaseous emissions, such as nitrogen and sulfur oxides, in the atmosphere. $PM_{2.5}$ composition is nonuniform, depending on source and chemical processing in the atmosphere, such as absorption of gases onto the surface of particles, adhesion, coagulation, and hydroscopic growth. Thus, the general term $PM_{2.5}$ does not capture significant differences in aerosol composition around the world. $PM_{2.5}$ is associated with more deleterious health effects

than coarse PM, because these tiny particles can penetrate deep into the lungs and may consist of more toxic materials (Pope and Dockery 2006).

Ground-level concentrations of O_3 and $PM_{2.5}$ have increased substantially since preindustrial times (Volz and Kley 1988; Staehelin et al. 2001; Ginoux et al. 2006; Horowitz 2006; Schulz et al. 2006). While O_3 mitigation has traditionally focused on urban areas in developed regions, observation and modeling studies show that O_3 produced in polluted regions can be transported long distances and that transport of precursors can enhance O_3 production in remote regions, impacting air quality on a global scale (TF HTAP 2007; Fiore et al. 2009; National Academy of Sciences 2009; West et al. 2009a; TF HTAP 2010). As a result, the global background concentration of O_3 has roughly doubled that in preindustrial times (Volz and Kley 1988; Akimoto 2003; Vingarzan 2004; TF HTAP 2010). Though the lifetime of $PM_{2.5}$ (days to weeks) is shorter than that of O_3 (weeks to months), it is also long enough that it can distribute to form elevated regional background concentrations (Akimoto 2003; Liu et al. 2009b; TF HTAP 2010).

1.1.1. Air pollution epidemiology

Evidence for health effects of air pollution come from both controlled exposure studies and epidemiology studies. Epidemiology studies find statistical relationships between observed ambient air pollutant concentrations and health effects over large populations. Unlike cellular, animal, and even human controlled exposure studies, epidemiology studies assess real-world human responses to air pollution and therefore

generally provide a more realistic assessment of the health effects of actual air pollution exposures.

The first air pollution epidemiology studies examined very severe air pollution episodes, such as the London Smog episode in 1952, where an air inversion kept pollution from coal combustion close to the ground. Researchers later compared daily mortality with pollution concentrations, finding about 12,000 deaths attributable to the incident (Figure 1.1) (Bell et al. 2001). Modern air pollution epidemiology studies leverage extensive monitoring networks in the US and Europe and detailed health information to find statistical relationships across many cities and over long time periods. These studies measure relative risk (RR), the ratio of the probability of an event occurring in an exposed group versus in an unexposed group. When RR=1, the risk factor has no effect. When RR>1 the risk factor causes a risk increase in the exposed group compared with the unexposed group. Conversely, if the RR<1, the risk factor actually has a protective effect. For example, estimated RR of mortality associated with ambient $PM_{2.5}$ concentration is greater than 1, particularly for lung cancer and cardiopulmonary mortality (Figure 1.2) (Pope et al. 2002; Pope and Dockery 2006).

As described in the next sections, the evidence for health effects of air pollution is now well established and widely accepted. Short-term studies from around the world and several large-scale long-term studies in the US and Europe find that $PM_{2.5}$ is associated with increased mortality. A large body of literature also finds that short-term O_3 exposure is associated with increased daily mortality, and recent evidence from one long-term study in the US also links O_3 with respiratory mortality. The major air pollution epidemiology studies generally find that the natural log of RR varies linearly with

concentration, with the slope of the association termed the "concentration-response factor" (CRF). Current epidemiological evidence finds that $PM_{2.5}$ generally has a stronger relationship with mortality than does O_3.

1.1.2. Ambient $PM_{2.5}$ concentrations and mortality

The health effects of chronic exposure to ambient $PM_{2.5}$ concentrations are well established by long-term epidemiology studies that examine associations between elevated $PM_{2.5}$ concentrations and deleterious health outcomes, such as premature mortality. The first major $PM_{2.5}$ cohort study was the "Harvard Six Cities study," which examined $PM_{2.5}$ concentrations and mortality in six US cities, finding a significant association between elevated $PM_{2.5}$ concentrations and mortality (Dockery et al. 1993). The Harvard Six Cities study was later reanalyzed with additional years of follow-up, during which $PM_{2.5}$ levels decreased in the six cities (Laden et al. 2006). This study found that when $PM_{2.5}$ concentrations decreased, mortality also decreased, reaffirming the strong association between $PM_{2.5}$ and mortality, and demonstrating that the association is reversible when $PM_{2.5}$ is controlled. In this latest reanalysis, relative risk of all-cause, cardiovascular, and lung cancer mortality was 1.16 (95% confidence interval [CI], 1.07-1.26), 1.28 (1.13-1.44), and 1.27 (0.96-1.69) for a 10 $\mu g/m^3$ increase in $PM_{2.5}$ (Laden et al. 2006).

Positive associations have also been found by the American Cancer Society (ACS) study, which has a larger cohort from all major urban areas within the US. The ACS study has been extended and reanalyzed several times with consistent findings of a strong association between $PM_{2.5}$ concentrations and excess all-cause, cardiopulmonary,

and lung cancer mortality (e.g. Pope et al. 2002; Krewski et al. 2009). The most recent reanalysis found that for a 10 $\mu g/m^3$ increase in $PM_{2.5}$, relative risk of total, cardiopulmonary, and lung cancer mortality was 1.06 (95% CI, 1.04-1.08), 1.13 (1.10-1.16), and 1.14 (1.06-1.23) (Krewski et al. 2009). The ACS study includes approximately 500,000 adults age 30 and older from over 150 metropolitan areas, a larger cohort than any other $PM_{2.5}$ cohort study.

Both the Harvard Six Cities and ACS studies are consistent in the strong positive association found between $PM_{2.5}$ concentration and mortality, but relative risk estimates from the Harvard Six Cities study are substantially larger than estimates from the ACS study. In 2008, US EPA sponsored an expert elicitation of this relationship which produced a mean that was between the relative risk estimates from these two studies (Roman et al. 2008). No long-term $PM_{2.5}$ cohort study to date has been conducted outside of the US and Europe, and extrapolation of these relationships found in the US to the rest of the world is uncertain, but is supported by meta-analyses finding that short-term mortality studies around the world find generally consistent results (Health Effects Institute 2010; Atkinson et al. 2011). While both studies are used by US EPA to estimate the health benefits of regulations in the US, the ACS study is generally used more often in global health impact assessments, since it includes the largest population. However, the ACS cohort overrepresented well-educated individuals in the US who were found to have a lower relative risk of $PM_{2.5}$-related mortality (Pope and Dockery 2005). Thus, health impact assessments based on the ACS cohort may be underestimates.

1.1.3. Ambient ozone concentrations and mortality

Many short-term epidemiology studies have implicated acute O_3 exposure as a serious health detriment, finding that elevated O_3 concentrations are associated with daily mortality (e.g. Bell et al. 2005; Ito et al. 2005; Levy et al. 2005). These studies typically examine O_3 concentrations and mortality in one US city, which limits the ability to generalize findings to the entire population. A larger study that included 95 US urban communities confirmed the earlier associations, finding that a 10 ppb increase in daily average O_3 concentrations was associated with a 0.52% (95% posterior interval [PI], 0.27%-0.77%) increase in total mortality and a 0.64% (95% PI, 0.31%-0.98%) increase in cardiovascular and respiratory mortality (Bell et al. 2004). Short-term O_3 mortality studies around the world generally find consistent O_3 mortality relationships (Anderson et al. 2004; Atkinson et al. 2011)

Only recently, a large-scale long-term cohort study based on the American Cancer Society cohort found an association between chronic O_3 exposure and mortality (Jerrett et al. 2009). This study found that only respiratory mortality was significantly associated with O_3 exposure when $PM_{2.5}$ concentrations were included in the model. For a 10 ppb increase in the seasonal (6 month) average of 1-hour daily maximum O_3 concentrations, respiratory mortality increased by 4% (95% CI, 1.3%-6.7%). While this is the first large-scale cohort study to demonstrate effects of long-term O_3 exposure on mortality, evidence of O_3 effects on developmental respiratory effects such as lung function and asthma induction and exacerbation suggest biological plausibility (National Academy of Sciences 2008). In addition, previous smaller scale cohort studies have also found positive associations (National Academy of Sciences 2008). Continuing research on

chronic O_3 exposure and mortality is expected to further elucidate long-term risk of mortality from O_3 exposure. Prior to this work, studies assessing the global health impacts of O_3 have used short-term mortality relationships. This work is the first to begin using chronic O_3 mortality estimates from Jerrett et al. (2009) for health impact assessment.

1.2. Air pollution in a global context

Evidence for associations between these pollutants and human health endpoints found by short-term and long-term epidemiology studies have formed the basis for regulatory action in the US, Europe, and many other countries. In the US, both O_3 and PM are regulated by National Ambient Air Quality Standards (NAAQS), which are set by US EPA to protect human health without regard to cost. NAAQS were first established in 1970 and are continually strengthened over time to reflect new scientific understanding. In 2008, the daily 8-hr. maximum standard for O_3 was lowered from 0.08 parts per million (ppm) to 0.075 ppm, and it is currently being reconsidered at a range that is more protective of public health (0.06-0.07 ppm). While the original NAAQS for PM was based on PM_{10}, a separate standard for $PM_{2.5}$ was set in 1997 after linkages were found between $PM_{2.5}$ and health problems, such as increased hospital admissions, emergency room visits, and premature death for people with lung and heart disease. The annual average PM_{10} standard was eventually revoked in 2006 because evidence does not suggest a link between long-term exposure to PM_{10} and deleterious health effects, although the 24-hr. average standard of 150 $\mu g/m^3$ was retained. The current standard for annual average $PM_{2.5}$ is 15 $\mu g/m^3$.

NAAQS have been very effective at reducing $PM_{2.5}$ and O_3 concentrations in the US (Figure 1.3) (US EPA 2008b) with large benefits to public health that continue as downward emission trends persist (Hubbell et al. 2004; Fann and Risley 2011). However, evidence suggests that air pollution affects health at levels lower than current standards (e.g. Jerrett et al. 2009; Krewski et al. 2009; Kim et al. 2011). Furthermore, emissions are rising in many places around the world, most notably in China and India, due to rapid economic development and limited regulation (Lamarque et al. 2010; TF HTAP 2010). Since air pollution can travel long distances, impacting air quality and public health far from the emission source (Figure 1.4) (e.g. National Academy of Sciences 2009; TF HTAP 2010), strategies to control local pollution that have been widely successful in the past may not be as sufficient to protect public health in the future as emissions around the world continue to rise (Keating et al. 2004). In sum, the contribution of local emission sources to concentrations is decreasing in many developed countries as a result of tight regulation while the contribution from foreign emissions is rapidly growing (Figure 1.5). These factors combined suggest a need for international cooperation in controlling air pollution.

Air pollution and global climate change are also interrelated, suggesting that these problems should be considered together in designing mitigation strategies. First, warming temperatures and more frequent air inversions are expected to exacerbate air pollution episodes (e.g. Bloomer et al. 2009; Jacob et al. 2009). Additionally, some pollutants traditionally regulated for their impacts on health, such as O_3 and components of $PM_{2.5}$, also affect climate by directly absorbing or reflecting solar radiation, indirectly impacting cloud lifetime and reflectivity, and reducing snow and ice albedo (e.g. Horvath

1993, Hansen and Nazarenko 2004, Koch and Del Genio 2010). Finally, the sources of greenhouse gases are often the major sources of air pollutants; therefore, actions aimed at mitigating either climate change or air pollution will likely also impact the other (e.g. West et al. 2004; Reynolds and Kandlikar 2008; Bollen et al. 2010; Haines et al. 2010; Nemet et al. 2010). Pollution mitigation strategies may either have climate benefits or disbenefits, and simultaneous consideration of both issues can result in identification of win-win strategies that might not otherwise be recognized.

Outdoor air pollution is thus increasingly recognized as a global problem requiring international solutions (Holloway et al. 2003; Keating et al. 2004; Global Atmospheric Pollution Forum 2010; TF HTAP 2010). On the national scale, sophisticated benefit-cost assessments have been employed to justify air pollution regulations, finding for example that the economic benefits of the Clean Air Act vastly outweigh the costs, largely due to reductions in air pollution-related mortality (US EPA 2010). Similar benefit-cost assessments on the global scale may be increasingly useful to inform domestic and international decision-making in the future (e.g. West et al. 2006).

1.3. Health impact assessment

The relationships between pollutant levels and health outcomes identified by the epidemiology literature described above can be used to calculate the overall health impacts attributable to air pollution and changes in air pollutant concentrations. The basis of health impact assessment is the health impact function, which relates changes in pollutant concentrations to changes in the burden of disease attributable to that pollutant. Health impact functions take into account exposed population, baseline incidence rates,

pollutant concentrations, and concentration-response factors identified by the epidemiology literature (Figure 1.6). First, present or future population is estimated. Pollutant concentrations from air quality models or monitors are then used in conjunction with the population estimates to simulate population exposure. Finally, adverse health impacts are calculated using a health function, baseline incidence rates, and population exposure from the previous step. This method is consistent with the US Environmental Benefits Mapping and Analysis program (BenMAP), developed by the US EPA for regulatory impact analysis.

Health impact assessment is based on the relationships between exposure and health outcome (Relative Risk, RR) from the epidemiology literature. Epidemiological studies of O_3 and $PM_{2.5}$ exposure and mortality demonstrate a generally log-linear relationship between ambient concentrations and RR (Equation 1):

(1)

Here, β is the concentration-response factor (CRF), or the slope of the line between the natural logarithm of ΔX, the change in concentration, and RR. Since RR=1 for unexposed populations, the AF is calculated by Equation 2:

(2)

AF is then multiplied by the baseline mortality rate (y_0) and exposed population (Pop) to yield the change in the health outcome resulting from the change in concentration (Equation 3):

(3)

Health impact assessments conducted by the US EPA focus solely on benefits accrued within the US, and have the benefit of highly resolved demographic and air quality data, including both monitored and simulated concentrations. On a global scale, health impact assessment must draw upon data that are substantially cruder than are available for just the US and are necessarily more coarsely resolved. Some global health impact assessment studies have used monitored concentrations to estimate global health impacts of air pollution (e.g. Cohen et al. 2004). These studies are limited due to the sparseness of monitored concentrations around the world, particularly in developing countries, and the inability to examine effects of future changes in emissions and environmental conditions on concentrations. Using global chemical transport models (CTMs) to simulate exposure concentrations allows estimation of health impacts with full spatial coverage, not just where monitors are located. Another benefit of using CTMs for health impact assessment is the ability to control emissions and atmospheric conditions, which allows for analyzing the effects of expected or proposed changes in conditions on health.

1.4. Motivation and objectives

Numerous global modeling studies of the long-range transport of air pollution and interactions between air pollution and climate have increased awareness that air pollution emissions affect the environment and health on large spatial scales (e.g. TF HTAP 2010 and references therein). However, these studies have largely focused on impacts of emissions on air pollution concentrations and do not account for population exposure and health impacts, historically the drivers of public concern for air quality. Prior to this work, few studies had used global CTMs to estimate global mortality, focusing on future changes in O_3 (West et al. 2006; 2007), long-range transport of O_3 from Europe (Duncan et al. 2008), emissions from shipping (Corbett et al. 2007), and air pollution changes associated with carbon dioxide emissions (Jacobson 2008). In the past two years, in addition to the current work, global CTMs have been used to estimate mortality due to long-range transport of O_3 and $PM_{2.5}$ (Liu et al. 2009a; West et al. 2009b), future changes in O_3 (Selin et al. 2009), aircraft emissions (Barrett et al. 2010), and fossil fuel and biofuel emissions (Jacobson 2010). These studies generally support the notion that air pollution is not just a local problem, but affects health on regional or hemispheric scales. However, the body of literature examining the health impacts of air pollution on such large spatial scales is thin, and these studies all use different assumptions and methods, limiting comparability among studies.

This dissertation is aimed at advancing understanding of the global health impacts of air pollution by examining different types and sources of air pollutants and the effects of major methodological choices on results. Consistent with previous studies, the impacts of air pollution on global mortality are estimated using global CTMs to simulate

O_3 and $PM_{2.5}$ concentrations and epidemiologically-derived concentration-response relationships to calculate health impacts. However, here, the previous methodology is improved by refining the demographic information used as inputs into the health impact function. For example, country-specific baseline mortality rates are used in place of broad regional averages. In addition, area-weighted average baseline mortality rates are used where gridcells overlap multiple countries. Finally, this work focuses on cause-specific mortality which is likely to be more comparable globally than all-cause mortality, since major causes of death vary dramatically around the world.

These methodological improvements are employed in three case studies that address varied aspects of the global health impacts of air pollution, including the impacts of both O_3 and $PM_{2.5}$ and of both total anthropogenic emissions and incremental emission reductions. Chapter 2 addresses the global burden of anthropogenic O_3 and $PM_{2.5}$ on premature human mortality (Anenberg et al. 2010). Chapter 3 examines the impacts of intercontinental transport of O_3 on mortality (Anenberg et al. 2009). Chapter 4 considers the impacts of global, regional, and sectoral black carbon emissions on surface air quality and premature mortality (Anenberg et al. in prep). Finally, key findings and implications from these case studies and future research needs are discussed in Chapter 5.

1.5. Tables and figures

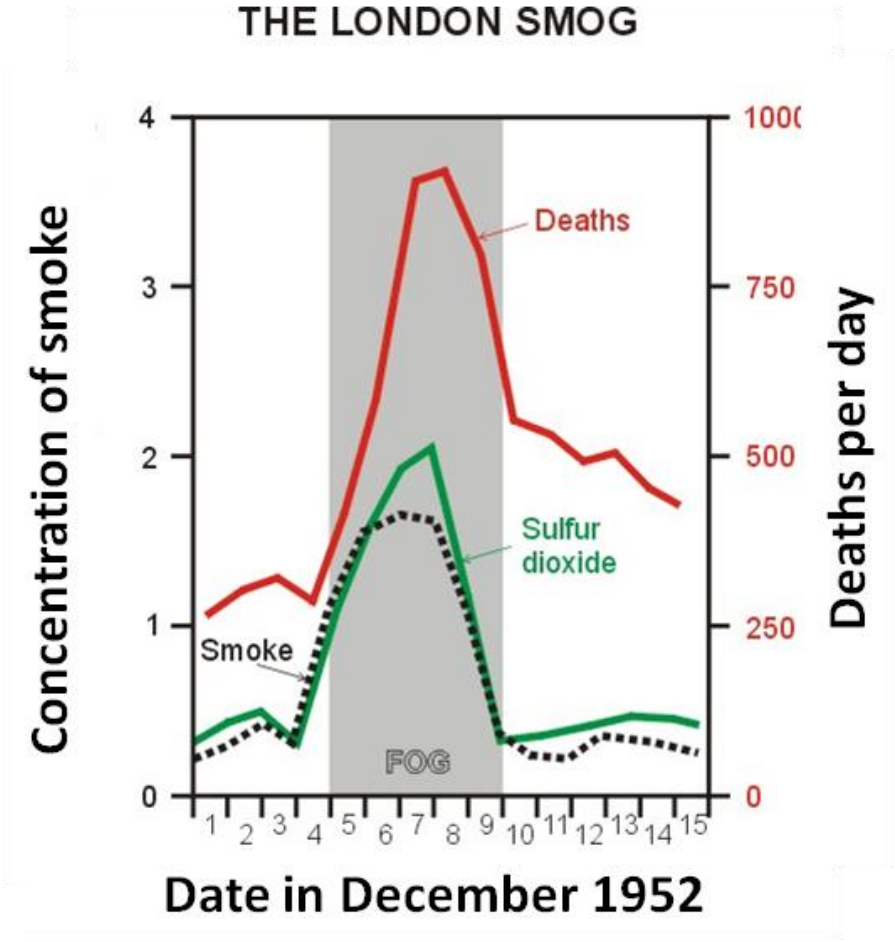

Figure 1.1. Concentration of smoke and sulfur dioxide and deaths per day for the London Smog air pollution episode of 1952. Image source:

http://www.ems.psu.edu/~lno/Meteo437.html

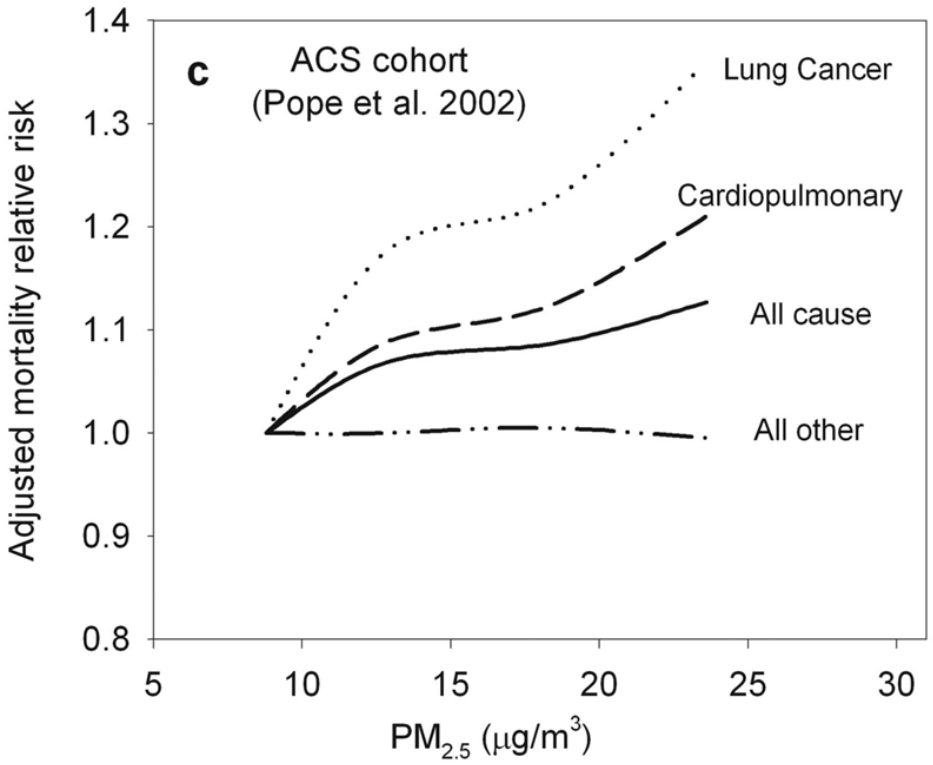

Figure 1.2. Concentration-response relationships estimated from the ACS cohort of long-term $PM_{2.5}$ exposure (Pope and Dockery 2006).

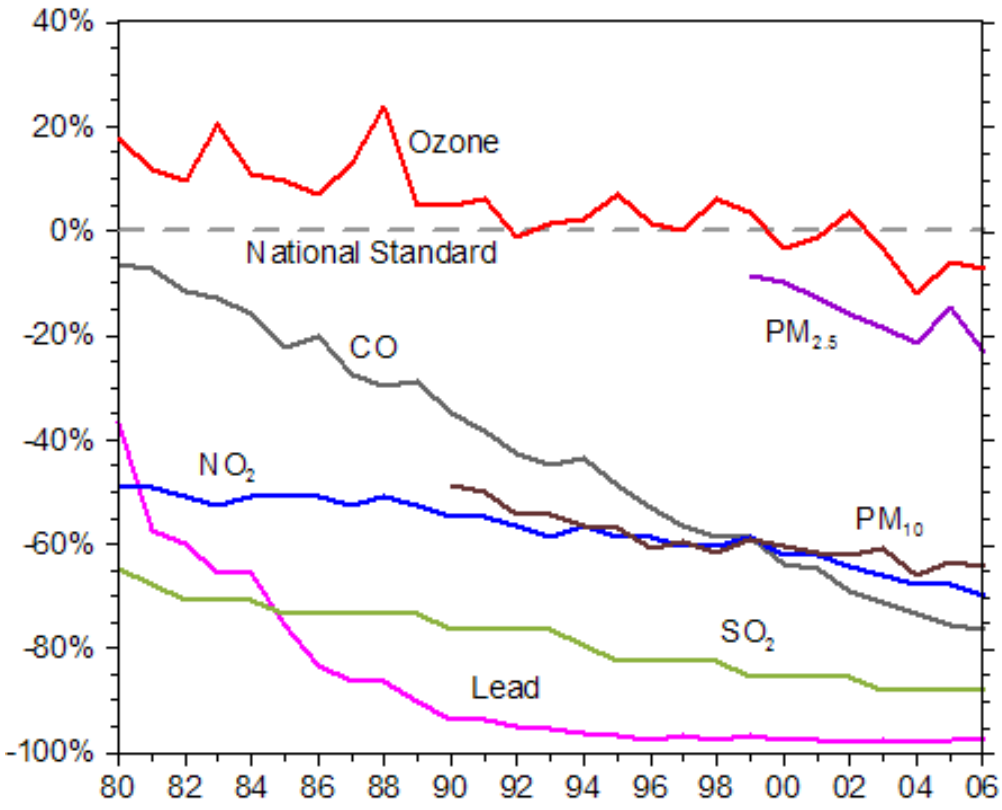

Figure 1.3. Comparison of national levels of the six principal pollutants to national ambient air quality standards, 1980-2006 (US EPA 2008b). National levels are averages across all sites with complete data for the time period.

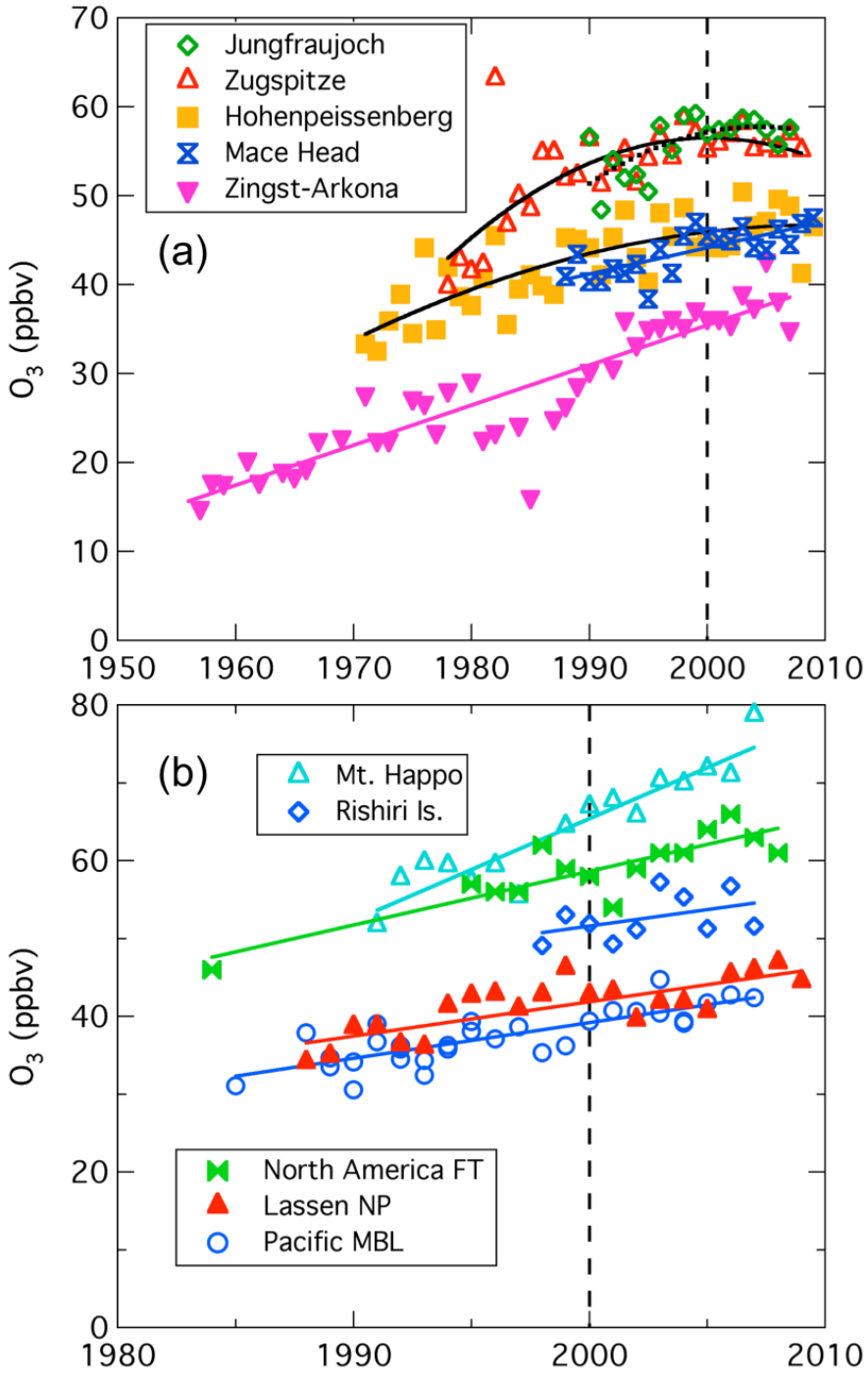

Figure 1.4. Springtime trends in O_3 concentrations measured in remote locations in (a) Europe and (b) western North America and Japan (TF HTAP 2010). Abbreviations: FT = free troposphere; NP = national park; MBL = marine boundary layer.

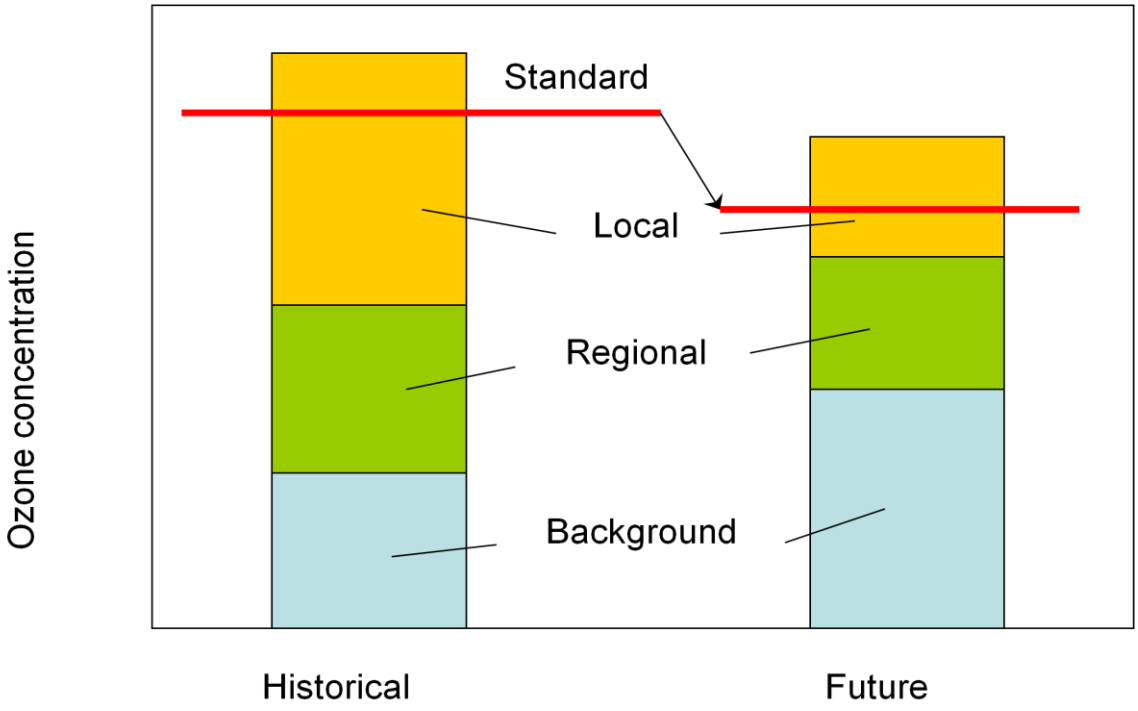

Figure 1.5. The "tightening vise" of air pollution management, shown here (schematically) for O_3 from the perspective of an industrialized nation. From the historical view to the future, air pollution managers succeed in reducing their local contribution to O_3, and work regionally with other jurisdictions to reduce the regional contribution. However, the hemispheric background increases, while their air quality standard becomes more stringent (Keating et al. 2004).

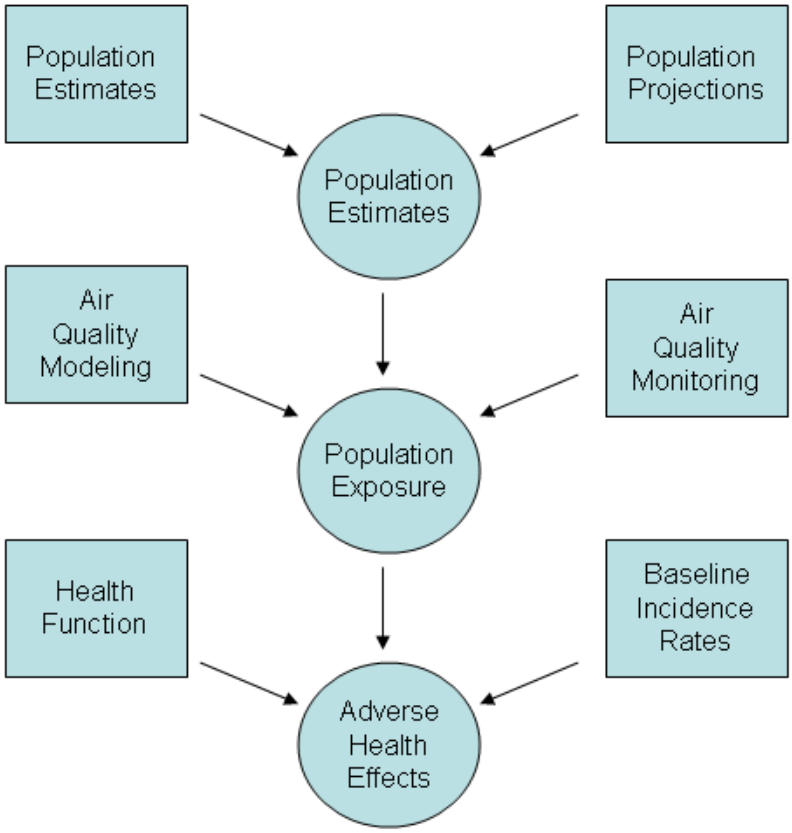

Figure 1.6. Flow diagram of health impact assessment methodology.

Chapter 2. An estimate of the global burden of anthropogenic ozone and fine particulate matter on premature human mortality using atmospheric modeling

(Anenberg, S. C., Horowitz, L. W., Tong, D. Q., West, J. J. (2010). Environmental Health Perspectives, 118, 1189-1195.)

2.1. Introduction

Ground-level ozone (O_3) and fine particulate matter ($PM_{2.5}$) have increased substantially since preindustrial times. While O_3 and $PM_{2.5}$ concentrations have increased most in industrialized areas, observations show that background concentrations have also increased in remote regions (Volz and Kley 1988; Staehelin et al. 2001; Akimoto 2003; Vingarzan 2004; Schulz et al. 2006). O_3 and $PM_{2.5}$ are associated with negative health impacts, including premature mortality (e.g. Jerrett et al. 2009; Krewski et al. 2009). Cohen et al. (2004) estimated that about 800,000 annual premature mortalities globally, or 1.2% of all deaths, are associated with urban outdoor $PM_{2.5}$. This was considered an underestimate because it excludes O_3 impacts and includes only urban areas for which econometric models trained with observations were used to predict concentrations.

We estimate the global burden of human mortality due to anthropogenic O_3 and $PM_{2.5}$ using a global atmospheric chemical transport model (CTM). Using an atmospheric CTM allows estimation of mortality where air quality measurements are sparse,

particularly in developing nations. By simulating preindustrial concentrations, we also isolate mortality due to anthropogenic pollution and avoid making assumptions for background O_3 and $PM_{2.5}$ concentrations. Global CTMs have been used to estimate mortalities due to long-range transport of air pollution (Anenberg et al. 2009; Liu et al. 2009a; West et al. 2009b), future changes in emissions (West et al. 2006; 2007), or changes in one sector's emissions (Corbett et al. 2007). CTMs have not been used previously to quantify the global burden of anthropogenic air pollution on human mortality.

2.2. Methods

We calculate mortalities associated with anthropogenic air pollution using health impact functions that relate changes in pollutant concentrations to changes in mortality. Here, we define anthropogenic air pollution as the geographically-distributed difference in O_3 and $PM_{2.5}$ concentrations between present-day (2000) and preindustrial, as simulated by a global chemical transport model (CTM). Health impact functions for both O_3 and $PM_{2.5}$ are based on a log-linear relationship between relative risk (*RR*) and concentrations defined by epidemiology studies (Jerrett et al. 2009; Krewski et al. 2009):

$$RR = exp^{\beta \Delta X} \qquad [1]$$

where β is the concentration-response factor (CRF) [i.e., the estimated slope of the log-linear relation between concentration and mortality], and ΔX is the change in

concentration. The fraction of the disease burden attributable to the risk factor, the attributable fraction (*AF*), is defined as:

$$AF = (RR\text{-}1)/RR = 1 - exp^{-\beta \Delta X} \quad [2]$$

AF is multiplied by the baseline mortality rate (y_0) and size of the exposed population (*Pop*) to yield an estimate of the excess mortalities attributable to air pollution (Δ *Mort*):

$$\Delta Mort = y_0 (1 - exp^{-\beta \Delta X}) Pop \quad [3]$$

Disease survival time varies among populations, and we calculate years of life lost (*YLL*) associated with mortalities using the baseline YLL (YLL_0) per death:

$$\Delta YLL = \Delta Mort * YLL_0/y_0 \quad [4]$$

Next, we describe the CRFs, simulated exposure concentrations, and demographic data used in the health impact functions for O_3 and $PM_{2.5}$.

For O_3, we base CRFs on the association between long-term O_3 exposure and RR of death from respiratory disease found by Jerrett et al. (2009), an American Cancer Society (ACS) cohort study of US adults ≥30 for 1977-2000. While many daily time-series epidemiology studies demonstrate short-term O_3-mortality impacts (e.g. Bell et al. 2004), Jerrett et al. (2009) provides the first clear evidence for long-term impacts. For the two pollutant model in which $PM_{2.5}$ was controlled, a 10 part per billion (ppb) increase in the seasonal (April-September) average daily 1-hr maximum O_3

(concentration range 33.3-104.0 ppb) was associated with a 4% (95% CI, 1.3%-6.7%) increase in RR of death from respiratory disease.

For $PM_{2.5}$, we use RRs from Krewski et al. (2009), which is the latest reanalysis of the ACS $PM_{2.5}$ studies (e.g. Pope et al. 2002) and has the largest population of the available $PM_{2.5}$ cohort studies (e.g. Hoek et al. 2002; Laden et al. 2006). We use RRs for 1999-2000 from the random effects Cox model analysis that adjusted for 44 individual-level and seven ecological covariates. A 10 $\mu g/m^3$ increase in $PM_{2.5}$ (concentration range 5.8-22.2 $\mu g/m^3$), was associated with 6% (95% CI, 4%-8%), 13% (10%-16%), and 14% (6%-23%) increases in total, cardiopulmonary, and lung cancer mortality. The linearity of the concentration-response function was also demonstrated up to 30 $\mu g/m^3$ in the 1979-1983 analysis. Krewski et al. (2009) found that $PM_{2.5}$ was associated most strongly with risk of death from ischemic heart disease, a subset of cardiopulmonary disease, and previous studies have found that controlling for O_3 concentrations had little effect on the $PM_{2.5}$-mortality relationships (Krewski et al. 2000). Compared with the relationships in an earlier expert elicitation (Roman et al. 2008), the total mortality RR in Krewski et al. (2009) is generally 3%-14% per 10 $\mu g/m^3$ lower with a tighter confidence interval.

We assume that these relationships found in the US are valid globally. For O_3, Jerrett et al. (2009) is the first study showing significant long-term impacts, but the short-term impact has been documented well in North America and Europe (Anderson et al. 2004; Bell et al. 2004). For $PM_{2.5}$, similar long-term mortality results have been demonstrated in Europe (Hoek et al. 2002), but to date no $PM_{2.5}$ cohort studies have been conducted in the developing world. Short-term O_3 and $PM_{2.5}$ studies in developing nations demonstrate relationships that are generally comparable with short-term studies in

North America and Europe (Health Effects Institute Scientific Oversight Committee 2004). Our assumption is further supported by evidence that concentration-mortality relationships do not vary significantly by sex, age, and race (Zanobetti et al. 2000; Jerrett et al. 2009; Krewski et al. 2009), though some sensitive populations may be at a higher risk. Because causes of death differ globally from those in North America and Europe, we emphasize cause-specific mortality, for which there may be less error than for estimates of all-cause mortality across different populations.

We use present day (2000) and preindustrial O_3 and $PM_{2.5}$ concentrations (Figure 2.1) simulated by Horowitz (2006) using the Model of Ozone and Related Chemical Tracers, version 2 (MOZART-2) (Horowitz et al. 2003). The preindustrial simulation, which corresponds to the 1860 simulation by Horowitz (2006), represents the "background" O_3 and $PM_{2.5}$ present in the absence of anthropogenic emissions, allowing us to isolate the anthropogenic contributions to concentrations and premature mortalities. MOZART-2 has a resolution of 2.8º latitude by 2.8º longitude with 34 vertical levels, and we use concentrations in the first vertical level as surface concentrations. Both simulations used the same meteorology from the National Center for Atmospheric Research Community Climate Model to isolate the impact of emission changes on concentration. We define $PM_{2.5}$ as all simulated sulfate (SO_4), nitrate (NO_3), ammonium, black carbon (BC), and primary organic carbon (OC). We exclude dust, sea salt, and secondary organic aerosols, which we assume are unchanged from preindustrial to present. We multiply OC mass by 1.4 to account for associated species other than carbon, and assume all SO_4 and NO_3 exists as $(NH_4)_2SO_4$ and NH_4NO_3, following Ginoux et al. (2006). For the preindustrial case, fossil fuel burning emissions were set to zero and

emissions from burning of biofuels, savannah, tropical forests, and agricultural waste were assumed to be 10% of 1990 values.

Consistent with the epidemiology studies, we use seasonal average 1-hr daily maximum concentrations for O_3 and annual average concentrations for $PM_{2.5}$. Because high O_3 occurs during different months globally, for each grid cell, we find the consecutive 6-month period with the highest average of the simulated daily 1-hr maximum O_3 concentrations, which we then use to calculate annual mortalities. Table 2.1 shows that the modeled global population-weighted seasonal average 1-hr. daily maximum O_3 increased by 37.1 ppb (from 19.6 ppb in 1860 to 56.7 ppb in 2000), using present population, and the global population-weighted annual average $PM_{2.5}$ increased by 15.0 $\mu g/m^3$ (from 1.1 $\mu g/m^3$ in 1860 to 16.1 $\mu g/m^3$ in 2000). Globally, OC, BC, NO_3, and SO_4 are 62.3%, 6.3%, 0.3%, and 31.0% of total $PM_{2.5}$ in 1860 and 45.6%, 9.1%, 4.9%, and 40.4% in 2000 (see Figure A.1).

We compare modeled present day surface O_3 concentrations with the Climate Monitoring and Diagnostics Laboratory (CMDL; http://www.esrl.noaa.gov/gmd/) monitoring network (mean bias=2.5ppb) for 11 remote locations around the world, and for three non-urban networks: the Clean Air Status and Trends Network (CASTNet; https://www.epa.gov/castnet/index.html) for the US (mean bias=2.9ppb), the European Monitoring and Evaluation Programme (EMEP; http://www.emep.int/) for Europe (mean bias=-0.2ppb), and the Acid Deposition Monitoring Network in East Asia (EANET; http://www.eanet.cc/) for Japan (mean bias=0.4ppb) (see Figure A.2-Figure A.5). Horowitz (2006) found that simulated preindustrial O_3 concentrations overestimate reconstructed observations from the late nineteenth century by ~5-10 ppb, with strong

sensitivity to assumed biomass burning. Modeled surface $PM_{2.5}$ concentrations were compared with observations by Ginoux et al. (2006) and were generally found to be estimated within a factor of 2 in remote locations and at non-urban stations in Europe and the US, with a tendency to be overestimated. These comparisons show that surface O_3 and $PM_{2.5}$ are simulated well by MOZART-2 for non-urban and remote measurements in the areas compared, and it is not apparent that corrections for bias are necessary. While simulated concentrations are not systematically biased outside of urban regions, the coarse resolution (grid cell area=$9.9x10^4$, $8.6x10^4$, and $5.2x10^4$ km^2 at 0°, 30°, and 60° latitude) used here may cause errors in mortality estimates, particularly in urban areas with strong population and concentration gradients.

Global premature mortalities are estimated separately for O_3 and $PM_{2.5}$ by applying Equation 3 in each of the MOZART-2 surface grid cells, using the corresponding population and baseline mortality rates for each cell. We use the global 2006 population (see Figure A.6) (Oak Ridge National Laboratory 2008), and, consistent with the ACS study population, the population fraction ≥30 (Table 2.1), estimated in 14 world regions (see Figure A.7) (World Health Organization 2004), to calculate mortality. We use baseline all-cause, cardiopulmonary, and lung cancer mortality rates for 14 world regions (World Health Organization 2004) and 66 countries (World Health Organization 2008b), back-calculating from regional rates where country-specific rates are unavailable (Table 2.1 and Figure A.8-Figure A.11). Country-specific mortality rates are broadly categorized with no cutoff at age 30, and we use rates for the population ≥25, assuming that differences between the rates are insignificant. We use baseline YLL rates for the population ≥30 in 14 world regions (global average=7.89, 9.77, and 8.93 for

cardiopulmonary disease, respiratory disease, and lung cancer; see Table A.1), assuming a 3% discount rate and non-uniform age-weighting, giving less weight to years lived at older ages (World Health Organization 2008b). Baseline mortality rates, baseline YLL, and the fraction of the population ≥30 are gridded to the MOZART-2 grid, and for grid cells overlapping multiple countries, we calculate area-weighted averages using a Geographic Information System (GIS) program.

We present mean results ± 1 standard deviation, calculating uncertainty from 500 Monte Carlo simulations that randomly sample from normal distributions of the CRF, as reported by the epidemiology studies, and modeled present-day concentrations (standard deviation=25% of simulated value). While the epidemiology literature provides little evidence for low-concentration (LCT) or high-concentration thresholds (HCT) for either O_3 or $PM_{2.5}$ (Schwartz and Zanobetti 2000; Jerrett et al. 2009; Krewski et al. 2009), mortality relationships beyond measured concentrations are unknown. Therefore, we estimate mortalities with and without assuming LCTs below which O_3 and $PM_{2.5}$ are assumed to have no effect on mortality. For O_3, we apply an LCT of 33.3 ppb, the lowest measured level in Jerrett et al. (2009). When applied, this threshold replaces the natural background everywhere except in some grid cells in Asia and South America, where preindustrial concentrations exceed the threshold (Table 2.1). We also examine an LCT of 56 ppb, which Jerrett et al. (2009) found to be close to statistical significance at an α-level of 5% (p=0.0600). The 56 ppb threshold exceeds preindustrial concentrations in all cells. Since no grid cells exceed the highest measured level (104.0 ppb) in Jerrett et al. (2009), we do not apply an HCT for O_3. For $PM_{2.5}$, we apply an LCT of 5.8 $\mu g/m^3$, the lowest measured level in Krewski et al. (2009), which exceeds preindustrial

concentrations in all grid cells (Table 2.1), effectively replacing the natural background. Some grid cells in Europe and Asia exceed the highest measured level (30.0 $\mu g/m^3$) in Krewski et al. (2009), and we examine HCTs of 30 $\mu g/m^3$ and 50 $\mu g/m^3$ in the sensitivity analysis. These thresholds apply only to our definition of $PM_{2.5}$ and would be affected by including dust, sea salt, and secondary organic aerosols.

2.3. Results

With no upper or lower concentration threshold, anthropogenic O_3 is estimated to result in about 0.7 ± 0.3 million respiratory mortalities annually worldwide (Table 2.2), corresponding to 6.3 ± 3.0 million YLL (Table 2.3). Estimated global respiratory mortalities are reduced by ~33% when we assume an LCT of 33.3 ppb, the lowest measured level in Jerrett et al. (2009). Regardless of threshold assumption, over 75% of O_3 mortalities are estimated to occur in Asia, which is densely populated and highly polluted, while only ~5% occur in North America. Estimated excess O_3 mortalities are most dense in highly populated areas, but are distributed more evenly across the globe when divided (normalized) by population size (Figure 2.2).

Assuming no upper or lower concentration threshold, we estimate that exposure to anthropogenic $PM_{2.5}$ results in 3.5 ± 0.9 million cardiopulmonary mortalities and 220,000 ± 80,000 lung cancer mortalities annually (Table 2.2), corresponding to 28 ± 6.8 and 2.2 ± 0.8 million YLL (Table 2.3). With an LCT of 5.8 μg/m3, estimated cardiopulmonary and lung cancer mortalities decrease by ~28%. Regardless of threshold, about 75% of excess mortalities would occur in Asia, due to high $PM_{2.5}$ concentrations and dense population, followed by Europe (17%). As for O_3, estimated $PM_{2.5}$ mortalities are most

dense in highly populated areas, but are more localized due to the shorter atmospheric lifetime of $PM_{2.5}$ vs. O_3 (Figure 2.1 and Figure 2.3). The highest estimated rates of mortalities per million people are in Europe, East Asia, and the Eastern US (Figure 2.3, right), owing to large baseline cardiopulmonary and lung cancer mortality rates and high $PM_{2.5}$ concentrations.

Applying an LCT of 25 ppb for O_3 results in ~14% fewer estimated respiratory mortalities compared with the estimate assuming no upper or lower threshold (Table 2.4). Using CRFs from the single-pollutant model in Jerrett et al. (2009), which did not control for $PM_{2.5}$, O_3 mortality estimates are ~25% lower, corresponding to the relative magnitudes of the CRFs. Applying the 56 ppb LCT from the threshold model reduces mortality estimates by ~75%. For $PM_{2.5}$, RRs from Krewski et al. (2009) are similar to the 1979-1983 and 1999-2000 average all-cause and lung cancer RRs from Pope et al. (2002), but are ~40% higher for cardiopulmonary mortality, thus causing a corresponding increase in our estimates when applied (Table 2.5 and Table A.2). Using RRs from Laden et al. (2006), an extended reanalysis of the Harvard Six Cities cohort study that found significantly higher RRs than did Krewski et al. (2009), increases estimated cardiopulmonary and lung cancer mortalities by ~30% and 50%. With no LCT, applying HCTs of 30 $\mu g/m^3$ and 50 $\mu g/m^3$ decreases estimated mortalities by ~10% and 1%, with larger decreases estimated for Europe and Asia where some modeled concentrations exceeded the upper threshold values.

2.4. Discussion and Conclusions

We estimate the global burden of mortality due to anthropogenic O_3 and $PM_{2.5}$ using a global atmospheric chemical transport model and health impact functions. Anthropogenic O_3 is associated with about 0.7 ± 0.3 million respiratory mortalities (1.1% ± 0.5% of all mortalities) and 6.3 ± 3.0 million YLL annually when no upper or lower concentration threshold is assumed. Anthropogenic $PM_{2.5}$ is associated with about 3.5 ± 0.9 million cardiopulmonary (5.6% ± 1.4% of all mortalities) and 220,000 ± 80,000 lung cancer mortalities (0.4% ± 0.1% of all mortalities) annually when no threshold is assumed, corresponding to 30 ± 7.6 million YLL. Global mortalities were reduced by ~30% when we assumed low-concentration thresholds of 33.3 ppb for O_3 and 5.8 $\mu g/m^3$ for $PM_{2.5}$, the lowest measured levels in Jerrett et al. (2009) and Krewski et al. (2009). Estimated excess mortalities are most dense in highly populated areas, but also occur in rural areas that have been affected by the increased regional or global background of air pollution since preindustrial times. These estimates based only on cardiopulmonary and lung cancer mortality may be conservative since O_3 and $PM_{2.5}$ may also affect other causes of mortality. In addition, to be consistent with the ACS study population, we included only the population ≥30, but evidence suggests that O_3 and $PM_{2.5}$ affect health negatively for all ages, including the very young (US EPA 2008a and references therein).

Estimated $PM_{2.5}$ mortalities are five times O_3 mortalities, suggesting $PM_{2.5}$ is the dominant contributor to the global health burden of outdoor air pollution. To minimize double counting of mortalities, we applied long-term RRs for O_3 and $PM_{2.5}$ based on the same ACS cohort. $PM_{2.5}$ RRs have been shown previously to be independent from O_3 concentrations (Krewski et al. 2000), and we use O_3 RRs from Jerrett et al. (2009) that

control for $PM_{2.5}$. Furthermore, Jerrett et al. (2009) and Krewski et al. (2009) reported that $PM_{2.5}$-related mortality was dominated by cardiovascular mortality, while O_3 was primarily associated with respiratory mortality. The independence of the exposure-response relationships and difference in dominant biological mechanisms of mortality for each pollutant implies that double counting is unlikely to be significant. If these implications are correct, O_3 and $PM_{2.5}$ mortalities may be summed together to yield total mortalities; otherwise, summing the results would overestimate total mortalities.

Mortality estimates were sensitive to concentration thresholds and concentration-mortality relationships, often changing by more than 50% of the estimated value under different assumptions. We assume that the CRFs found by epidemiology studies conducted in North America apply globally, despite differences in health status, lifestyle, age structure, and medical care, and emphasize cause-specific mortality. The CRFs used here could also be subject to confounders, including temperature (Jerrett et al. 2009). Although some evidence suggests differential toxicity of $PM_{2.5}$ components (Franklin et al. 2008; Ostro et al. 2008), we assume that all $PM_{2.5}$ species exert effects similar to aggregated $PM_{2.5}$, despite differences in $PM_{2.5}$ composition throughout the world. These assumptions, while necessary due to limited data, may have substantial impacts on the results.

Using the same assumptions for CRFs (Pope et al. (2002) for 1979-1983) and low-concentration threshold (7.5 $\mu g/m^3$, applied to total $PM_{2.5}$ in Cohen et al. (2004), but here only to the species in our definition of $PM_{2.5}$), our mortality estimates for urban and rural areas (Table 2.5) are ~50% higher than the previous estimate of 800,000 mortalities from urban air pollution reported by Cohen et al. (2004). The discrepancy results from

two competing differences in methods. First, we include rural populations, which were excluded by Cohen et al. (2004). Because the urban population in Cohen et al. (2004) is ~30% of the total global population, and air pollution has increased in rural regions, inclusion of rural populations suggests many more air pollution mortalities globally. Second, we use a coarse resolution global CTM that spreads emissions across large grid cells. While rural O_3 and $PM_{2.5}$ are simulated well, the coarse resolution may suppress high urban $PM_{2.5}$ concentrations, causing us to underestimate $PM_{2.5}$ mortalities. Compared with a previous US estimate of 144,000 $PM_{2.5}$ mortalities (all causes) found using a regional CTM (US EPA 2009), our estimate of $PM_{2.5}$ mortalities in North America is similar but slightly lower (by 2% for cardiopulmonary and lung cancer mortalities and 7% for all cause mortalities). The coarse resolution model may either overestimate or underestimate O_3 pollution in urban areas, as O_3 precursors are diluted into a large volume. Previous studies have found that regional O_3 can be overestimated by 13% at the resolution used here, but that background concentrations are not greatly affected by resolution (Wild and Prather 2006). A finer resolution model would capture urban populations and concentrations more accurately, but adequate resolution is not currently possible in global air quality models.

Despite these limitations, this study highlights regions where improvements to air quality may be particularly effective at reducing air pollution-related mortality. Previous estimates rank urban air pollution ($PM_{2.5}$ only) as the 13th leading global risk factor and 3rd among environmental risks (Ezzati et al. 1999). Our results suggest a larger burden of disease due to outdoor air pollution than was previously estimated, but should only be compared with other risk factors when all are updated consistently. Future estimates of

the global burden of air pollution on mortality should strive to combine information from global and regional models with rural and urban concentrations from measurements. CRFs from new studies on O_3 and $PM_{2.5}$ mortality relationships that examine individual $PM_{2.5}$ components, that are conducted in different parts of the world, that include populations of all ages, and that resolve relationships at low and high concentrations should also be incorporated. In the future, global economic development will likely shift the disease burden from infectious disease and malnutrition to chronic conditions, which are more strongly affected by air pollution exposure. While some countries have implemented policies to improve air quality, without further action, the global burden of anthropogenic air pollution on mortality may be even larger in the future than is estimated for the present.

2.5. Tables and figures

Table 2.1. Population ≥30, average baseline mortality rates (Resp.=respiratory, CP=cardiopulmonary, LC=lung cancer), and population-weighted average and range (below, shown for the highest and lowest individual grid cells) of the seasonal average (6-month) 1-hr. daily maximum O_3 concentrations and annual average $PM_{2.5}$ concentrations from MOZART-2 simulations of the preindustrial (1860) and present (2000) (Horowitz 2006).

	Pop ≥ 30[b] (billions)	Baseline mortality rates (%/year)[c]			O_3 (ppb)[a]				$PM_{2.5}$ (μg/m^3)[a]			
					1860		2000		1860		2000	
		Respiratory	CP	LC	Average	Range	Average	Range	Average	Range	Average	Range
Africa	0.28	0.206	0.739	0.011	23.32	11.4–31.9	54.46	20.2–71.5	0.92	0.28–3.19	7.50	0.50–13.9
North America	0.27	0.081	0.502	0.071	21.42	12.5–32.3	59.75	27.0–89.3	1.50	0.14–4.65	8.44	0.31–16.6
Europe	0.44	0.127	1.22	0.056	18.26	15.2–27.5	48.92	32.3–74.3	0.93	0.11–2.96	14.77	0.40–39.0
Asia	1.8	0.171	0.746	0.037	18.91	6.15–35.9	59.64	10.8–83.7	1.19	0.23–3.06	20.41	0.34–55.9
South America	0.15	0.121	0.515	0.025	18.44	12.2–35.8	44.59	22.3–90.3	1.00	0.33–3.89	6.35	0.40–13.9
Oceania	0.02	0.074	0.346	0.035	13.37	3.74–22.8	26.75	6.41–44.4	0.96	0.22–2.27	2.59	0.25–5.01
World	2.9	0.134	0.754	0.042	19.61	3.74–35.9	56.70	6.41–90.3	1.13	0.11–3.89	16.11	0.25–55.9

Abbreviations: CP, cardiopulmonary; LC, lung cancer; Pop, population. Data are average and range for the highest and lowest individual grid cell.

[a]Simulated by Horowitz (2006). [b]Population ≥ 30 years of age for the year 2006 from the Landscan database (Oak Ridge National Laboratory 2008). [c]Baseline mortality rates are country-specific for the latest year after 2000 where data were

available (World Health Organization 2008b). Where country-specific rates after the year 2000 were not available, we back-calculate country-specific rates from regional rates for the year 2002.

Table 2.2. Annual estimated mortalities ± 1 SD due to anthropogenic O_3 and $PM_{2.5}$, assuming natural background only or LCTs (33.3 ppb for O_3 and 5.8 µg/m^3 for $PM_{2.5}$) (x1000).

	O_3 respiratory		$PM_{2.5}$ cardiopulmonary		$PM_{2.5}$ lung cancer	
	Background	Threshold	Background	Threshold	Background	Threshold
Africa	63 ± 34	45 ± 30	154 ± 44	52 ± 33	3 ± 1	1 ± 1
North America	35 ± 17	25 ± 15	124 ± 37	65 ± 30	17 ± 7	10 ± 5
Europe	41 ± 21	23 ± 17	586 ± 149	383 ± 143	47 ± 17	31 ± 14
Asia	543 ± 253	370 ± 220	2,584 ± 618	1,991 ± 603	152 ± 53	122 ± 47
South America	18 ± 9	8 ± 6	48 ± 15	16 ± 9	2 ± 1	1 ± 1
Oceania	1 ± 1	0 ± 0	2 ± 1	0 ± 0	0 ± 0	0 ± 0
World	700 ± 335	470 ± 288	3,499 ± 864	2,506 ± 816	222 ± 80	164 ± 68

SDs reflect uncertainty in the CRF and simulated present-day concentrations (SD=25% of simulated concentration).

Table 2.3. Estimated annual YLL ± 1 SD due to anthropogenic O_3 and $PM_{2.5}$, assuming natural background or LCTs (33.3 ppb for O_3 and 5.8 µg/m^3 for $PM_{2.5}$) (x1000).

	O_3 respiratory		$PM_{2.5}$ cardiopulmonary		$PM_{2.5}$ lung cancer	
	Background	Threshold	Background	Threshold	Background	Threshold
Africa	901 ± 486	644 ± 429	1,694 ± 484	572 ± 363	40 ± 13	13 ± 13
North America	285 ± 138	203 ± 122	804 ± 240	421 ± 194	152 ± 62	89 ± 45
Europe	243 ± 125	136 ± 101	4,336 ± 1,103	2,834 ± 1,058	472 ± 171	311 ± 141
Asia	4,322 ± 2,014	2,945 ± 1,751	20,620 ± 4,932	15,888 ± 4,812	1,594 ± 556	1,280 ± 493
South America	137 ± 68	61 ± 46	365 ± 114	122 ± 68	19 ± 10	10 ± 10
Oceania	7 ± 7	0 ± 0	11 ± 6	0 ± 0	0 ± 0	0 ± 0
World	6,251 ± 2,992	4,197 ± 2,572	27,607 ± 6,817	19,772 ± 6,438	2,169 ± 782	1,602 ± 664

SDs reflect uncertainty in the CRF and simulated present-day concentrations (SD=25% of simulated concentration)

Table 2.4. Estimated annual global O_3 mortalities (mean ± 1 SD) to CRFs from the multipollutant model (in which $PM_{2.5}$ was controlled) and single-pollutant model in Jerrett et al. (2009), and LCTs (x1000).

	Cardiopulmonary	Respiratory
Multipollutant model	—	700 ± 335
LCT = 25 ppb	—	605 ± 317 (–13.6%)
LCT = 33.3 ppb	—	470 ± 288 (–32.9%)
Single-pollutant model	1,076 ± 493	524 ± 252 (–25.1%)
LCT = 25 ppb	925 ± 467	452 ± 238 (–35.4%)
LCT = 33.3 ppb	705 ± 423	350 ± 215 (–50.0%)
Threshold model[a]		
LCT = 56 ppb	—	178 ± 187 (–74.6%)

Data in parentheses are percentage change from estimates assuming CRFs from Jerrett et al. (2009) multipollutant model with no LCT (top row). Uncertainty is from the CRF and simulated present-day concentrations (SD=25% of simulated concentration).

[a]Calculated using the CRF (0.00432 ppb^{-1}) and corresponding standard error (0.00121 ppb^{-1}) for respiratory mortality when a threshold of 56 ppb is included in the O_3-mortality model (Jerrett et al. 2009). Although Jerrett et al. (2009) found that no threshold model was clearly a better fit to the data than a linear representation of the overall O_3-mortality association, a threshold of 56 ppb was close to statistical significance (p=0.06).

Table 2.5. Estimated annual global $PM_{2.5}$ mortalities (mean ± 1 SD) using alternative CRFs with and without LCTs and HCTs (x1000).

	Mortality		
	All causes	Cardiopulmonary	Lung cancer
Krewski et al. (2009)	3,381 ± 986	3,499 ± 864	222 ± 80
LCT = 5.8 μg/m^3	2,378 ± 876 (–29.7%)	2,506 ± 816 (–28.4%)	164 ± 68 (–26.1%)
LCT = 7.5 μg/m^3	2,077 ± 822 (–38.6%)	2,201 ± 780 (–37.1%)	146 ± 64 (–34.2%)
HCT = 30 μg/m^3	3,059 ± 774 (–9.5%)	3,205 ± 676 (–8.4%)	201 ± 68 (–9.5%)
HCT = 50 μg/m^3	3,338 ± 940 (–1.3%)	3,464 ± 826 (–1.0%)	219 ± 78 (–1.4%)
Pope et al. (2002), 1979–1983[a]	2,333 ± 1,196 (–31.0%)	1,800 ± 742 (–48.6%)	139 ± 72 (–37.4%)
Laden et al. (2006)[b]	7,714 ± 2,736 (+128.2%)	4,549 ± 1,439 (+30.0%)	336 ± 198 (+51.4%)

Data in parentheses are percentage change from estimates using CRFs from Krewski et al. (2009) and no LCT or HCT (top row). Uncertainty is from the CRF and simulated present-day concentrations (SD=25% of simulated concentration).

[a] Pope et al. (2002) reported RR estimates for two time periods (1979-1983 and 1999-2000) and for the integrated average of both. The RR estimates for 1979-1983 were more conservative than those from 1999-2000 and the integrated average. See Table A.2 for results from the average of both time periods and with concentration thresholds.

[b] Laden et al. (2006) extended the follow-up of the Harvard Six Cities adult cohort study for 8 years, finding significantly higher RR estimates for overall mortality than the original study and Krewski et al. (2009). See Table A.2 for results with concentration thresholds.

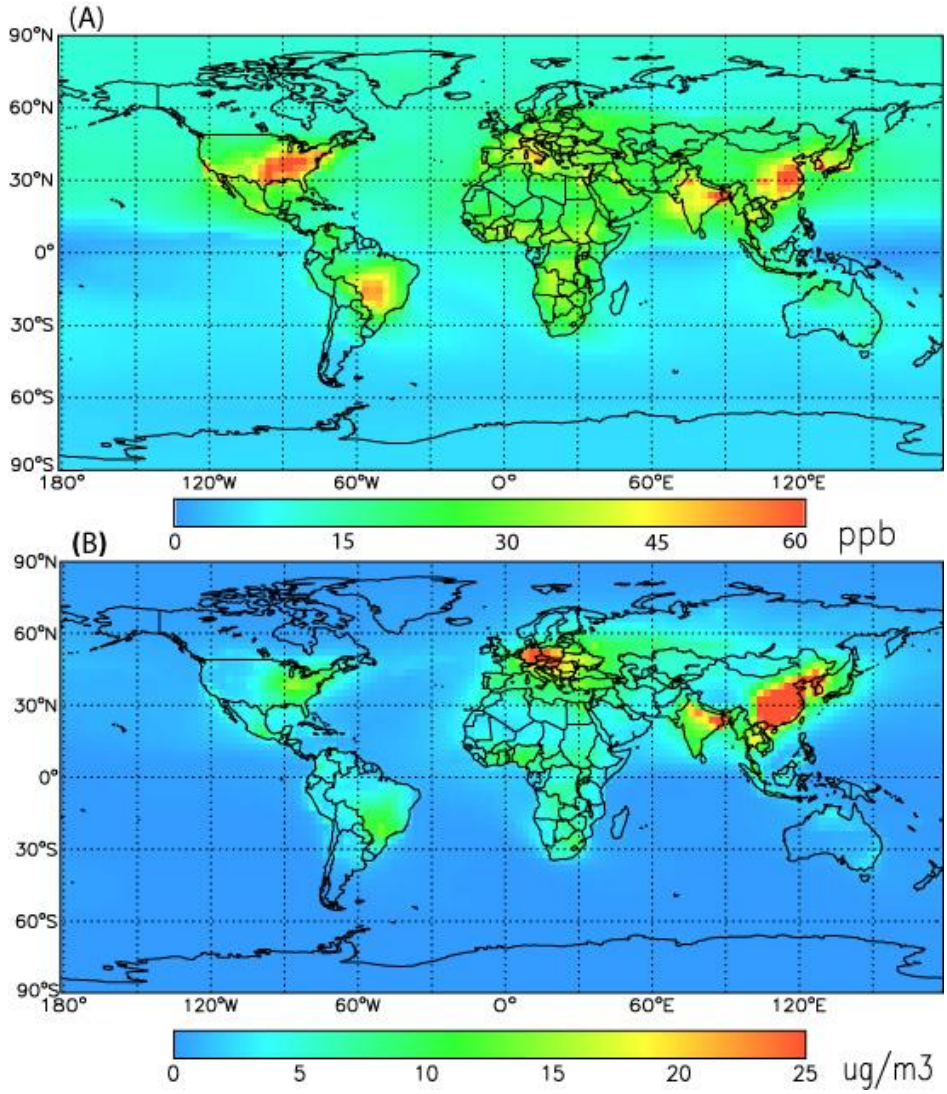

Figure 2.1. Estimated change (present minus preindustrial) in (A) seasonal average (6-month) 1-hr. daily maximum O_3 concentrations (ppb) and (B) annual average $PM_{2.5}$ ($\mu g/m^3$) from Horowitz (2006) simulations.

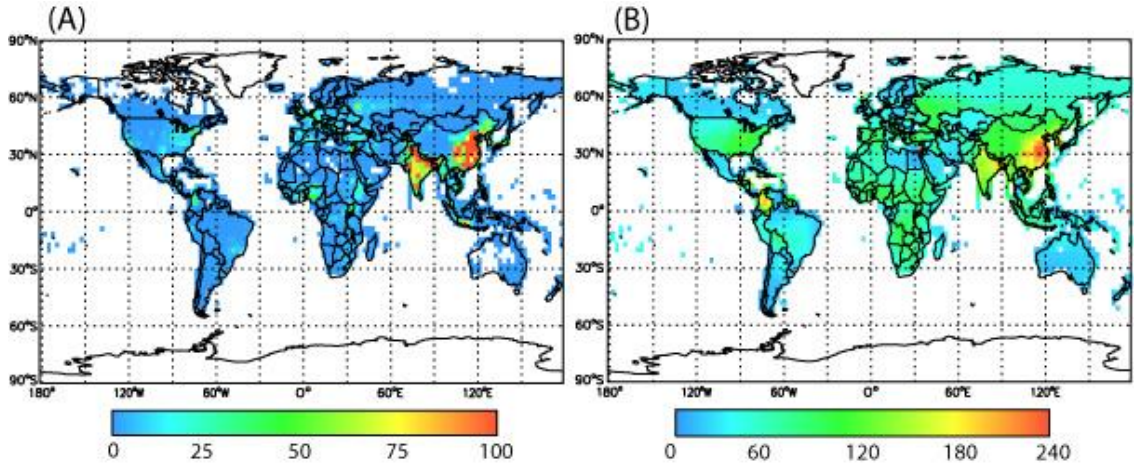

Figure 2.2. Estimated annual premature respiratory mortalities attributed to anthropogenic O_3 when no threshold is assumed, for respiratory mortalities (A) per 1000 km^2 and (B) per 10^6 people.

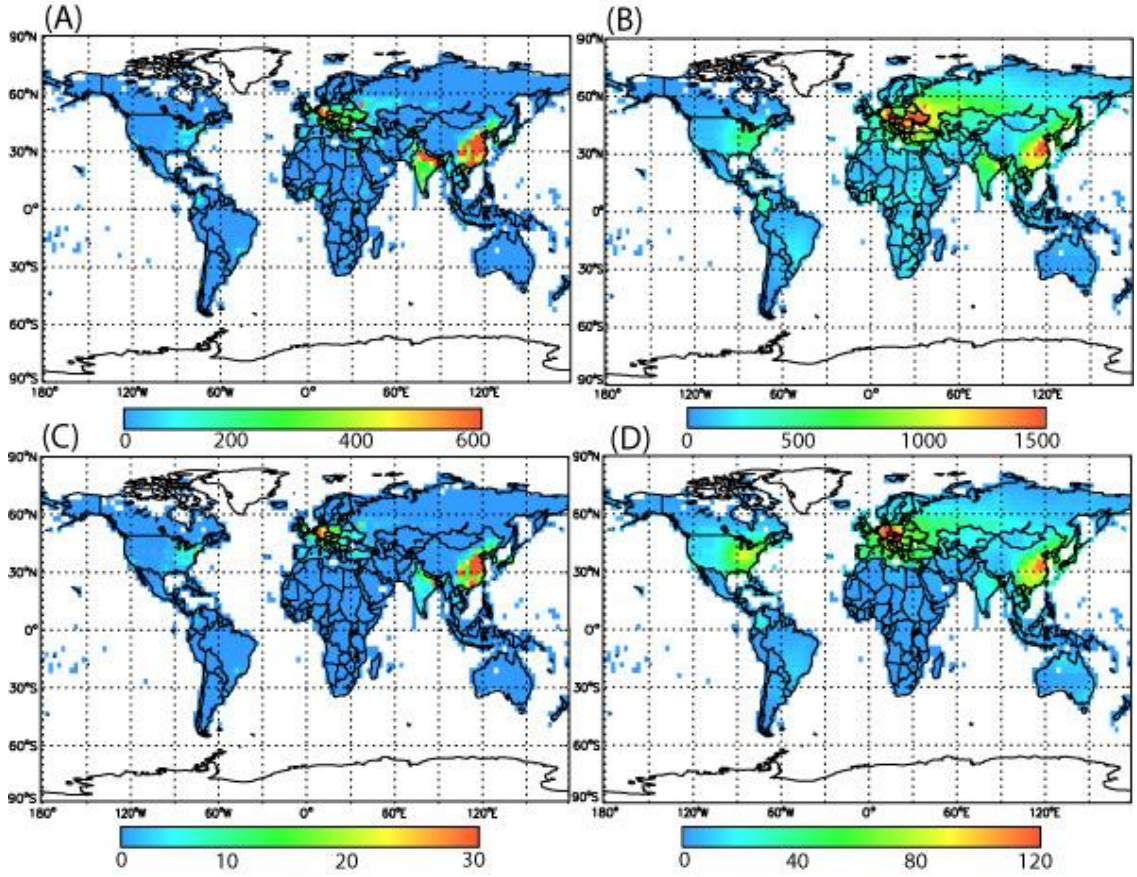

Figure 2.3. Estimated annual premature mortalities attributed to anthropogenic $PM_{2.5}$ when no upper or lower concentration threshold is assumed, for (A) cardiopulmonary mortalities per 1000 km^2, (B) rate of cardiopulmonary mortalities per 10^6 people, (C) lung cancer mortalities per 1000 km^2, and (D) rate of lung cancer mortalities per 10^6 people.

Chapter 3. Intercontinental impacts of ozone pollution on human mortality

(Anenberg, S. C., West, J. J., Fiore, A. M., Jaffe, D. A., Prather, M. J., Bergmann, D., Cuvelier, K., Dentener, F. J., Duncan, B. N., Gauss, M., Hess, P., Jonson, J.- E., Lupu, A., MacKenzie, I. A., Marmer, E., Park, R. J., Sanderson, M. G., Schultz, M., Shindell, D. T., Szopa, S., Vivanco, M. G., Wild, O., and G. Zeng. (2009). Environmental Science and Technology, 43, 6482-6487.)

3.1. Introduction

Ground-level ozone (O_3) causes deleterious impacts to human health, including cardiovascular and respiratory mortality (Bell et al. 2004; Bell et al. 2005; Ito et al. 2005; Levy et al. 2005). O_3 is photochemically produced in the troposphere by oxidation of methane (CH_4), non-methane volatile organic compounds (NMVOCs), and carbon monoxide (CO) in the presence of nitrogen oxides ($NO_x = NO + NO_2$). Observations and modeling studies demonstrate that O_3 produced in polluted regions can be transported long distances and that transport of precursors can enhance O_3 production in remote regions, impacting air quality on a global scale (TF HTAP 2007; Fiore et al. 2009). Understanding the impacts of O_3 precursor emissions from one region on health in distant regions may inform future air pollution mitigation strategies.

The impacts of O_3 on human mortality are influenced by demographic characteristics, including population density and baseline mortality rates. We calculate

the premature mortalities within the entire Northern Hemisphere (NH) and within four major industrial regions – North America (NA), East Asia (EA), South Asia (SA), and Europe (EU) – that could be avoided by decreasing O_3 precursor emissions in each region. We use results from the Task Force on Hemispheric Transport of Air Pollution (TF HTAP, www.htap.org) multi-model study which showed that surface O_3 in one region decreases following 20% reductions of anthropogenic NO_x, NMVOCs, and CO emissions in any of the foreign regions, and that the O_3 decrease is similar to that from a 20% reduction in anthropogenic CH_4 emissions in the same foreign region (TF HTAP 2007; Fiore et al. 2009). We estimate avoided premature mortalities using these simulated long-range O_3 responses and a health impact function.

3.2. Methods

The TF HTAP coordinated an effort to quantify source-receptor relationships for four regions (NA, EA, SA, and EU; Figure B.1), using multiple chemical transport models (CTMs) (Fiore et al. 2009). We use the resulting multi-model mean surface O_3 responses for 20% reductions in NO_x, NMVOC, and CO emissions in each region (SR6) and a 20% reduction in the global CH_4 mixing ratio (SR2), relative to the base case (SR1). Fourteen models participated in the SR6 vs. SR1 cases and 17 models in the SR2 vs. SR1 case, all with horizontal resolution ranging from 5° x 5° to 1° x 1° (Table B.1), meteorology and emissions from 2001, and a constant CH_4 mixing ratio (1760 ppb for base case). All models have fixed meteorology, and do not model changes in meteorology due to atmospheric composition. For the 20% reductions in NO_x, NMVOC, and CO emissions, we do not account for long-term changes in O_3 due to the resulting

change in CH_4 (Wild et al. 2001; West et al. 2007; Fiore et al. 2009), which is estimated to be small for this scenario. Compared with surface O_3 observations, the model ensemble mean captured seasonal cycles in the northern mid-latitude regions, except for a 10-20 ppb summertime positive bias over the eastern United States (US) and Japan, which did not correlate with estimates of the O_3 response to foreign emission reductions. Surface O_3 concentrations (monthly averages) from the individual models are regridded to a common 0.5° x 0.5° grid, and the ensemble average concentration is calculated for each grid cell and perturbation scenario.

Following previous studies using one global CTM (West et al. 2006; Corbett et al. 2007; Duncan et al. 2008; West et al. 2009b), avoided premature mortalities resulting from each perturbation scenario are calculated using a health impact function based on a log-linear relationship between O_3 concentration and relative risk (*RR*) (Bell et al. 2004). *RR* is used to calculate the attributable fraction (*AF*), the fraction of the disease burden attributable to the risk factor (Equation 1). When *RR*>1, O_3 exposure increases risk of mortality.

Equation (1) $$AF = \frac{RR - 1}{RR} = 1 - exp^{-\beta \Delta X}$$

Here, β is the concentration-response factor (CRF) and ΔX is the change in O_3 concentration. *AF* is multiplied by the baseline mortality rate (y_0) and exposed population (*Pop*) to yield avoided mortalities due to the O_3 concentration change (Equation 2).

Equation (2) $$\Delta\, Mort = y_0\,(1 - exp^{-\beta \Delta X})\, Pop$$

We apply Equation 2 in each grid cell for each month using the corresponding population and baseline mortality rates, and sum the results to yield annual avoided premature mortalities ("avoided mortalities").

CRFs are from a daily time-series study of the average relative risk of mortality associated with short-term ambient O_3 concentrations in 95 US cities (Bell et al. 2004). For each 10 ppb increase in 24-hr. average O_3, total non-accidental (includes cardiovascular and respiratory) mortality increased by 0.52% (95% posterior interval (PI), 0.27%-0.77%) and cardiovascular and respiratory mortality in particular increased by 0.64% (95% PI, 0.31%-0.98%). These values are relatively low compared with other studies in the US (Ostro et al. 2006), and we assume that they are valid globally, as similar results have been demonstrated in Europe and in developing nations (Health Effects Institute Scientific Oversight Committee 2004; Ostro et al. 2006). Compared with estimates of avoided non-accidental mortalities, estimates of avoided cardiopulmonary mortalities may be less influenced by differences in mortality causes around the world. We present results for both cardiopulmonary and non-accidental mortalities, but emphasize the cardiopulmonary results, which alone may underestimate the impact of decreased O_3 on mortality by excluding other causes of death potentially associated with O_3.

Epidemiology studies relating O_3 and mortality may be subject to confounding by correlated co-pollutants, weather, and other factors, such as demographics and health status. As recommended previously (National Academy of Sciences 2008), we use data from Bell et al. (2004), who controlled for known confounders, and examine the sensitivity of our results to *RR* estimates from meta-analyses of single-city time-series

studies (Bell et al. 2005; Ito et al. 2005; Levy et al. 2005). While little evidence exists for a low-concentration threshold below which O_3 causes no adverse impacts (National Academy of Sciences 2008), we calculate results with and without a low-concentration threshold of 35 ppb, as recommended for European analyses (Holland et al. 2005).

We map the gridded global population in 2006 (Oak Ridge National Laboratory 2008; NH total is 5.71 billion) to the coarser grid of the multi-model mean O_3 concentrations. Baseline cardiopulmonary and non-accidental mortality rates are from the World Health Organization for 14 world regions (World Health Organization 2004) and 66 countries (World Health Organization 2008b). For countries with no available data, we back-calculate population-weighted average mortality rates from regional rates. We use a Geographic Information System to calculate area-weighted average rates for grid cells that overlap multiple countries and to calculate avoided mortalities within US borders.

Our estimates of O_3 responses are subject to uncertainty due to the coarse resolution of global models. While global models are currently necessary to estimate long-range transport, their coarse resolution influences O_3 production within the source region, and our results may differ from those of a fine-resolution regional model. Errors due to resolution are expected to be smaller for long-range transport, as changes in concentration are more spatially uniform (Wild et al. 2006). Errors for mortality estimates may be greatest within source regions, particularly in urban regions with strong population gradients.

3.3. Results

3.3.1. Regional NO_x, NMVOC, and CO emission reductions

For simultaneous 20% reductions of anthropogenic NO_x, NMVOC, and CO emissions in each of the four regions, the largest impact on the multi-model mean change in surface O_3 occurs in the "domestic" region (i.e. where emissions are reduced) (Table 3.1). We note that "domestic" impacts include transport between metropolitan regions, states, and neighboring nations. Emission reductions in SA yield the greatest disparity between the domestic and "foreign" (i.e. within the three regions outside of the source region) population-weighted O_3 response, with a ratio of the domestic change to the change in each foreign region of 17-32. EA emission reductions also cause a large domestic vs. foreign difference (ratio of domestic to foreign response of 6.5-8.2), while this ratio is smaller for NA (2.8-6.4) and EU (2.7-3.9).

Regardless of where emission reductions occur, avoided mortalities are concentrated in highly populated areas (e.g. Northern India and China; Figure 3.1, left). The greatest rates of avoided mortalities per million people occur near the source region (Figure 3.1, right), except for EU, where NO_x reductions increase O_3 during the winter (Fiore et al. 2009), increasing domestic mortalities. For each receptor region, reducing domestic emissions is more effective at decreasing mortalities than reducing emissions in any of the three foreign regions (Table 3.2 and Table B.2). In response to domestic emission reductions, more avoided mortalities are calculated in EU with a threshold than without, since the wintertime domestic mortality increase often occurs when O_3 concentrations are lower than 35 ppb.

Reducing anthropogenic precursor emissions by 20% in all regions together avoids 21,800 (95% confidence interval (CI), 10,600-33,400) cardiopulmonary mortalities in the NH annually, assuming no threshold (Table 3.2), corresponding to about 6% of global cardiopulmonary mortalities attributable to O_3 (Anenberg et al. 2010) and about 0.03% of mortalities of all causes globally. Avoided non-accidental mortalities are about 1.7 times higher than the cardiopulmonary results (Table B.2). Foreign emission reductions contribute about 30% of the total avoided mortalities in NA (63-72% of these in the US) and EA, 20% for SA, and >50% for EU, indicating that more mortalities would be avoided in EU by reducing emissions in the three foreign regions compared with reducing domestic emissions.

Focusing on the impacts of each source region, 64-76% of the total annual NH avoided mortalities following NA emission reductions occur outside of NA (the range reflects different causes of mortality and threshold assumptions). Without a threshold, 55-58% of the total annual NH avoided mortalities following EU emission reductions occur outside of EU, though this conclusion reverses when a threshold of 35 ppb is applied (38-40% outside of EU). These findings agree with recent studies indicating that emission reductions in NA and EU have greater impacts on mortality outside the source region than within (Duncan et al. 2008; West et al. 2009b). NA is the only region where reducing emissions avoids more mortalities in a foreign receptor region (EU) than domestically, reflecting higher population and baseline mortality rates in EU. However, this conclusion does not hold when a threshold is applied (Table 3.2 and Table B.2). Emission reductions in SA yield the most annual avoided mortalities overall, but influence foreign regions the least, (90% of the resulting NH avoided mortalities are in

SA) due to its large population and minor influence of emissions on O_3 in the three foreign regions (Table 3.1). Emission reductions in EA also result in more avoided mortalities within the region (about 70% of the total NH avoided mortalities) than in the rest of the NH.

We analyze the sensitivity of the avoided non-accidental mortality results to the uncertainty in the O_3 responses simulated by the model ensemble for each grid cell (Table B.3 and Figure 3.2). Different resolutions, O_3 precursor emissions, and representations of chemical and transport processes in the individual models contribute to a large standard deviation among O_3 responses, particularly within the source region (Fiore et al. 2009). The range of avoided mortalities given by the 68% CI (± 1 standard deviation) in the modeled O_3 responses is similar in magnitude to the 95% CI in the CRF from Bell et al. (2004) for foreign source-receptor pairs, but is larger for each region in response to domestic emission reductions, except for SA. This large range in O_3 response to domestic emission reductions influences the relative importance of source-receptor pairs for mortality. For example, whereas using the ensemble mean O_3 concentration for NA emission reductions results in similar annual avoided mortalities in NA and EU, using the mean minus 1 standard deviation leads to more avoided mortalities in EU than in NA, and using the mean plus 1 standard deviation leads to more avoided mortalities in NA than in EU (Table B.3). A similar effect occurs for foreign vs. domestic avoided mortalities from EU emission reductions.

We also examine the sensitivity of the avoided non-accidental mortalities to the mean CRF from three meta-analyses of single-city daily time-series studies (Table B.3 and Figure 3.2), which have generally consistent results (Bell et al. 2005; Ito et al. 2005;

Levy et al. 2005) and do not report CRFs for cardiopulmonary mortalities. The mean CRF from the meta-analyses is larger than the CRF from Bell et al. (2004); consequently, avoided mortality estimates are 1.6-1.9 times larger. While the range in modeled O_3 responses to emission changes contributes more to uncertainty in our estimated avoided mortalities than does the uncertainty associated with the CRF from Bell et al. (2004) for some regions, using the mean CRF from the meta-analyses yields avoided mortality estimates that are often near or higher than the upper end of the range from the uncertainty in modeled O_3 concentrations (Figure 3.2). Therefore, source-receptor relationships for mortality are highly sensitive to both the CRF and modeled O_3 responses to emission reductions.

3.3.2. Global CH_4 mixing ratio reduction

Reducing the global CH_4 mixing ratio by 20% decreases O_3 fairly uniformly around the world, so that the population-weighted changes in O_3 concentration in all receptor regions are comparable and slightly higher in SA and EU (

Table 3.3), in agreement with previous studies (West et al. 2006; West et al. 2007; Fiore et al. 2008). About 80% of the 16,000 (95% CI, 7,700-24,400) NH annual avoided cardiopulmonary mortalities (assuming no concentration threshold) occur in the four regions, 8% of which occur in NA (57-82% of these in the US), 28% in EA, 35% in SA, and 29% in EU. Since the concentration change in each region is similar, the differences in avoided mortalities are largely driven by population and baseline mortality rates. Avoided non-accidental mortalities are about 1.7 times the cardiopulmonary results, and both are 0.6-0.8 times the results with a threshold of 35 ppb (Table B.4). These results are similar to a previous estimate of about 30,000 avoided non-accidental mortalities in 2030 due to 20% global anthropogenic CH_4 emission reductions (West et al. 2006), when accounting for differences in steady-state assumptions, modeled CH_4 reductions, and future population growth. CH_4 responds to emission reductions over decades, during which population growth increases the ultimate health benefits of CH_4 reductions.

Following methods used by Fiore et al. (2009), we infer the contribution of 20% anthropogenic CH_4 emission reductions in each region to the simulated O_3 response from reducing the global CH_4 mixing ratio by 20% (see Appendix B). We find about equivalent resulting reductions in population-weighted O_3 concentrations and avoided mortalities in the NH (Table 3.4), with the greatest mortality decrease in SA and smallest in NA (Figure B.5). Without a threshold, reducing anthropogenic CH_4 emissions by 20% in all source regions collectively avoids 8,600 (4,100-13,100) cardiopulmonary mortalities annually. Avoided non-accidental mortalities are about 1.7 times the cardiopulmonary results, and both are about 0.7 times the results with a threshold of 35 ppb (Table B.5). The domestic impacts of reducing regional CH_4 emissions are 0.1-0.3

times those from reducing domestic NO_x, NMVOC, and CO emissions by the same percentage, due to the large domestic effects of these precursors (Table 3.2 and Figure B.5). However, for each region, reducing emissions of NO_x, NMVOC, and CO in the three foreign regions has similar impacts on mortality as an equivalent percentage decrease in CH_4 emissions (Table 3.2 and Figure B.5).

3.3.3. Foreign vs. domestic influences within North America

Foreign anthropogenic NO_x, NMVOC, and CO emission reductions decrease mortalities in NA throughout the year, but compared with domestic emission reductions, cause fewer avoided mortalities in the summer and more in the winter due to the seasonality of O_3 in response to domestic NO_x emission reductions (Figure 3.3 and Figure B.6). We compare foreign and domestic impacts in NA using Health Import Sensitivity (HIS), the ratio of the summed avoided mortalities following NO_x, NMVOC, and CO emission reductions in the three foreign regions to the avoided mortalities following emission reductions in NA only. When HIS<1, the avoided mortalities due to domestic emission reductions are greater than the sum of those from emission reductions in the three foreign regions. The annual HIS for NA is 0.56, indicating that reducing domestic emissions is more effective than reducing foreign emissions for avoiding mortalities. The HIS for NA is lowest in the summer due to the large influence of domestic vs. foreign emissions on mortality and approaches infinity in the winter, when foreign emission reductions decrease O_3 but domestic emission reductions increase O_3 (Figure 3.3).

3.4. Discussion

We estimate the intercontinental impacts of O_3 on human mortality using a health impact function and multi-model estimates of the surface O_3 response to precursor emission reductions in four large industrial regions. Reducing O_3 precursor emissions by 20% within each receptor region ("domestic") avoids more mortalities than does reducing emissions in any of the three foreign regions. However, for all regions, emission reductions in the three foreign regions contribute significantly to the avoided mortalities resulting from emission reductions in all regions combined (30% for NA and EA, 20% for SA, and >50% for EU). For EU, the larger foreign impact is due to the influence of NA emissions.

Intercontinental health impacts of O_3 are influenced by the contribution of foreign emissions to O_3 in each region and by regional population and baseline mortality rates. Using the mean O_3 responses from the multi-model ensemble, more mortalities are avoided outside the source region than within following emission reductions in NA (64-76% of resulting NH annual avoided mortalities occur outside the source region) and EU (55-58%, assuming no threshold). The opposite is true for EA (about 70% within the source region) and SA (about 90%). Due to large populations, reducing emissions in any of the regions avoids many mortalities in EA and SA. Similarly, lowering the global CH_4 abundance by 20% reduces mortality most in SA, followed by EU, EA, and NA.

The relative importance of source-receptor pairs for mortality is strongly influenced by the accuracy and consistency of global CTMs in estimating O_3 responses to domestic and foreign precursor emission reductions. The substantial inter-model variation, particularly in the domestic O_3 response, causes uncertainty that influences our

conclusions about the relative numbers of domestic vs. foreign avoided mortalities. We expect that the coarse resolution of global models captures long-range transport, but may cause error particularly for domestic emission reductions. In assessing mortalities, systematic positive biases in the model ensemble mean O_3 should not affect our results when no threshold is assumed, but would when we assume a threshold, as the number of days above the threshold is affected. Future research should explore the possible bias in using coarse global models for health impact assessments, considering the relationships between concentration and population in metropolitan regions, by comparing with regional models, and should increasingly use finer-resolution or nested CTMs.

Our results focus solely on O_3-related mortality and do not account for possible effects on particulate matter mortality from the same changes in emissions. We examine only the short-term impacts of O_3 on mortality, for which years of life saved are unknown. We assume that the CRFs found in the US are valid globally, but populations across the world have different health characteristics that may influence O_3 impacts. The CRFs used here are corroborated by meta-analyses of short-term O_3 epidemiology studies in Europe and the developing world, which show a similar association between O_3 and mortality, but are somewhat inconsistent in the magnitude of the relationship. In addition, epidemiology studies could be subject to confounders, including correlated co-pollutants, that are as yet unknown.

Our results suggest that emission controls in one region affect O_3 air quality and O_3-related mortality in other world regions, with impacts outside the source region that are comparable to or even exceed the domestic (intra-regional) impacts. Confidence in these estimates would be increased by resolving uncertainties, including domestic O_3

responses to emission reductions and O_3 CRFs around the world. Despite uncertainties, our results point to widespread impacts of emission reductions, suggesting that collective international agreements over larger spatial scales may be needed to address local mortalities due to O_3 pollution (Holloway et al. 2003; Keating et al. 2004).

3.5. Tables and figures

Table 3.1. Population-weighted reduction in annual mean O_3 concentration (ppb) in receptor regions following 20% NO_x, NMVOC, and CO emission reductions in each source region, based on 2006 population (billions, italics) (Oak Ridge National Laboratory 2008).

Source Region	**Receptor Region**			
	NA	**EA**	**SA**	**EU**
	0.481	*1.67*	*1.55*	*1.02*
NA	0.960	0.183	0.149	0.349
EA	0.184	1.200	0.146	0.168
SA	0.059	0.112	1.890	0.066
EU	0.150	0.221	0.165	0.589

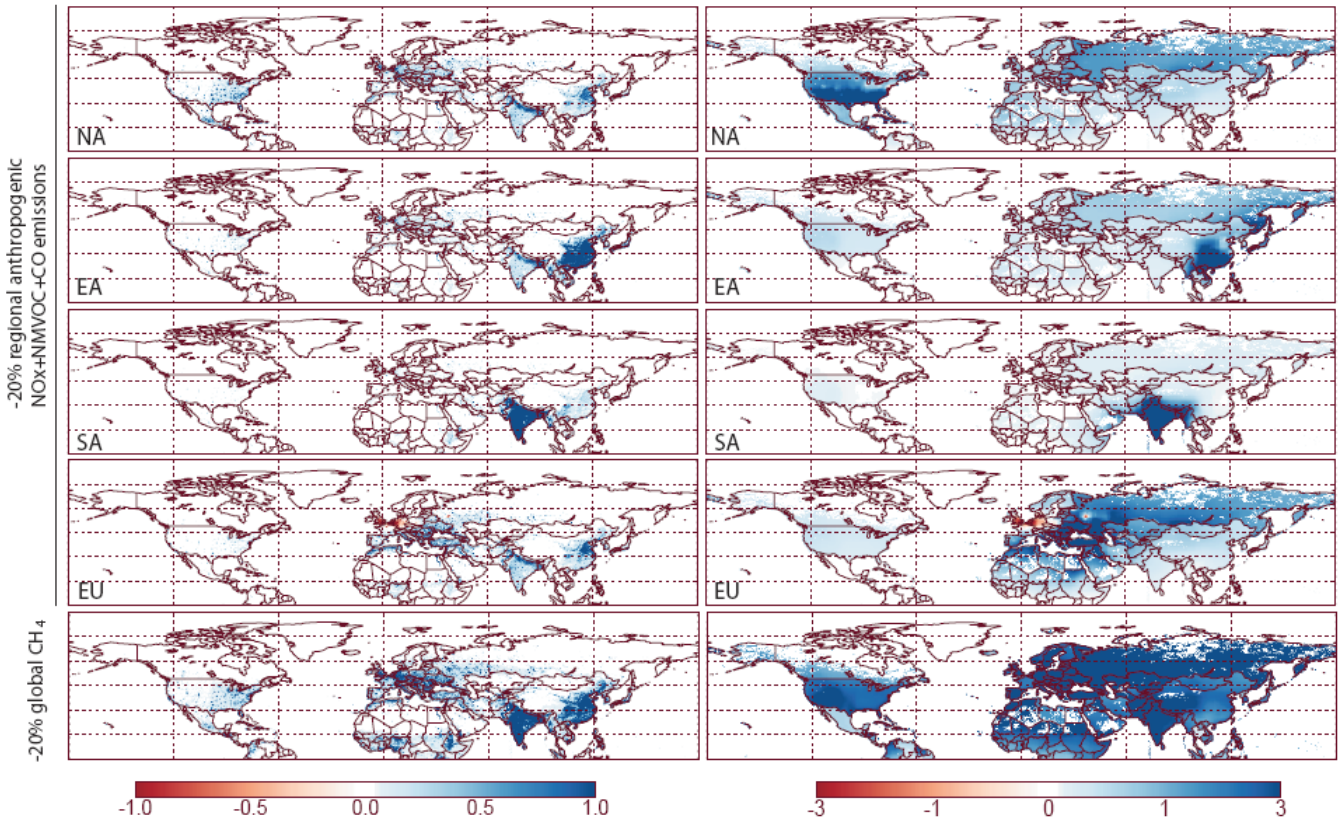

Figure 3.1. Annual avoided cardiopulmonary mortalities per 1000 km^2 (left) and per million people (right) resulting from 20% NO_x, NMVOC, and CO emission reductions in the region shown and a 20% global CH_4 mixing ratio reduction, assuming no low-concentration threshold.

Table 3.2. Annual avoided cardiopulmonary mortalities (hundreds) following 20% NO_x, NMVOC, and CO emission reductions in each region, assuming no concentration threshold and assuming a concentration threshold of 35 ppb (italics). Confidence intervals (95%) reflect uncertainty in the CRF only (Bell et al. 2004).

Source Region	**Receptor Region**				
	NA	**EA**	**SA**	**EU**	**NH**
NA	9 (4 - 13) *9 (4 - 14)*	7 (3 - 10) *4 (2 - 6)*	6 (3 - 9) *5 (3 - 8)*	11 (5 - 17) *6 (3 - 9)*	36 (18 - 55) *27 (13 - 41)*
EA	2 (1 - 3) *1 (1 - 2)*	43 (21 - 66) *40 (19 - 61)*	6 (3 - 9) *5 (2 - 8)*	5 (3 - 8) *3 (1 - 4)*	59 (29 - 91) *49 (24 - 76)*
SA	1 (0 - 1) *0 (0 - 1)*	4 (2 - 6) *3 (1 - 4)*	76 (37 - 117) *66 (32 - 101)*	2 (1 - 3) *1 (0 - 2)*	85 (41 - 130) *71 (34 - 108)*
EU	2 (1 - 3) *1 (0 - 1)*	8 (4 - 12) *6 (3 - 8)*	6 (3 - 10) *6 (3 - 9)*	17 (8 - 26) *25 (12 - 38)*	38 (18 - 58) *40 (19 - 61)*

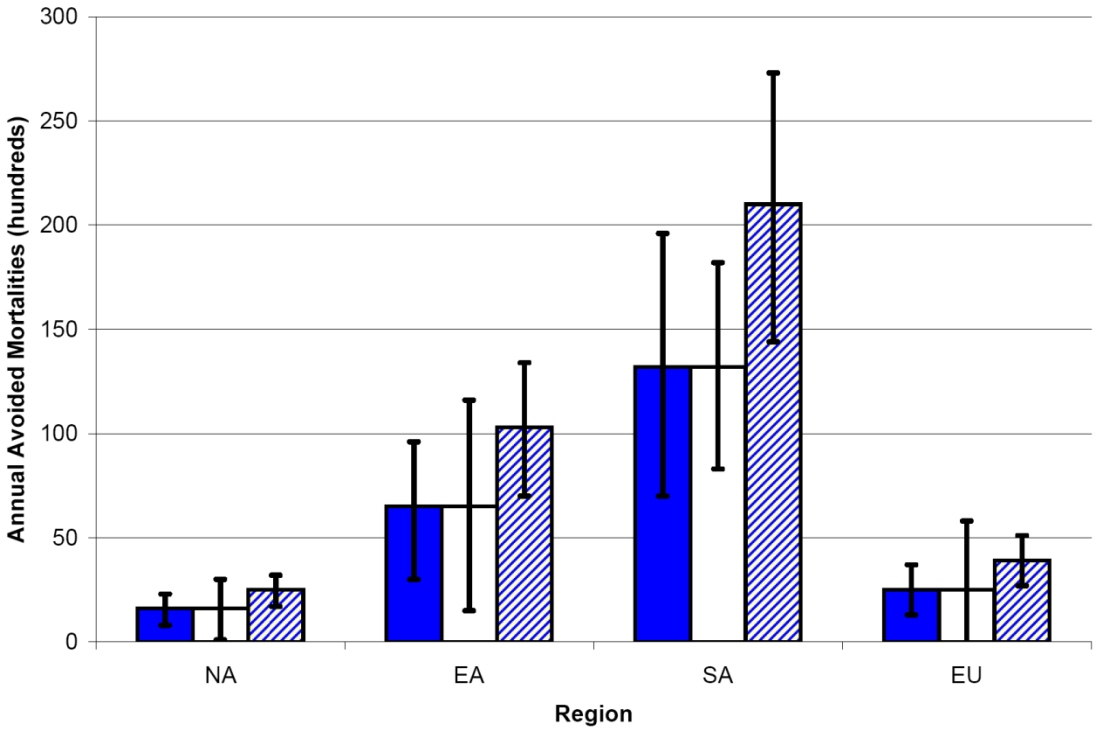

Figure 3.2. Annual avoided non-accidental mortalities (hundreds) in each region from 20% NO_x, NMVOC, and CO emission reductions in the same region using the CRF and confidence interval (95%) from Bell et al. (2004) (solid bars), using the CRF from Bell et al. (2004) and confidence intervals (68%) from ±1 standard deviation of the model ensemble ozone perturbation in each grid cell (Fiore et al. 2009) (white bars), and using the mean and confidence intervals (95%) of the CRFs from three meta-analyses of O_3 mortality (Bell et al. 2005; Ito et al. 2005; Levy et al. 2005) (striped bars). We convert the CRFs of Ito et al. (2005) and Levy et al. (2005) for 1-hr maximum O_3 concentrations to 24-hr mean using a ratio of 1-hr maximum to 24-hr mean equal to 2 (Levy et al. 2005).

Table 3.3. Population-weighted reduction in annual mean surface O_3 (ppb) and annual avoided cardiopulmonary and total non-accidental mortalities (hundreds) over each region and the entire NH following a 20% reduction in the global mean CH4 abundance, assuming no concentration threshold. Confidence intervals (95%) reflect uncertainty in the CRF only (Bell et al. 2004).

Receptor Region	Population-weighted ΔO_3 (ppb)	Avoided Cardiopulmonary Mortalities (hundreds)	Avoided Non-accidental Mortalities (hundreds)
NA	1.11	11 (5 - 17)	19 (10 - 29)
EA	1.08	38 (19 - 59)	58 (30 - 86)
SA	1.19	48 (23 - 73)	83 (43 - 123)
EU	1.23	39 (19 - 59)	58 (30 - 86)
NH	1.12	160 (77 - 244)	271 (141 - 401)

Table 3.4. Population-weighted reduction in annual mean surface O_3 (ppb) and annual avoided cardiopulmonary and total non-accidental mortalities (hundreds) in the NH following a 20% reduction in anthropogenic CH_4 emissions in each region relative to the base simulation, assuming no concentration threshold. Confidence intervals (95%) reflect uncertainty in the CRF only (Bell et al. 2004).

Source Region	Population-weighted ΔO_3 (ppb)	Avoided Cardiopulmonary Mortalities (hundreds)	Avoided Non-accidental Mortalities (hundreds)
NA	0.145	21 (10 - 31)	35 (18 - 52)
EA	0.166	24 (11 - 36)	40 (21 - 59)
SA	0.150	21 (10 - 33)	36 (19 - 54)
EU	0.140	20 (10 - 31)	34 (18 - 50)

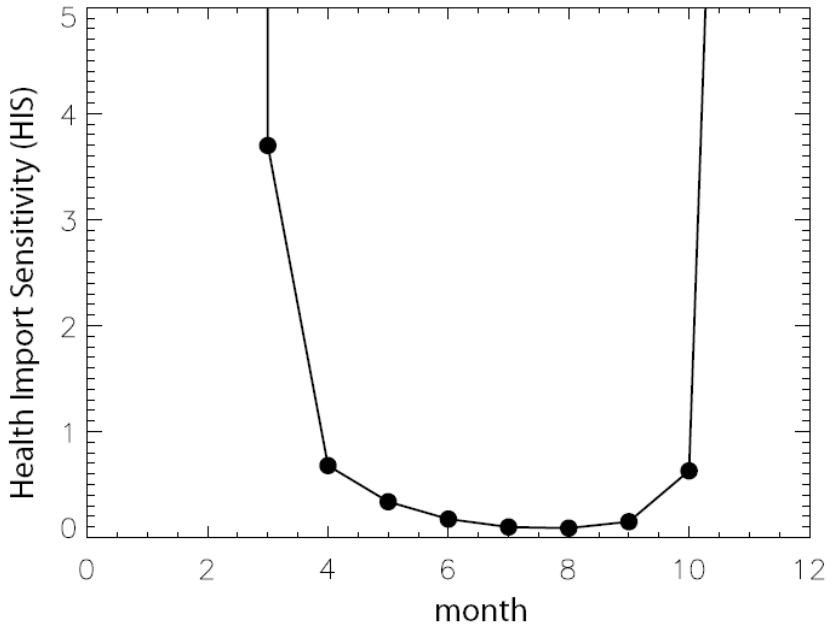

Figure 3.3. Seasonality of Health Import Sensitivity (the ratio of foreign vs. domestic impacts on cardiopulmonary mortalities) in NA, assuming no threshold.

Chapter 4. Impacts of global, regional, and sectoral black carbon emission reductions on surface air quality and human mortality

(Anenberg, S. C., Arunachalam, S., Talgo, K., Dolwick, P., Jang, C., West, J. J. In preparation for Atmospheric Chemistry and Physics)

4.1. Introduction

Black carbon (BC) is a component of fine particulate matter ($PM_{2.5}$) produced by incomplete combustion of fuel and is mainly emitted by residential, transportation, and industrial sources (Bond et al. 2004). $PM_{2.5}$ is associated with negative health impacts, including premature mortality (e.g. Krewski et al. 2009), and some evidence suggests that $PM_{2.5}$ mixtures containing high BC fractions may have larger mortality effects than other mixtures (e.g. Smith et al. 2010b). BC also warms the atmosphere by absorbing solar radiation (Horvath 1993), indirectly impacts cloud lifetime and reflectivity (e.g. Koch and Del Genio 2010), and deposits on snow and ice, reducing albedo and quickening melting (Hansen et al. 2004). Although the net effects of BC on climate remain uncertain, mitigation of BC emissions offers an opportunity to address climate change and air pollution simultaneously (e.g. Jacobson 2002; Bond and Sun 2005; Ramanathan and Carmichael 2008; Kopp and Mauzerall 2010). Both climate and health benefits should therefore be considered when evaluating mitigation strategies.

While several recent studies have examined the climate impacts of BC emissions (e.g. Koch et al. 2007; Reddy et al. 2007; Levy et al. 2008; Shindell et al. 2008; Fuglestvedt et al. 2009), the associated health impacts have been studied less extensively. In contrast with direct atmospheric warming by BC absorption of sunlight, which depends on total column BC concentrations, BC health impacts depend on population exposure at the surface, where humans breathe. In addition, the net climate impacts of BC emitting sources can be offset by co-emitted $PM_{2.5}$ components that reflect radiation, such as organic carbon (OC) and sulfate (SO_4) (Unger et al. 2010), but all $PM_{2.5}$ components are thought to be damaging to health. Since the drivers for climate and health impacts of BC emissions differ, mitigation strategies that achieve the greatest near-term climate benefits may not yield the greatest co-benefits for public health, and vice versa.

Previous studies of the health impacts of outdoor air pollution have found that the greatest burden of outdoor air pollution on human health occurs in Asia, where large populations are exposed to high ozone and $PM_{2.5}$ concentrations (Cohen et al. 2004; Anenberg et al. 2010), and that biofuel combustion causes eight times more premature deaths globally than fossil fuel emissions, largely because biofuel combustion occurs mainly in very populated regions of the world (Jacobson 2010). Surface BC concentrations, specifically, have also been found to be highest over East Asia, South Asia, and Southeast Asia (e.g. Koch et al. 2009). The co-location of high BC concentrations and large populations may translate into a substantial impact on global public health, and significant potential benefits of BC mitigation.

Quantifying the health benefits of BC emission reductions and their variation by source region and sector may inform strategies to mitigate near-term climate change and

air pollution simultaneously. Here, we calculate the surface air quality and premature human mortality impacts of halving anthropogenic BC emissions globally, regionally, and from three major economic sectors. We also examine a scenario in which BC and OC emissions are reduced together, as they are co-emitted and likely to both be affected by BC mitigation strategies. We simulate $PM_{2.5}$ concentration changes with a global chemical transport model (CTM) and calculate mortality changes using a health impact function based on epidemiologically-derived concentration-response relationships.

4.2. Methods

4.2.1. Model setup

We simulate a base case and several sensitivity cases using the global CTM MOZART-4 (Model of Ozone And Related Tracers, version 4) (Emmons et al. 2010). MOZART-4 has 85 gas-phase species and 39 photolysis and 157 gas-phase reactions. The representation of tropospheric aerosols includes sulfate (SO_4; assumed here to exist as ammonium sulfate), BC, OC, secondary organic aerosol (SOA), ammonium nitrate (NO_3), and sea salt (Emmons et al., 2010). An online photolysis scheme accounts for the impact of aerosols on photolysis rates, affecting production of photochemical oxidants (Tie et al. 2005; Emmons et al. 2010). Here, MOZART-4 is configured with a horizontal resolution of 1.9˚x1.9˚, 28 vertical levels, and is driven with meteorology from the NCEP/NCAR reanalysis (6 hour timestep) (Kistler et al. 2001; Kalnay et al. 1996) for the year 2002 with six months of spinup starting in July 2001. BC and OC are initially emitted as 80% and 50% hydrophobic and are converted to hydrophilic with a time

constant of 1.6 days to simulate the gradual coating of hydrophobic particles with sulfate and other compounds (Emmons et al. 2010). Dry deposition of BC and OC is set to 0.1 cm s^{-1} and wet deposition of hydrophilic BC and OC is set to 20% of the wet deposition rate of HNO_3 (Tie et al. 2005; Emmons et al. 2010).

Anthropogenic BC and OC emissions for the year 2000 are from the inventory developed for the Intergovernmental Panel on Climate Change Fifth Assessment Report (IPCC AR5), based on Bond et al. (2007) and Junker and Liousse (2008) with updates described by Lamarque et al. (2010). Since this inventory includes only submicron particles, we multiply BC and OC emissions by 1.15 and 1.4 to include all particles up to 2.5 μm in diameter for these species (Cooke et al. 1999), as in Liu et al. (2009b). The IPCC AR5 inventory reports emissions from the residential, transportation, and industrial sectors (includes non-road transportation), and smaller sectors, such as waste treatment, agricultural waste burning, and shipping. The residential, industrial, and transportation sectors together comprise >90% of the total anthropogenic BC inventory (Figure 4.1). As BC and OC are generally co-emitted with CO (e.g. Dickerson et al. 2002), we vary these emissions monthly by scaling to the monthly profile of CO from the RETRO emissions inventory (http://retro.enes.org/data_emissions.shtml), which does not include BC and OC, in each grid cell and sector (Figure C.1 and Figure C.2).

Anthropogenic emissions of all other species are those used by Emmons et al. (2010b), which are from the POET (Precursors of Ozone and their Effects in the Troposphere) (Olivier et al. 2003; Granier et al. 2005) inventory for the year 2000, with Asian emissions replaced by the annually varying Regional Emissions Inventory in Asia (REAS) (Ohara et al. 2007) (Table C.1). Biomass burning emissions for all species are

from the Global Fire Emissions Database version 2 (GFED2) (Van der Werf et al. 2006) for the specific months in 2001 and 2002 modeled here. To account for emission altitude and plume buoyancy, we distribute all biomass burning emissions vertically up to 6 km above the surface using the vertical profile from Dentener et al. (2006). All other emissions are injected at the surface, including power generation (<1% of global BC emissions) and industrial emissions, which include non-road transportation and small sources with no smokestacks.

Relative to this base case, we calculate changes in $PM_{2.5}$ concentration and mortality for 12 sensitivity cases wherein anthropogenic BC emissions are halved globally, individually in eight major world regions (North America, South America, Europe, the Former Soviet Union, Africa/Middle East, South Asia (India), East Asia (China), and Southeast Asia/Australia) plus in the United States (US) alone, and individually in three major economic sectors (residential, industrial, transportation). These regions are defined in Table 4.1 and Figure C.3. We also examine a scenario in which global anthropogenic BC+OC emissions are halved together, since they are co-emitted. Because each source emits BC and OC in different ratios and each control measure may reduce them in different percentages, this experiment is meant to be illustrative of including OC reductions and does not represent the impacts of actual mitigation measures. We use simulated concentrations in the first vertical level (height=~80m) as surface concentrations. We multiply simulated hydrophobic and hydrophilic OC concentrations by 1.3 and 1.7 to account for associated species other than carbon (Ming et al. 2005) and add this to SOA to give total organic mass (OM). We estimate $PM_{2.5}$ as $BC+OM+SO_4+NO_3$, assuming that these species exist entirely as $PM_{2.5}$

and ignoring other species (dust and sea salt) that are dominated by natural emissions and are unaffected by changing BC and OC emissions.

4.2.2. Evaluation of base case surface concentrations

Simulated annual average $PM_{2.5}$ concentrations are highest in EA and IN, due to large anthropogenic and biomass burning emissions (Table 4.1 and Figure C.4Figure C.8). BC is 3-5% of total $PM_{2.5}$ among world regions and OM is 14-46% (Figure 4.2 and Table C.2). SO_4 generally contributes the most to $PM_{2.5}$, except for IN and EA, where OM and NO_3 also contribute significantly, and SE/AU, where OM is high due to wildfires. Population-weighted average BC and NO_3 concentrations are generally larger than simple average concentrations (Figure C.2), indicating closer co-location with population compared with OM and SO_4, which are more widespread.

MOZART-4 has been evaluated extensively against satellite data and measurements at altitude and at the surface by Emmons et al. (2010) and Tie et al. (2005), who comprehensively evaluated the aerosol scheme specifically. Here we focus on changes in $PM_{2.5}$ components at the surface, and therefore evaluate simulated BC, OC, and SO_4 concentrations in the first vertical level. Since modeled concentrations are volume averages over large grid cells, they are expected to represent concentrations in remote locations that are more homogenous better than in urban areas. We therefore compare simulated concentrations to surface observations in remote locations from the Interagency Monitoring of Protected Visual Environments (IMPROVE; http://vista.cira.colostate.edu/improve/) network for the US and the European Monitoring and Evaluation Programme (EMEP; http://www.emep.int/) network for Europe. Surface

observations outside of the US and Europe are limited. We compare modeled BC and OC with observations at 15 locations in China (Zhang et al. 2008) and eight in India (Beegum et al. 2009) from 2006. Each of these monitoring networks reports elemental carbon (EC), which is measured by optical rather than thermal-optical techniques and may be between 30% and 100% of BC; since the emissions inventory is more representative of EC than BC, comparing modeled concentrations with EC is most appropriate (Vignati et al. 2010). For OC, we compare observations with simulated concentrations prior to conversion to OM, and include SOA. We compare SO_4 prior to mass conversion to ammonium sulfate. Although we simulate 2002 for our base case, for the model evaluation only, we ran the base case through 2003 to leverage additional observations from IMPROVE (available for both 2002 and 2003) and EMEP (available for July 2002-June 2003).

Compared with observations from IMPROVE (average 2002-2003) for the US (Figure 4.3 andFigure C.9), BC is generally simulated within a factor of two (inside the dashed lines), with some simulated concentrations higher than observations in the Northwest, California, and Northeast, and lower than observations in the South. Simulated OC is generally lower than observations, particularly in the Southeast, likely due to unrealistically low simulated SOA concentrations, consistent with previous studies using MOZART-4 (Dunlea et al. 2009; Emmons et al. 2010). However, simulated OC is higher than observations in the Northwest. Simulated SO_4 generally matches observations in the East, but is higher than observations in the West (Figure C.10). Compared with observations from EMEP in Europe (average July 2002 to July 2003), simulated BC concentrations are generally lower than observations, particularly in the

West (Figures 4.3 and C.9). As for IMPROVE, simulated OC is lower than observations in Europe (Figures 4.3 and C.9) and simulated SO_4 is higher than observations (Figure C.10). For the few observations available from China and India, simulated concentrations are within a factor of two of observations in remote locations, but are lower than observations in regional and urban locations (Figure C.11Figure C.12). Some of these discrepancies may be due to differences between volume averaged modeled concentrations in large grid cells and point measurements (Swall and Foley, 2009; Gilardoni et al. 2011), or the mismatch between 2006 measurements in Asia and 2002 simulated concentrations. Measurement methods may also cause overestimation of ambient EC concentrations (Novakov et al. 2005), with the reflectance method for IMPROVE potentially measuring higher EC concentrations than the transmittance method used by EMEP (Pope et al. 2006).

Simulated simple (population-weighted) regional average surface NO_3 concentrations range as high as 10.6 (30.6) $\mu g/m^3$ in EA and 6.3 (15.1) $\mu g/m^3$ in IN (Figure 4.2 and Table C.2). While a lack of global NO_3 measurements limits our ability to evaluate simulated concentrations, these concentrations are consistent with those simulated by other global CTMs (Park et al. 2004). Any biases in simulated NO_3 concentrations would not significantly affect our results, since NO_3 varies little among the BC emission scenarios.

4.2.3. Health impact function

We calculate avoided premature deaths in each grid cell using the change in simulated $PM_{2.5}$ concentration between the base case and the emission reduction scenario

and a health impact function (HIF). Global CTMs have been used previously to estimate mortality due to total anthropogenic air pollution (Anenberg et al. 2010), long-range transport of air pollution (Duncan et al. 2008; Anenberg et al. 2009; Liu et al. 2009a; West et al. 2009b), future changes in emissions (West et al. 2006; West et al. 2007; Selin et al. 2009), changes in one sector's emissions (Corbett et al. 2007; Barrett et al. 2010), fossil fuel and biofuel emissions (Jacobson 2010), and air pollution changes associated with carbon dioxide emissions (Jacobson 2008).

Here we use a log-linear relationship between long-term $PM_{2.5}$ exposure and relative risk (RR), following Anenberg et al. (2010). RR>1 indicates that $PM_{2.5}$ exposure increases risk of mortality. We use RR to calculate β, the concentration-response factor (CRF), and, as shown in Eq. (1), the attributable fraction (AF), the fraction of the disease burden attributable to the change in annual average $PM_{2.5}$ (ΔX). This HIF is applied in each grid cell by multiplying the AF by the baseline mortality rate (y_0) and exposed population (Pop), as shown in Eq. (2).

$$AF = (RR-1)/RR = 1 - \exp^{-\beta\Delta X} \quad (1)$$

$$\Delta Mort = y_0 (1 - \exp^{-\beta\Delta X}) Pop \quad (2)$$

Some evidence suggests that air pollution mixtures with high BC fractions, "black smoke," "diesel $PM_{2.5}$," and "traffic $PM_{2.5}$," have stronger associations with mortality than other mixtures (Cooke et al. 2007; Brunekreef 2009). Studies that use ambient BC concentrations as a marker for air pollution mixtures also find stronger associations with mortality than those using total $PM_{2.5}$ (Ostro et al. 2007; Ostro et al. 2008; Bell et al.

2009; Peng et al. 2009; Smith et al. 2009). These studies are subject to substantial exposure error since BC is very spatially heterogeneous, potentially resulting in risk underestimation (Smith et al. 2009; Bell et al. 2010). However, evidence for differential toxicity of BC and BC-containing mixtures remains inconclusive. We therefore assume that all mixtures of $PM_{2.5}$ are equally potent in causing premature mortality and use the change in total $PM_{2.5}$ in Eq. (2).

We calculate CRFs using estimates of RR of chronic mortality due to total $PM_{2.5}$ from Krewski et al. (2009), the latest reanalysis of the American Cancer Society $PM_{2.5}$ studies (e.g. Pope et al. 2002) and the largest among long-term $PM_{2.5}$ mortality studies (e.g. Laden et al. 2006). For a 10 $\mu g/m^3$ increase in $PM_{2.5}$, RR was 1.06 (95% CI, 1.04-1.08), 1.13 (95% CI, 1.10-1.16), and 1.14 (95% CI, 1.06-1.23) for total, cardiopulmonary, and lung cancer mortality in adults age 30+. These RRs were determined for the observed range of concentrations, 5.8-22.2 $\mu g/m^3$, and the linearity of the concentration-response relationship was also demonstrated up to 30 $\mu g/m^3$ based on 1979-1983 $PM_{2.5}$ data. Causes of death differ globally from those in the US, and we estimate cardiopulmonary and lung cancer mortality, as they are more comparable around the world than all-cause mortality. We assume these CRFs apply globally, despite differences in health status, lifestyle, age structure, and medical care among global populations.

We use baseline cardiopulmonary and lung cancer mortality rates from the World Health Organization (2004; 2008b), population from the LandScan database (Oak Ridge National Laboratory 2008) from 2006 (Figure C.13), and the fraction of the population age 30+ (World Health Organization 2004) to be consistent with Krewski et al. (2009), as described by Anenberg et al. (2010) (see Table C.3).

4.3. Results

4.3.1. Global emission reductions

Halving global anthropogenic BC emissions reduces the global annual average $PM_{2.5}$ concentration by 33 ng/m^3 (1.2%), ranging among regions from 43 ng/m^3 in NA to 453 ng/m^3 in EA (Table 4.1 and Figure 4.4). Population-weighted average $PM_{2.5}$ concentrations decrease by 542 ng/m^3 (1.8%) globally, ranging from 126 ng/m^3 in AF/ME to 1201 ng/m^3 in EA. Regional BC concentrations decrease 25-49%, with smaller percentage reductions in regions with frequent wildfires (e.g. SA, AF/ME, SE/AU; Figure 4.5a and Figure C.14). Wildfires are assumed to be natural and are therefore excluded from the emission reduction. We estimate that these $PM_{2.5}$ reductions would avoid ~157,000 (95% CI, 120,000-194,000) annual premature deaths worldwide (Table 4.1 and Figure 4.6). In all regions except NA which has a relatively high baseline lung cancer mortality rate, >90% of avoided deaths are from cardiopulmonary disease. Over 80% of global avoided deaths occur in EA, with 81,000 (95% CI, 61,000-100,000) avoided deaths, and IN, with 48,000 (95% CI, 37,000-59,000). These regions have large emissions and exposed populations, and IN also has high baseline cardiopulmonary mortality rates.

Estimated reductions in $PM_{2.5}$ concentrations are generally smaller than reductions in BC concentrations due to increased SO_4 production (Figure 4.5a). Aerosols affect gas-phase chemistry by absorbing or scattering radiation that drives photochemistry (He et al. 1999; Liao et al. 1999; Castro et al. 2001). Previous studies using regional models

(Jacobson 1998; Li et al. 2005) and global models (Martin et al. 2003), including using the aerosol scheme used in MOZART-4 specifically (Tie et al. 2005), find that high BC concentrations lead to reduced photolysis rates for O_3 and nitrogen dioxide and, therefore, reduced O_3 concentrations. Here, we find that reduced BC concentration increases photolysis and leads to increased concentrations of O_3, hydroxyl radical (OH), and hydrogen peroxide (H_2O_2), as shown in Figure C.15. As described by Tie et al. (2001), gas-phase production of SO_4 in MOZART-4 occurs via R1, while aqueous phase (in-cloud) production occurs via R2 and R3, where S(IV) is total dissolved sulfur (HSO_3 and SO_3).

$SO_2 + OH \rightarrow SO_4$ (R1)

$S(IV) + O_3 \rightarrow SO_4 + products$(R2)

$S(IV) + H_2O_2 \rightarrow SO_4 + products$ (R3)

Through these reactions, increased concentrations of OH, O_3, and H_2O_2 in response to BC emission reductions lead to enhanced SO_4 production. The resulting SO_4 increases are very small percentages of total $PM_{2.5}$ (up to 0.7% in EA; Figure C.14) but since SO_4 concentrations are much larger than BC concentrations, they can offset up to 28% (in EA) of regional BC reductions (Figure 4.5a). We include changes to all $PM_{2.5}$ species in our mortality calculation, but do not include O_3 increases.

Halving global anthropogenic BC and OC emissions together reduces BC concentrations by the same amount as halving BC emissions alone, but OM is also reduced (Figure 4.5b), such that annual average $PM_{2.5}$ reductions are larger by a factor of

four in NA to over eight in IN (Table 4.1). These $PM_{2.5}$ reductions are associated with ~8 times more annual avoided deaths than is estimated for halving BC alone (Table 4.1). Here, changes in radiation absorption by BC and scattering by OM, which can increase the pathlength of solar radiation and accelerate photochemistry (e.g. Dickerson et al. 1997), have opposing effects on gas-phase chemistry. We find increases in OH and O_3 concentrations but decreases in H_2O_2 concentrations, resulting in mixed effects on SO_4 (Figure C.16).

Estimated avoided deaths from halving anthropogenic BC and BC+OC are consistent with estimates by Anenberg et al. (2010) of the global burden of anthropogenic $PM_{2.5}$ on mortality (~3.7 million deaths) when multiplied by the fraction of $PM_{2.5}$ that is BC (9%, 300,000 deaths) and OM (46%, 1.7 million deaths) in that study. The global burden estimate is twice our estimated deaths from halving BC, but only 1.6 times those from halving OC (1.16 million from halving BC+OC minus 0.2 million from halving BC alone). While both studies use the MOZART model, we use here an updated version, MOZART-4, which includes aerosol chemistry and interactions with radiation. Our methodology also differs for BC and OC emissions, assumptions for converting OC to OM, and years of emissions and meteorology.

4.3.2. Regional BC emission reductions

We now examine the surface $PM_{2.5}$ and mortality impacts of halving anthropogenic emissions in eight world regions individually. EA contributes 32% of global anthropogenic BC emissions, more than double the contribution from any other region (Figure 4.1). AF/ME and IN follow, with 13% and 12%.

We find the greatest reductions in population-weighted $PM_{2.5}$ occur within the EA (1262 ng/m^3) and IN (733 ng/m^3) source regions, due to high emissions (Table 4.2). For all regions, the contribution of BC emissions from other regions to surface $PM_{2.5}$ concentrations is very small, although some transport occurs between FSU, AF/ME, and EU, which are close in proximity. For some regions, halving BC emissions leads to small increases in OH, O_3, and H_2O_2 in distant regions, which enhance SO_4 production where SO_2 emissions are high, such as in EA (Figure C.17Figure C.18). Since BC concentrations are not greatly impacted outside of the source region, small SO_4 increases in distant regions can lead to overall $PM_{2.5}$ increases (Table 4.2). For example, halving BC emissions in IN increases population-weighted average $PM_{2.5}$ by 20 ng/m^3 in EA. The limited influence of extra-regional BC emissions on regional surface $PM_{2.5}$ concentrations is consistent with other studies finding that BC comprises 0-3% of background surface aerosol concentrations (Liu et al. 2009b) and that foreign BC emissions contribute 0-5% of regional surface BC concentrations (TF HTAP 2010).

Halving BC emissions in EA avoids 85,000 (95% CI, 64,000-105,000) annual premature deaths globally, more than any other region, followed by IN with 47,000 (95% CI, 36,000-58,000). EA and IN contribute 53% and 31% to all avoided deaths from halving global BC emissions, 1.6 and 2.5 times greater than their contributions to global anthropogenic BC emissions, owing to large populations in both regions and high cardiopulmonary mortality rates in IN. The small SO_4 increases in distant regions resulting from some regional BC emission reductions have very little impact on mortality. To compare mortality impacts of BC emissions across regions, we calculate the mortality impacts per unit BC emissions reduced (Figure 4.7). Per unit emission, the

mortality impact of BC emissions is largest for IN (136 premature deaths avoided per Gg BC emitted), followed by EA (90). This is likely due to smaller per-unit impacts of within-region emission reductions on BC concentration for EA (Table 4.2) and higher baseline cardiopulmonary mortality rates in IN (Table C.3).

Halving NA emissions reduces $PM_{2.5}$ in that region by 151 ng/m^3 and avoids 4,000 (95% CI, 3,000-5,000) annual premature deaths (12 per Gg BC reduced), 91% of which occur within the US. Compared with halving BC emissions in the US only, halving all NA emissions causes avoided deaths in NA to increase by 12% and in the US by 1.6%, mostly in the Northeast and California near national borders (Figure C.19).

4.3.3. Sectoral BC emission reductions

We next examine the impacts of halving global BC emissions from each major economic sector individually. Globally, 93% of anthropogenic BC emissions are estimated to be from three sectors: residential (38%), industrial (includes non-road transportation; 29%), and transportation (on-road only; 26%) (Figure 4.1). Each sector's contribution to total anthropogenic BC emissions differs considerably by region, with transportation emissions estimated to contribute most in developed regions (55% in NA and 53% in EU), and the residential sector contributing most in developing regions (62% in IN and 56% in both AF/ME and FSU). In EA, 50% and 35% are from the industrial and residential sectors.

Globally, halving residential BC emissions impacts population-weighted average $PM_{2.5}$ and mortality most, with 250 ng/m^3 $PM_{2.5}$ reduced and 74,000 (95% CI, 57,000-91,000) annual avoided deaths (Table 4.3). Avoided deaths are likely underestimated for

the residential sector since we exclude changes in indoor exposure. The global mortality impacts of reducing industrial BC emissions are also large, while those from reducing transportation emissions are fewer. Halving residential, industrial, and transportation emissions contributes 46%, 35%, and 15% to the avoided deaths from halving all anthropogenic BC emissions. These contributions are 1.3, 1.2, and 0.6 times each sector's portion of global BC emissions, owing to the degree of co-location with population globally. As for BC emissions, the relative magnitude of each sector's impact differs substantially in developed versus developing regions. For example, in IN, residential, industrial, and transportation emissions contribute 66%, 18%, and 14% of the $PM_{2.5}$ decrease, while in NA these sectors contribute 15%, 19%, and 59%. Of the total avoided deaths from halving global anthropogenic BC emissions, 26% occur in EA from the industrial sector, and 20% occur in each of IN and EA from the residential sector. Impacts of residential BC emissions are underestimates since impacts due to indoor $PM_{2.5}$ exposure are excluded.

The mortality impact per unit BC emitted ("mitigation efficiency") in each region is similar regardless of the sector from which emissions were reduced (Figure 4.8) and follows the same pattern as for the regional reductions (Figure 4.7). The only exception is for the transportation sector in EA, for which reducing BC emissions has a smaller per unit impact on mortality relative to the residential and industrial sectors. While the industrial and residential sectors in EA have the greatest BC emissions ("mitigation potential"), all three sectors in IN have the greatest overall mitigation efficiency. Outside of IN and EA, mitigation efficiency is greatest for FSU, SE/AU, and EU, while

mitigation potential is greatest for the residential sector in AF/ME and the transportation sector in EU and NA.

4.4. Sensitivity analysis

For the results presented above, we assume that the CRFs estimated for the US apply globally, although simulated concentrations in some grid cells in Asia are higher than the range included in the ACS study (Table C.3). Current evidence does not support the existence of low or high thresholds beyond which changes in $PM_{2.5}$ concentration have no impact on mortality (Krewski et al. 2009). However, while no long-term epidemiology studies have examined the relationship between $PM_{2.5}$ concentration and mortality at higher concentrations, the marginal impact of $PM_{2.5}$ on mortality may be smaller at higher concentrations (Pope et al. 2009; Smith and Peel 2010). Without quantitative evidence describing the concentration-response relationship at a wide range of concentrations, we examine the effect of low and high health effect thresholds on estimated deaths.

For the case where BC emissions are halved globally, applying a high-concentration threshold of 50 $\mu g/m^3$ (an assumption consistent with previous studies, e.g. Cohen et al. 2004) reduces global avoided deaths by 56%, 99.6% of which occurs in EA and IN (Figure 4.9) where concentrations most frequently exceed the threshold, but the majority (60%) of estimated avoided deaths still occur in these regions. Applying a low-concentration threshold of 5.8 $\mu g/m^3$, the lowest measured level in Krewski et al. (2009), reduces global avoided deaths by 2.1%, 33% and 22% of which occur in AF/ME and SE/AU.

We also examine the effect of applying the significantly higher CRFs from the latest reanalaysis of the Harvard Six Cities cohort study (Laden et al. 2006) which found that for a 10 $\mu g/m^3$ increase in $PM_{2.5}$, RRs of cardiovascular and lung cancer mortality were 1.28 (95% CI, 1.13-1.44) and 1.27 (95% CI, 0.96-1.69). Consistent with the relative magnitudes of the RR estimates, using the RRs from Laden et al. (2006) increases estimated global avoided deaths by 45.1%, which is distributed around the world.

4.5. Uncertainties

While we quantify uncertainty for mortality impacts from statistical error in the CRF, we are unable to quantify several other important uncertainties. Uncertainty in global BC emission inventories is estimated to be about a factor of 2, and could be comparatively larger for the residential and industrial sectors in developing regions, where emissions are more difficult to estimate (Bond et al. 2004; 2007). Global anthropogenic BC emissions are also generally allocated to grid cells according to population, an assumption that may be more accurate for some regions and sectors than others. Simulated BC concentrations vary widely among global CTMs due to differing assumptions for emissions and parameterization of aerosol processes, such as aging and wet deposition (Koch et al. 2009; Vignati et al. 2010). These model variations may affect estimated mortality impacts more than uncertainty in the CRF, as has been shown for ozone (Anenberg et al. 2009). The coarse grid resolution of the global CTM also contributes to uncertainty, since it does not capture fine spatial gradients of concentrations, particularly around urban areas. As BC and a component of OM are directly emitted, this uncertainty may be particularly important for this study.

Several uncertainties are also associated with health impact function parameters. We assume that all $PM_{2.5}$ mixtures are equally toxic, despite substantial compositional variation around the world and some evidence suggesting that BC-containing mixtures may be more toxic than the average. Additional research is needed to identify differential toxicity of air pollutant mixtures (e.g. Smith et al. 2009; Dominici et al. 2010; Vedal and Kaufman 2011). We also assume that CRFs found in the US apply globally, despite differences in concentration levels, populations, lifestyle, age structure, and medical care. This assumption is supported by evidence suggesting that $PM_{2.5}$-mortality associations are similar among different sub-populations in the US (Pope et al. 2009), though different sub-populations around the world likely have larger differences than those in the US, and by similar findings among short-term $PM_{2.5}$ mortality studies around the world (Health Effects Institute 2010; Atkinson et al. 2011). We emphasize cause-specific mortality which may be more comparable around the world than all-cause mortality, but may result in underestimates of the total mortality impacts since other causes of death are likely also associated with $PM_{2.5}$.

4.6. Conclusions

We have estimated the impacts of global, regional, and sectoral BC emission reductions on surface air quality and human mortality using a global chemical transport model (CTM) to simulate $PM_{2.5}$ concentrations and a health impact function to calculate mortality changes. We find that halving global anthropogenic BC emissions would reduce global population-weighted average $PM_{2.5}$ by 542 ng/m^3 (1.8%) and avoid 157,000 (95% confidence interval, 120,000-194,000) annual premature deaths

worldwide, corresponding to 4% of $PM_{2.5}$-related deaths (Anenberg et al. 2010) and 0.3% of all deaths. Since the chemical and physical processes governing BC concentrations in MOZART-4 and our health impact function are approximately linear, these results can be scaled to estimate the surface air quality and health impacts of larger or smaller changes in BC emissions. We exclude the likely substantial morbidity benefits of reducing BC due to lack of data on baseline morbidity rates. Morbidity impacts may not be directly proportional to mortality impacts because of differences in hospitalization rates and medical care around the world.

The vast majority of surface $PM_{2.5}$ and health benefits from BC emission reductions occur within the source region. Some inter-regional transport occurs between FSU, AF/ME, and EU, which are close in proximity. Regional definitions used here are very broad, encompassing many countries, which obscures smaller-scale transport of pollution across political boundaries. While most of the avoided deaths from halving global anthropogenic BC can be achieved by halving EA emissions (54%), followed by IN emissions (31%), IN emissions have 50% greater mortality impacts per unit BC emitted than EA emissions.

Globally, the contribution of residential, industrial, and transportation BC emissions to $PM_{2.5}$-related mortality is 1.3, 1.2, and 0.6 times each sector's contribution to anthropogenic BC emissions, owing to the degree of co-location between that sector's emissions and global population. Within each region, mortality per unit emission varies little by source sector; however, impacts of residential BC emissions are underestimates since impacts due to indoor $PM_{2.5}$ exposure are excluded. In addition, the coarse grid resolution used here does not capture the spatial scale at which actual exposure to

emissions from these sectors occurs (e.g. near roadways for the transportation sector). These results should be further studied at finer resolutions to better simulate actual exposure.

We find that reducing BC emissions increases regional SO_4 concentrations up to 28% of regional BC concentration reductions due to reduced absorption of radiation that drives photochemistry. The SO_4 increase lessens the health benefits of BC reductions, which are calculated based on total $PM_{2.5}$ concentrations, but may enhance the climate benefit since SO_4 scatters radiation. We estimate ~8 times more avoided deaths when BC and OC emissions are halved together, suggesting that these results greatly underestimate the full air pollution-related mortality benefits of BC mitigation. Several studies have examined the net climate impacts of the total emission mixture from individual economic sectors, finding that for some sectors, cooling agents such as SO_4 and OM offset the warming impacts of BC (e.g. Koch et al. 2007; Unger et al. 2010). Since no pollutant is beneficial for health, future studies should assess the health impacts of individual economic sectors and mitigation measures, accounting for the full mixture of emissions and both outdoor and indoor exposure. Confidence in our results would also be strengthened by reducing uncertainties from emissions, model parameterization of aerosol processes, grid resolution, and $PM_{2.5}$ concentration-mortality relationships over a range of concentrations, component mixtures, and populations.

4.7. Tables and figures

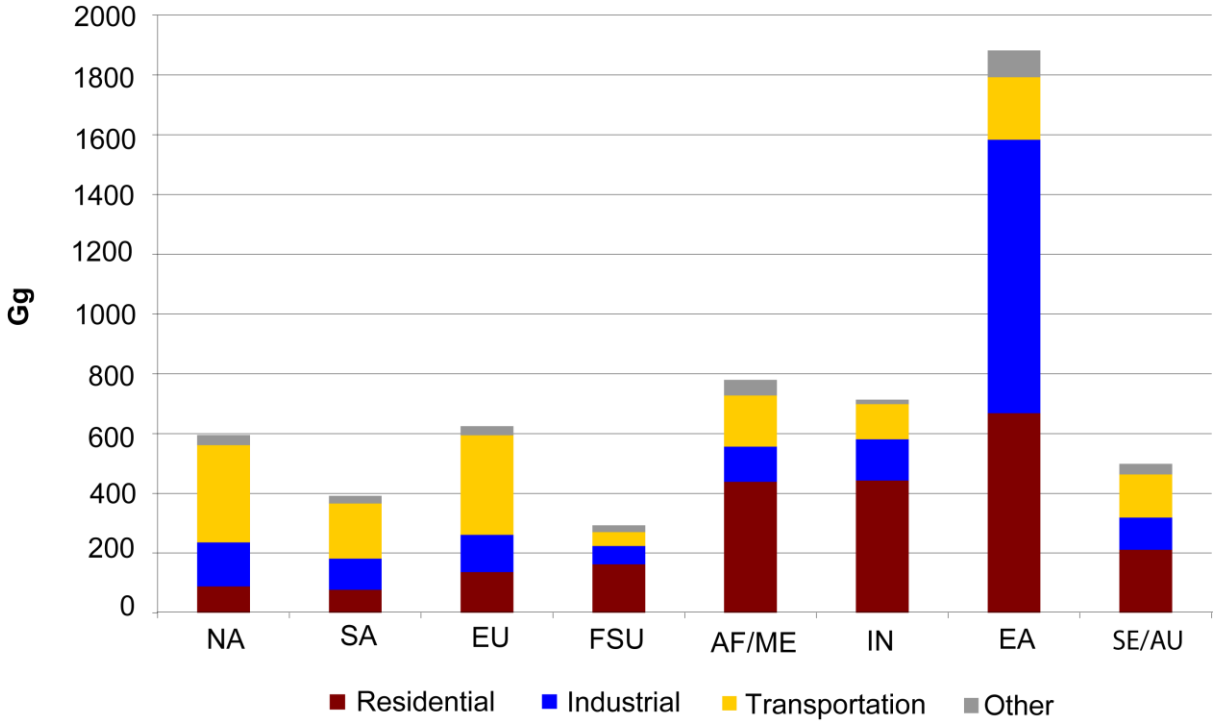

Figure 4.1. Anthropogenic BC emissions by region and sector after the IPCC emissions are scaled by 1.15 to account for particles larger than 1 µm in diameter.

Table 4.1. Simple and population-weighted annual average $PM_{2.5}$ (ng/m^3) concentrations for the base case and $PM_{2.5}$ reduction, avoided cardiopulmonary and lung cancer deaths (in thousands), and percent of these deaths from cardiopulmonary disease due to halving global anthropogenic BC emissions and BC+OC emissions. Confidence intervals (95%, in parentheses) reflect uncertainty in the CRF only.

	Base Case $PM_{2.5}$ Concentration ($\mu g/m^3$)		Global 50% BC Reduction				Global 50% BC+OC Reduction			
Receptor region	Simple Average	Population -weighted Average	Simple Average $\Delta PM_{2.5}$ (ng/m^3)	Population -weighted $\Delta PM_{2.5}$ (ng/m^3)	Avoided Deaths (x1000)	% CP	Simple Average $\Delta PM_{2.5}$ (ng/m^3)	Population -weighted $\Delta PM_{2.5}$ (ng/m^3)	Avoided Deaths (x1000)	% CP
North America (NA)	3.54	8.28	43	150	4 (3 - 5)	87.3	151	655	14 (11 - 18)	87.8
South America (SA)	3.84	6.02	44	130	1 (1 - 2)	94.9	218	735	8 (6 - 9)	95.1
Europe (EU)	9.77	13.4	147	230	8 (6 - 10)	91.1	772	1116	41 (31 - 51)	92.1
Former Soviet Union (FSU)	5.87	12.29	60	177	5 (4 - 6)	96.1	466	1582	45 (34-55)	96.1
Africa/ Middle East	5.32	7.21	64	126	5 (4 - 6)	97.4	454	941	36 (28-43)	97.5

(AF/ME)	19.28	36.29	420	732	48 (37-59)	96.7	3533	6409	399 (312-482)	96.7
South Asia (India; IN)										
East Asia (China; EA)	27.98	70.17	453	1201	81 (61-100)	92.8	3483	9938	622 (480-755)	93.0
Southeast Asia/ Australia (SE/AU)	4.81	9.55	54	247	6 (4 - 7)	94.2	361	1713	40 (31 - 49)	94.3
World	2.75	29.7	33	542	157 (120-194)	94.1	221	4379	1205 (932-1463)	94.4

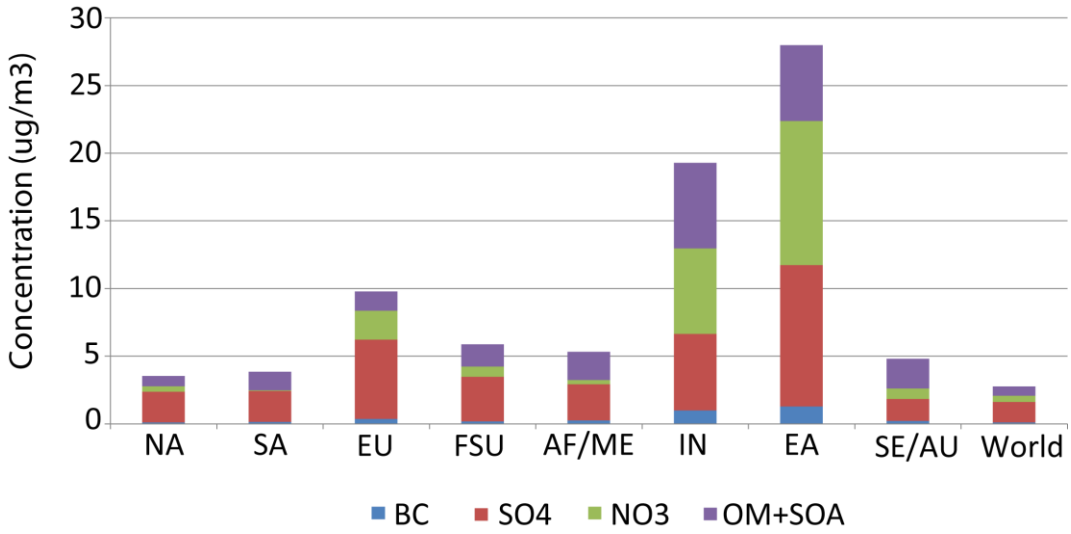

Figure 4.2. Simulated annual average concentration (µg/m^3) of $PM_{2.5}$ components for the base case (2002) by geographic region.

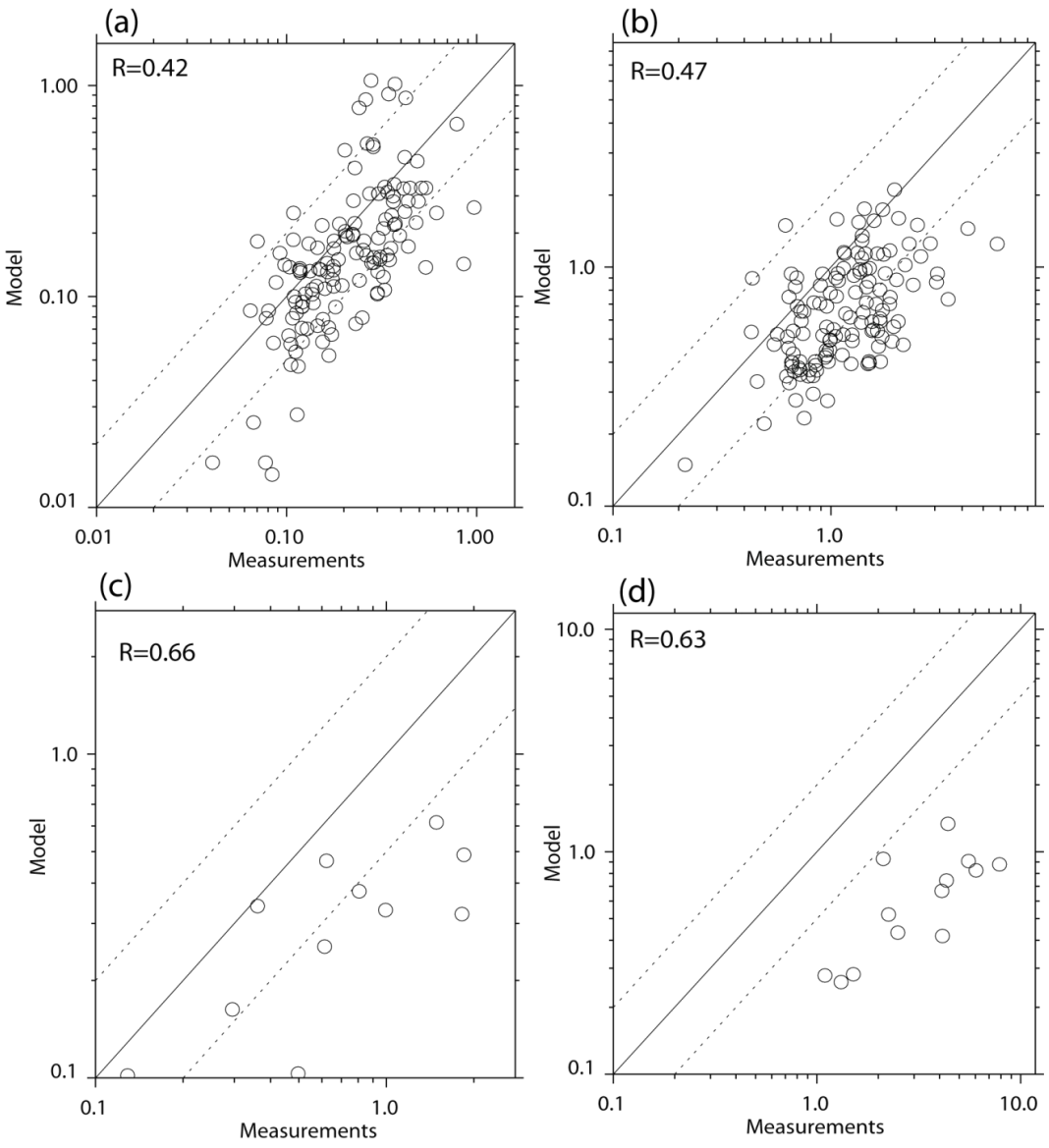

Figure 4.3. Comparison of simulated annual average surface BC and OC concentrations ($\mu g/m^3$) with the IMPROVE surface monitoring network for remote locations in the United States (average of 2002 and 2003) for a) BC and b) OC (includes SOA), and with the EMEP surface monitoring network for Europe (average for July 2002 to June 2003) for c) BC and d) OC (includes SOA).

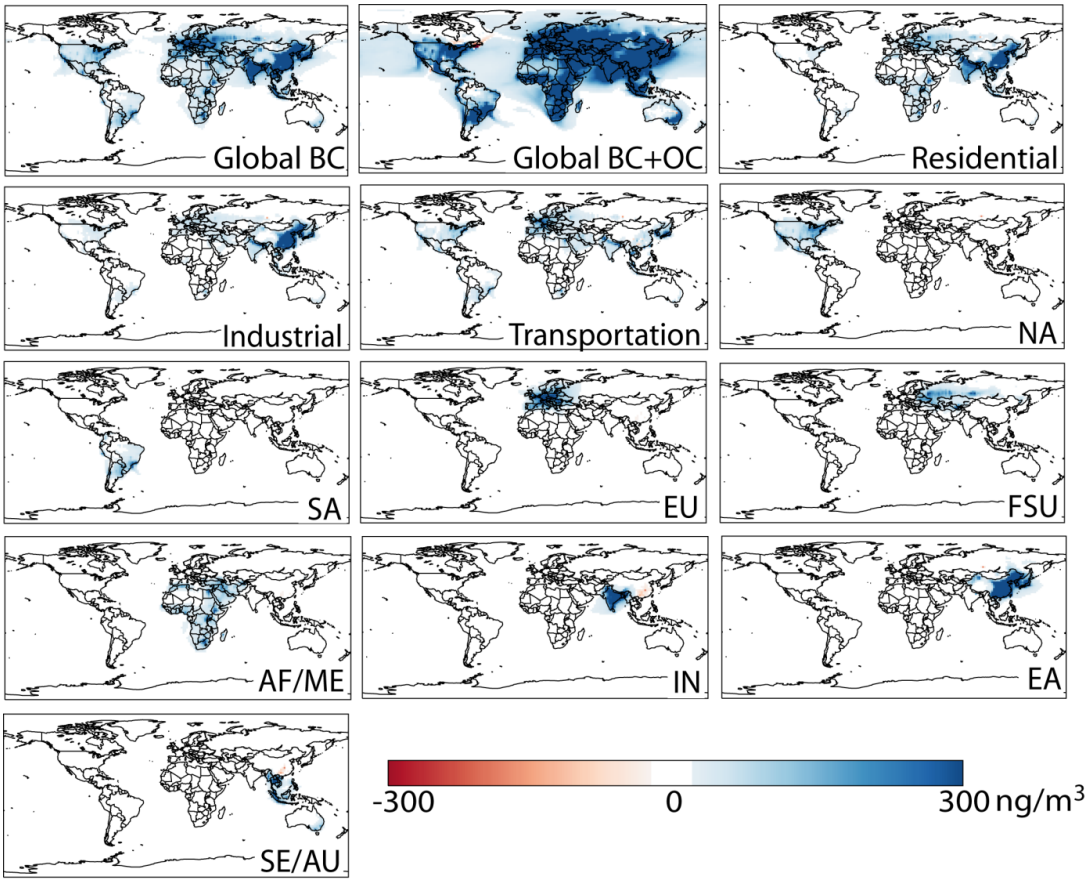

Figure 4.4. Reduction in annual average surface $PM_{2.5}$ concentration (ng/m^3) for the global, sectoral, and regional emission reductions relative to the base case.

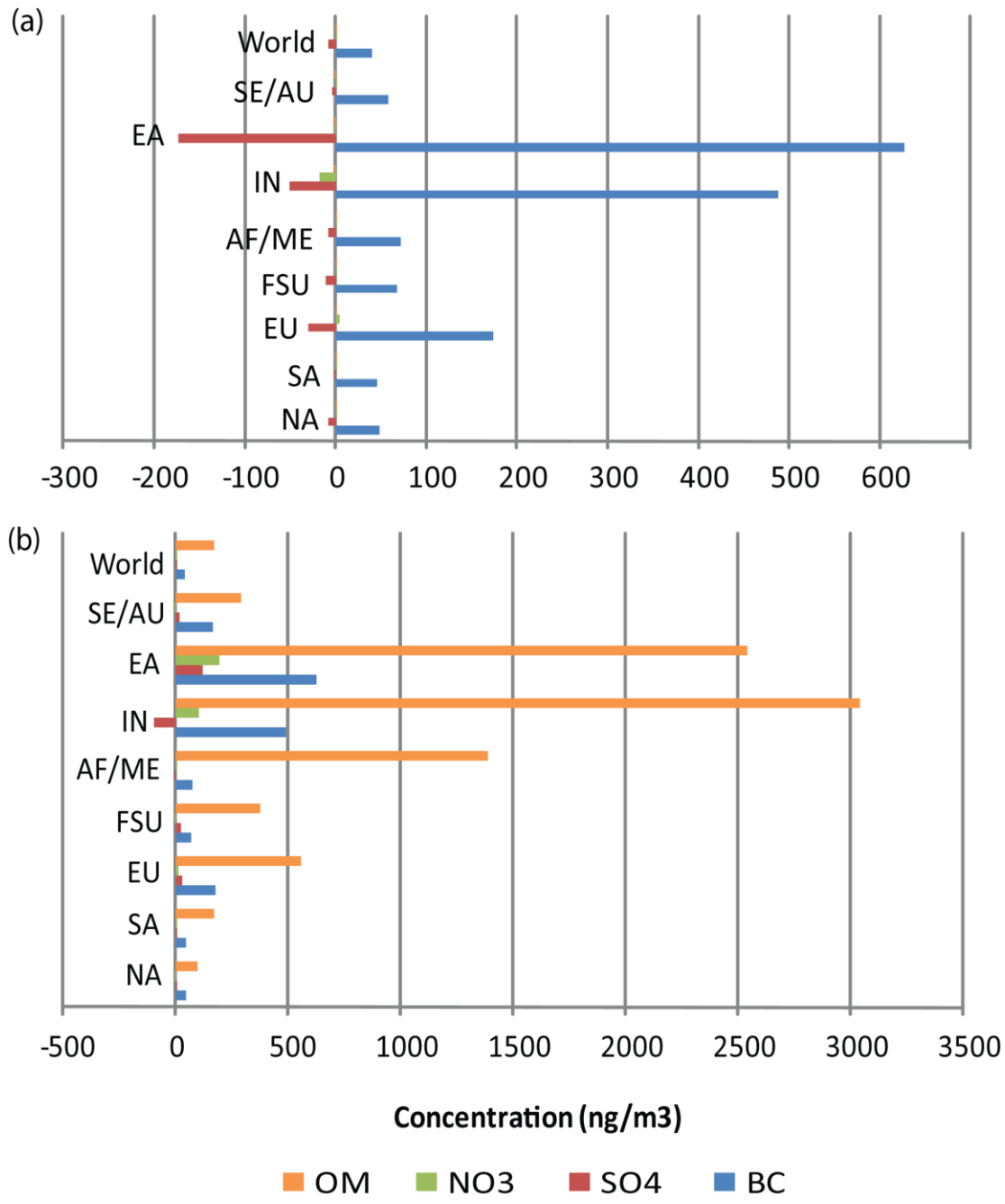

Figure 4.5. Reduction in global and regional annual average concentrations (ng/m^3) of $PM_{2.5}$ species for halving global anthropogenic (a) BC emissions and (b) BC+OC emissions, relative to the base case.

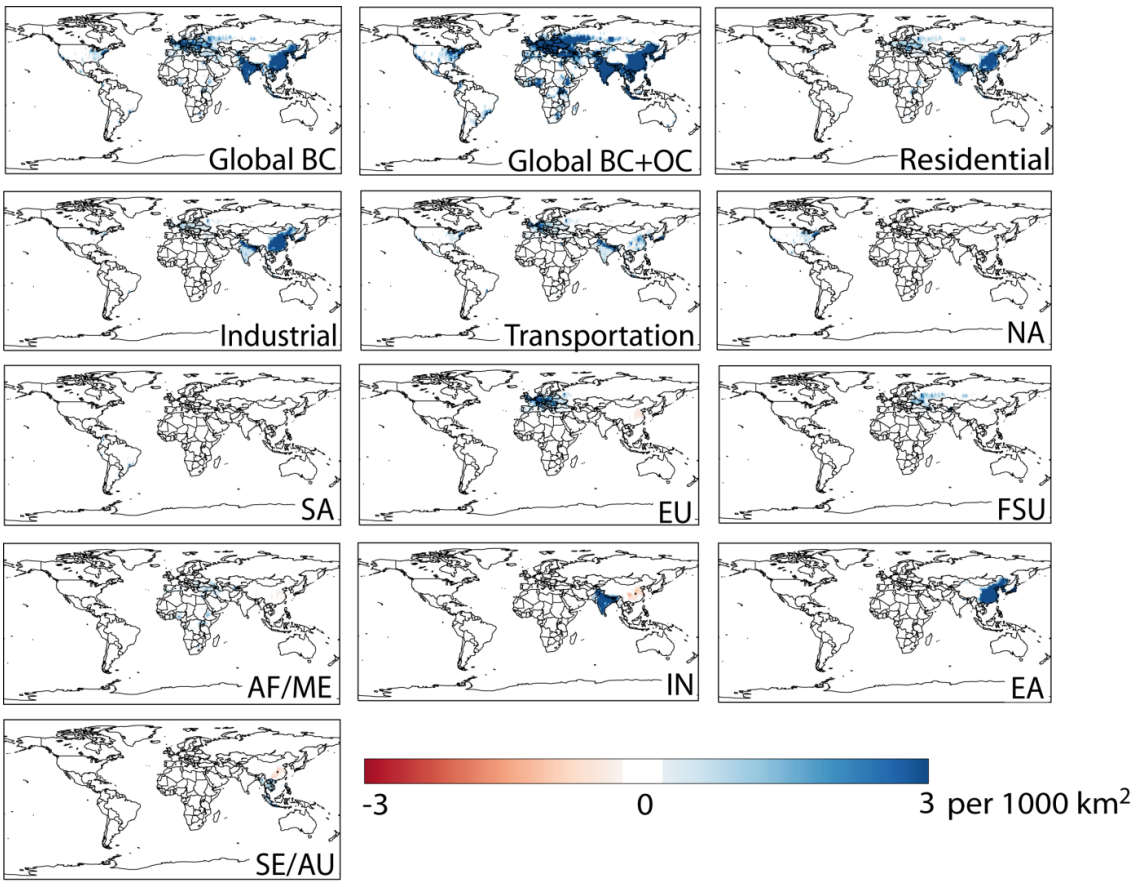

Figure 4.6. Avoided annual cardiopulmonary and lung cancer deaths per 1000 km^2, for the global, sectoral, and regional emission reductions relative to the base case.

Table 4.2. Reduction in population-weighted average $PM_{2.5}$ concentration (first row for each receptor region, ng/m^3) and annual avoided premature cardiopulmonary and lung cancer deaths (second row, thousands) in each receptor region after halving anthropogenic BC emissions in each source region. Confidence intervals (95%, in parentheses) reflect uncertainty in the CRF only.

	Source Region							
Receptor Region	NA	SA	EU	FSU	AF/ME	IN	EA	SE/AU
NA	151	-1	-1	-1	-1	-1	-2	-1
	4 (3 - 5)	0	0	0	0	0	0	0
SA	0	129	0	0	0	0	0	0
	0	1 (1 - 2)	0	0	0	0	0	0
EU	0	0	225	5	9	-1	-3	10
	0	0	8 (6 - 10)	0	0	0	0	0
FSU	-1	0	39	135	23	-1	1	0
	0	0	1 (1 - 1)	4 (3 - 5)	0	0	0	0
AF/ME	0	0	7	5	116	1	0	0
	0	0	0	0	4 (3 - 5)	0	0	0
IN	-1	-1	-1	-1	0	733	4	0
	0	0	0	0	0	49 (37 - 59)	0	0
EA	-4	0	-9	-3	-6	-20	1262	-9
	0	0	-1 (-1 - -1)	0	-1 (0 - -1)	-2 (-1 - -2)	85 (64 - 105)	-1 (-1 - -1)
SE/AU	0	0	0	0	1	8	9	230
	0	0	0	0	0	0	0	5 (4 - 7)

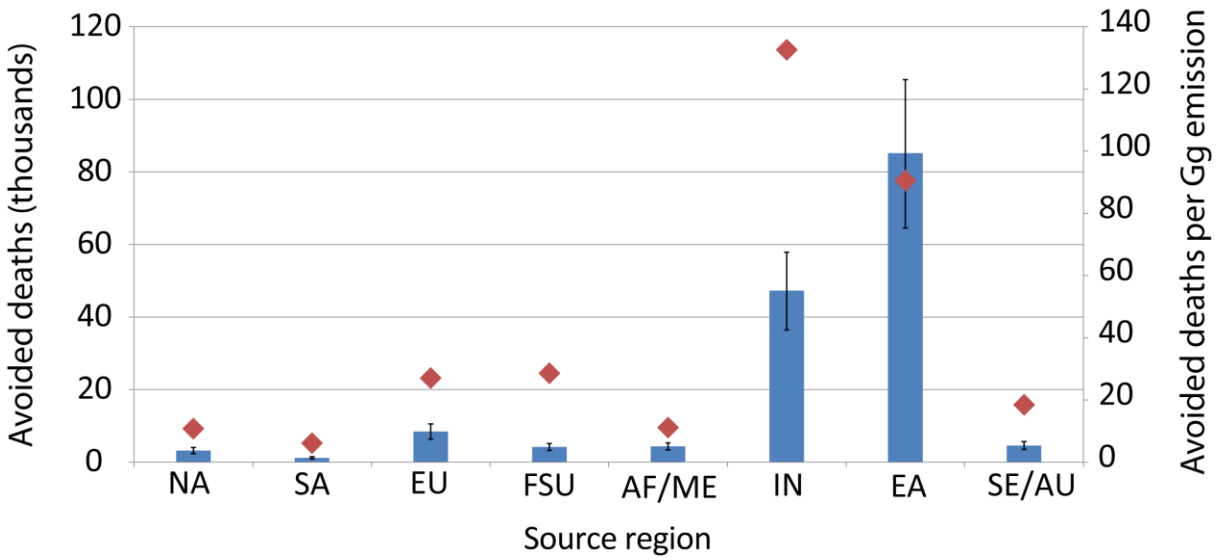

Figure 4.7. Global annual avoided premature deaths (thousands; blue bars) and avoided premature cardiopulmonary and lung cancer deaths per Gg BC emissions reduced (red diamonds), for halving anthropogenic BC emissions in each source region relative to the base case. Confidence intervals (95%) reflect uncertainty in the CRF only.

Table 4.3. Population-weighted reduction in annual average $PM_{2.5}$ (ng/m^3) and annual avoided premature cardiopulmonary and lung cancer deaths (in thousands) for halving global BC emissions from each sector, relative to the base case. Confidence intervals (95%, in parentheses) reflect uncertainty in the CRF only.

	Residential		Industrial		Transportation	
Receptor region	Population-weighted $\Delta PM_{2.5}$ (ng/m^3)	Avoided deaths x1000	Population-weighted $\Delta PM_{2.5}$ (ng/m^3)	Avoided deaths x1000	Population-weighted $\Delta PM_{2.5}$ (ng/m^3)	Avoided deaths x1000
NA	22	1 (0 - 1)	29	1 (1 - 1)	88	2 (2 - 3)
SA	28	0 (0 - 0)	30	0 (0 - 0)	65	1 (0 - 1)
EU	50	2 (1 - 2)	42	1 (1 - 2)	124	4 (3 - 5)
FSU	99	3 (2 - 3)	32	1 (1 - 1)	33	1 (1 - 1)
AF/ME	65	2 (2 - 3)	21	1 (1 - 1)	31	1 (1 - 1)
IN	480	32 (25 - 39)	135	9 (7 - 11)	105	7 (5 - 9)
EA	461	32 (24 - 39)	602	41 (31 - 50)	89	5 (4 - 7)
SE/AU	115	3 (2 - 3)	50	1 (1 - 1)	71	2 (1 - 2)
World	250	74 (57 - 91)	191	55 (42 - 68)	80	23 (17 - 28)

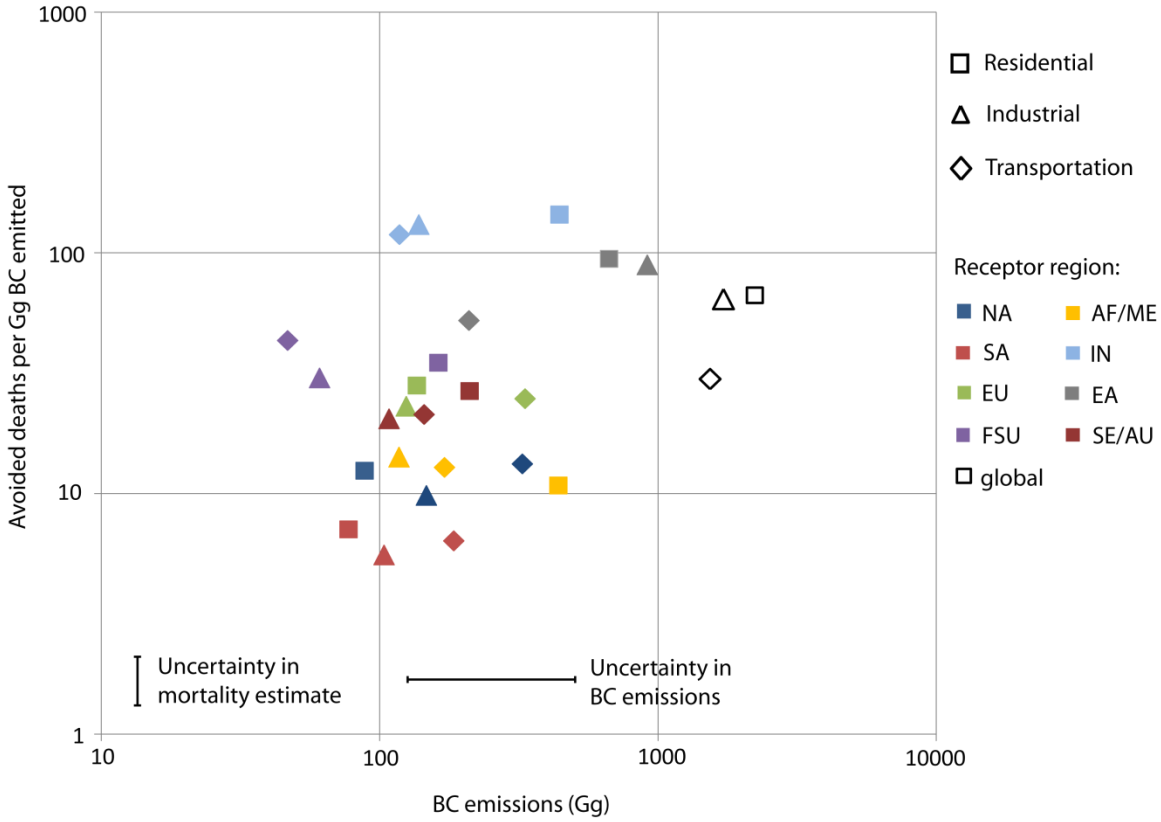

Figure 4.8. Annual avoided premature cardiopulmonary and lung cancer deaths per unit BC emissions reduced vs. total BC emissions (Gg) for particular source sectors within each region. Avoided deaths are estimated in the three simulations where global emissions in each sector are halved, and shown for each receptor region; these deaths are compared with emissions from each region, assuming that deaths from inter-regional transport are negligible (Table 4.2). Uncertainty in the mortality estimates is a factor of 0.23 from the central estimate, which includes uncertainties in the cardiopulmonary and lung cancer CRFs only. Uncertainty in BC emissions is assumed to be a factor of 2 from the central estimate (Bond et al. 2004; 2007). Since these uncertainties are factor differences from the central estimate, they are identical for each data point.

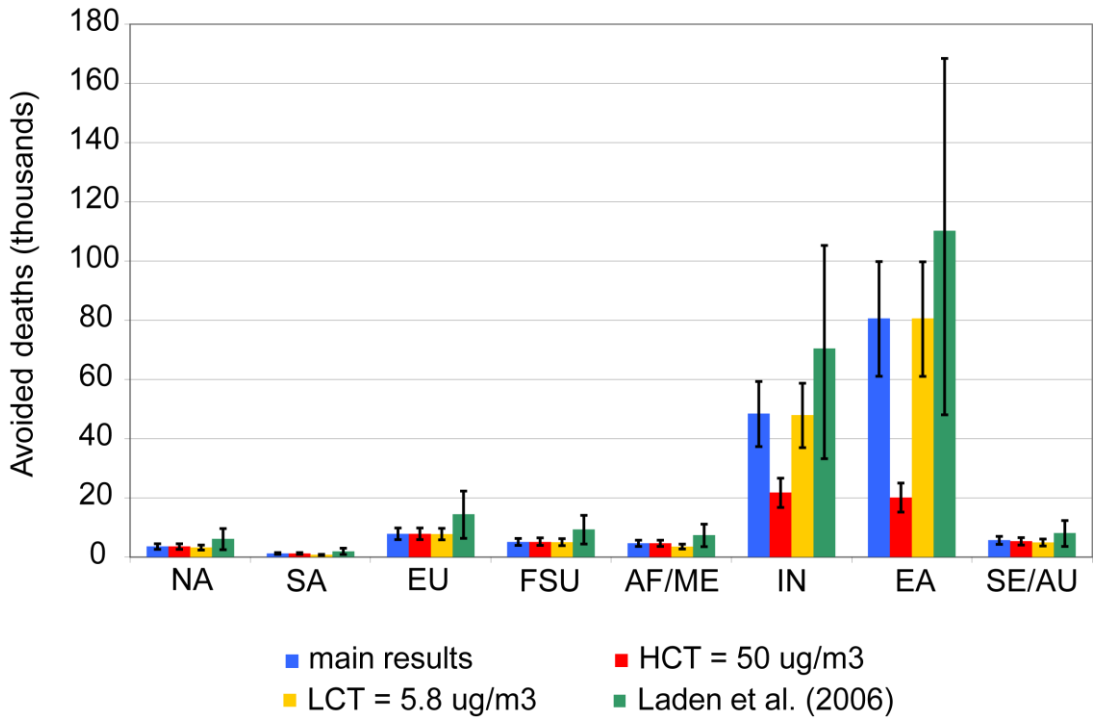

Figure 4.9. Sensitivity of estimated avoided annual premature cardiopulmonary and lung cancer deaths from halving global anthropogenic BC emissions to a high concentration threshold (HCT) of 50 µg/m^3, a low-concentration threshold (LCT) of 30 µg/m^3, and relative risk estimates from Laden et al. (2006; cardiovascular and lung cancer mortality only). Confidence intervals (95%) reflect uncertainty in the CRF only.

Chapter 5. Concluding remarks

Air pollution has historically been considered a local problem and has thus been regulated mainly on the national scale. In some developed regions, health-based regulations such as the National Ambient Air Quality Standards (NAAQS) in the US have led to drastic declines in air pollution concentrations in the past few decades, even as economic development and industrial production expanded (US EPA 2008b). These improvements are associated with substantial public health benefits that continue to accrue as downward emission trends persist (Hubbell et al. 2004; Fann and Risley, 2011). However, many areas within the US remain in nonattainment for O_3 and $PM_{2.5}$ (US EPA 2008b), and evidence suggests that these pollutants affect health at levels below current standards (e.g. Jerrett et al. 2009; Krewski et al. 2009; Kim et al. 2011). In addition, emissions are rising dramatically in some countries, particularly in developing regions, due to rapid population growth and economic development coupled with the absence of serious mitigation measures (Lamarque et al. 2010; TF HTAP 2010). The proximity of these rising emissions with the greatest population centers of the world results in millions of people worldwide exposed to air pollution concentrations significantly higher than US and European standards (e.g. Health Effects Institute 2010).

This dissertation addresses several aspects of the global health impacts of air pollution, using global CTMs to simulate O_3 and $PM_{2.5}$ concentrations and epidemiologically-derived concentration-response relationships to calculate health impacts. Three case studies on the mortality impacts of all anthropogenic O_3 and $PM_{2.5}$

(Chapter 2; Anenberg et al. 2010), intercontinental O_3 transport (Chapter 3; Anenberg et al. 2009), and BC emission reductions (Chapter 4; Anenberg et al. in prep.) demonstrate that air pollution remains a substantial problem for global public health with far-reaching impacts due to long-range transport and interactions with climate. This chapter considers the key findings from Chapters 2-4 and their implications, as well as future research needed to address several critical knowledge gaps and uncertainties.

5.1. Key findings and implications

5.1.1. Global public health burden

Air pollution remains a serious public health problem globally. O_3 and $PM_{2.5}$ concentrations have been declining in developed regions as a result of regulation, but still likely cause widespread health effects, while air pollution is becoming worse in most developing nations. In 2004, the World Health Organization (WHO) estimated that urban $PM_{2.5}$ causes 800,000 annual premature deaths worldwide (Cohen et al. 2004). This was considered an underestimate, as it was based on globally sparse surface concentration measurements in urban areas only and excluded ozone impacts. Chapter 2 demonstrated that using a global CTM to simulate concentrations, including both $PM_{2.5}$ and O_3 in both urban and rural areas, yields an estimated 3.7 million annual premature deaths due to total anthropogenic $PM_{2.5}$ and 700,000 due to O_3, much larger than was previously estimated by Cohen et al (2004). Results were about 50% larger using the same assumptions for concentration-response function and health effect thresholds, mainly due to two competing differences in methods. While using a global CTM includes the total global

population, suggesting larger estimates, the coarse grid resolution may suppress high urban $PM_{2.5}$ concentrations and, therefore, estimated $PM_{2.5}$ mortalities. The unique advantages of both observed and simulated concentrations should be leveraged in future studies to include the total population and exposure estimates at finer resolutions. The Global Burden of Disease 2010 project (www.globalburden.org), expected to be completed in 2011, will address this goal by using global CTMs in conjunction with surface and satellite measurements to estimate the global burden of outdoor air pollution on mortality.

Each of the case studies examined here demonstrate that air pollution health impacts are driven not just by concentration, but also by population exposure and demographics. For example, over 80% of the global air pollution-related deaths estimated in Chapter 2 occur in Asia, where population and concentrations are high, in addition to high baseline mortality rates in some areas. Chapter 4 also found that compared with the transportation sector, BC emissions from the global residential and industrial sectors disproportionately impact health since they are predominantly located in highly populated areas of the world. As modernization of medicine and healthcare in developing economies shifts major causes of death from infectious disease to chronic and degenerative diseases that are more affected by air pollution (e.g. cardiovascular disease, respiratory disease, and lung cancer) (Murray et al. 1997), the global burden of outdoor air pollution on mortality may rise in the future unless significant mitigation measures are enacted. Some evidence also shows that temperature and air pollution may synergistically affect health (Ren et al. 2008; 2009), suggesting that future climate change may increase vulnerability to air pollution. Additional research is needed to estimate how

the burden of outdoor air pollution on global mortality is expected to change in the future, taking shifting demographics and climate into account.

5.1.2. Impacts on local and hemispheric scales

Aair pollution-related deaths result from exposure to both local air pollution and air pollution transported from foreign sources. The atmospheric lifetime of $PM_{2.5}$ (days to weeks) is shorter than that of O_3 (weeks to months), and thus generally impacts concentrations and populations closer to the emission source. Chapter 2 demonstrated that $PM_{2.5}$ is the dominant contributor to the global burden of outdoor air pollution on premature mortality, suggesting that local emission controls are essential for mitigating air pollution-related mortality. Chapter 4 also showed that per unit emission, reducing BC emissions from some world regions and economic sectors achieves greater health benefits than reducing emissions from others, due to atmospheric processes governing transport and lifetime, as well as co-location with susceptible populations. Therefore, designing these local mitigation policies must consider local emission and exposure patterns which may differ by region.

However, Chapter 3 demonstrated that regional reductions of O_3 precursor emissions affect health all around the world, even in areas far from the source region. Emission reductions in North America and Europe were estimated to avoid more premature deaths in other parts of the world than locally, due to large exposed populations in the receptor regions. Of the avoided deaths from reducing emissions in North America, Europe, South Asia, and East Asia combined, foreign emission reductions contribute 30% in both North America, due to transported concentrations that

are large relative to concentrations from local emissions, and East Asia, due to large local populations exposed to smaller concentrations transported from other regions. In Europe, foreign emission reductions contribute over 50% of resulting avoided deaths, largely due to the influence of North American emissions. These results suggest that while local air pollution control is a critical component of efforts to prevent air pollution-related premature mortality, international cooperation in mitigation may be needed to address air pollution transported across political, and even continental, boundaries, as has been suggested elsewhere (Holloway et al. 2003; Keating et al. 2004; Global Atmospheric Pollution Forum 2010; TF HTAP 2010). In addition, cost-benefit analyses for domestic air pollution policies such as those conducted routinely by the US EPA and European Commission are likely to underestimate the total health benefits by not accounting for benefits internationally (West et al. 2009b).

5.1.3. Interactions with climate

Air pollution also interacts with climate, suggesting that limiting impact assessments to air pollution-related health impacts in a particular region excludes other important impact pathways occurring on both regional and global scales. First, warming temperatures are expected to exacerbate air pollution through increased biogenic emissions, photochemical reaction rates, and more frequent air inversions (e.g. Bloomer et al. 2009; Jacob et al. 2009). In addition, some pollutants traditionally regulated for their impacts on health, such as O_3 and black carbon, affect climate by directly absorbing or reflecting solar and infrared radiation, indirectly impacting cloud lifetime and reflectivity, and reducing snow and ice albedo (e.g. Horvath 1993, Hansen and

Nazarenko 2004, Koch and Del Genio 2010). Finally, greenhouse gases and air pollutions are often emitted by the same sources; therefore, actions aimed at mitigating either climate change or air pollution will likely also impact the other (e.g. West et al. 2004; Reynolds and Kandlikar 2008; Bollen et al. 2010; Haines et al. 2010; Nemet et al. 2010). These case studies demonstrate that substantial benefits for global public health can be achieved by mitigating O_3 (Chapter 3), methane (Chapter 3), and black carbon (Chapter 4), all of which are important climate warmers. Controlling these short-lived climate warmers in the atmosphere may therefore achieve co-benefits for both health and climate (Hansen et al. 2000; Jacobson 2002; Bond and Sun 2005; West et al. 2006; Ramanathan and Carmichael 2008; Molina et al. 2009; Kopp and Mauzerall 2010).

Considering air pollution in a global context may allow identification of strategies that benefit both climate and air pollution simultaneously ("win-win") or those that achieve benefits for one without worsening the other ("win-no-lose"). Several integrated assessments that estimate the multiple benefits of air pollution mitigation on climate, health, agriculture, and ecosystems are currently underway. These analyses focus on the integrated benefits of widespread international adoption of tighter on-road vehicle emissions standards, such as those currently in place in Europe (Shindell et al. in prep), and the benefits of mitigating short-lived climate forcers such as BC, O_3, and methane (UNEP in prep). Such integrated assessments should be increasingly used to inform policy decisions aimed at achieving both health and climate benefits.

5.1.4. Global health impact assessment methodology

Given the far-reaching impacts of air pollution on health, global health impact assessment is a useful tool to inform international policy decisions related to air pollution and climate change. However, the methodology is complicated by data limitations and requires many assumptions and extrapolations of data from the US and Europe to the rest of the world. Here, we improve upon the methodology used in the previous literature by refining the demographic information used as inputs into the health impact function. Specifically, country-specific baseline mortality rates are used in place of broad regional averages. In addition, area-weighted average baseline mortality rates are used where gridcells overlapped multiple countries. Finally, this work focuses on cause-specific mortality which is likely to be more comparable globally than all-cause mortality, since major causes of death vary dramatically around the world.

Despite these improvements, several critical knowledge gaps and uncertainties should be addressed to advance the quality of this methodology. Figure 5.1 shows the cascade of uncertainties that permeates these case studies, as well as other global health impact assessments in the literature. While these uncertainties should compound to produce a wide uncertainty range on the final health impact estimate, many of these uncertainties have not yet been studied extensively and are thus very difficult to quantify. The outcome is that these major uncertainties are discussed qualitatively and are left out of the quantitative uncertainty bounds around the mortality estimate. Most global health impact assessments therefore include uncertainty only from the error in the relative risk estimate produced by the epidemiology studies, which gives a false illusion of precision.

This work showed that the choice of the concentration-response function, in terms of magnitude, functional shape, and assumptions for the existence of health effect thresholds, substantially impacts mortality estimates. For $PM_{2.5}$, relative risk estimates from the latest American Cancer Society study (Krewski et al. 2009) were applied and linearly extrapolated to high concentrations in both Chapters 2 and 4. However, in both cases, examining the effect of using the Harvard Six Cities Study relative risk estimates (Laden et al. 2006) and health effect thresholds showed that mortality estimates were sensitive to these choices, often changing by >50% of the estimated value under different assumptions. Applying a log concentration-response function as has been suggested (Pope et al. 2009; Smith and Peel 2010) would also have a significant impact on estimated deaths, as evidenced by the substantial impact of high-concentration thresholds. For O_3, we estimate short-term mortality in Chapter 3 but long-term mortality in Chapter 2. The body of evidence for short-term O_3 mortality is much larger than that for long-term mortality, but toxicology and controlled human exposure studies demonstrate biological plausibility for a long-term effect on respiratory mortality (National Academy of Sciences 2008). Using long-term relative risk estimates for O_3 yields mortality estimates that are about a factor of 2 higher than is estimated using short-term relative risk estimates (Anenberg et al. 2011). Assumptions for concentration-response functions are thus critical choices in global health impact assessment.

In addition, while simulating exposure estimates with global CTMs allows full spatial coverage and examination of the impacts of hypothetical emission changes, surface concentrations simulated by CTMs remain uncertain. Neither global CTMs nor their inputs such as emissions were developed for the purpose of producing human

exposure estimates, and disagreements remain between simulated surface concentrations and observations, as well as among different CTMs (e.g. Fiore et al. 2009, Koch et al. 2009). Major advancements in global CTMs have improved their quality in simulating concentrations that match observations. However, current methods to evaluate simulated surface concentrations (as performed in Chapters 2 and 4) compare the simulated volume average of very large gridcells to measurements taken at specific points in space and time by surface monitors. Such comparisons provide a reasonable ballpark evaluation, especially when measurements taken in remote locations are used, but future studies should increasingly supplement point measurements taken at the surface with data from other observational sources, such as satellite observations which can be used to infer surface concentrations (van Donkelaar et al. 2010).

Multi-model ensembles may remove potential biases introduced by individual models, increasing the confidence in simulated concentrations. The multi-model ensemble analysis of long-range transport of O_3 in Chapter 3 demonstrated that the models in the ensemble had a very large standard deviation for local impacts of O_3 precursor emission reductions. The large standard deviation substantially influenced results, such that the relative magnitude of regional avoided deaths from local and foreign emission reductions changed when the mean + sd was used versus when the mean - sd was used. In Chapter 2, Monte Carlo analysis was used to include uncertainty in simulated O_3 and $PM_{2.5}$ concentrations, but necessarily used crude assumptions for model uncertainty due to lack of established estimates. A dedicated effort is necessary to examine the effect of uncertainty from simulated concentrations and other sources on

estimated deaths and to design methods to incorporate these various sources of uncertainties into the uncertainty bounds around the mortality estimate.

5.2. Future research

5.2.1. Incorporating future demographic shifts

This work found that the health impacts of air pollution are driven by both concentration and demographics of the exposed population. Since air pollution mitigation policies can take years or even decades to implement and often remain in effect for decades, the health benefits of potential policies should be evaluated based on the demographics of the future population. To date, studies examining the impacts of future changes in air pollution on human health include population growth according to socioeconomic assumptions (West et al. 2006; West et al. 2007; Selin et al. 2009; Shindell et al. in prep; UNEP in prep), but none have incorporated shifts in baseline mortality rates.

Two methods of calculating future changes in cardiovascular, respiratory, and lung cancer mortality rates, the causes of death found to be most strongly associated with O_3 and $PM_{2.5}$ (Jerrett et al. 2009; Krewski et al. 2009), should be explored. First, assuming economic development has a similar impact on mortality shifts in all regions of the world, income, as an indicator of economic development, can be used to relate epidemiological transitions that have already occurred in developed regions to those that are expected to occur in currently developing regions. A second method is to leverage large-scale studies that monitor risk factors around the world, such as the World Health

Organization (WHO) Multinational Monitoring of Trends and Determinants in Cardiovascular Disease (MONICA) project, to predict future mortality changes.

Once future mortality rates are projected, they can be used in a case study on the health impacts of future changes in air pollution. Projected changes in emissions that account for various degrees of economic development and pollution regulation have been developed for the Intergovernmental Panel on Climate Change (IPCC) Fifth Assessment Report (AR5) Representative Concentration Pathways (RCPs) and are readily available (http://www.iiasa.ac.at/Research/ENE/IAMC/rcp.html). These emission inventories can be leveraged to examine the future changes in surface air quality and human mortality for a variety of economic and policy scenarios. Such an analysis would produce the first estimates of how the total burden of air pollution on mortality may change in the future, while simultaneously advancing the global health impact assessment methodology to incorporate future demographic shifts.

5.2.2. Evaluating benefits of actual mitigation strategies

The changes in individual air pollutant emissions examined in Chapters 3 and 4 are unrealistic since each emission source emits a mixture of pollutants. Any mitigation strategy is likely to impact the entire emission mixture, rather than individual components alone. Chapter 4 showed that halving co-emitted OC emissions along with BC emissions avoids eight times more premature deaths compared with halving BC alone, suggesting that mortality results greatly underestimate the full air pollution-related benefits of BC mitigation strategies, which generally decrease both OC and BC. Each sector also produces emissions that result in different patterns of exposure, depending on where the

emissions occur (both horizontally and vertically) and the degree of co-location with population.

To identify emission sources that can be controlled to achieve the greatest benefits, the health impacts of individual economic sectors should be assessed, as has been done for climate (Koch et al. 2007; Reddy et al. 2007; Balkanski et al. 2010; Unger et al. 2010). Only two studies have estimated the health burden of individual emission source sectors, focusing specifically on shipping and aircraft (Corbett et al. 2007; Barrett et al. 2010). A natural first step would be to leverage the air quality modeling from Unger et al. (2010), in which each sector's emissions were eliminated from the model individually, as inputs to the health impact assessment. This would allow for estimation of gridded sector-specific mortality impacts, which can then be aggregated by world region. However, the horizontal resolution of the air quality model used by Unger et al. (2010) is 4°x5°, much coarser than the resolutions used in Chapters 2-4 and too coarse to reliably capture spatial gradients of population and concentrations. Running a similar experiment on a finer resolution would be an improvement from these methods and can be performed relatively easily using emissions from the IPCC AR5 inventory, which are disaggregated by sector. Finally, a more long-term and novel extension of this project would be to develop a tagging approach where each sector's emissions and subsequent chemical products are included in the CTM simultaneously but are assigned as discrete variables. This method would account for any non-linearities in the photochemical system that would be affected by removing emissions from individual sectors.

Since the IPCC AR5 inventory projects emissions through 2100 following several assumptions of economic growth and air pollution regulation, building a framework to

assess the health impacts of individual economic sectors can be expanded to examine how the relative impacts of each sector can be expected to change in the future. In the long run, this approach can be used to support international policy decisions by examining the benefits of actual international air pollution mitigation strategies.

5.2.3. Understanding uncertainties and the value of information

The case studies examined here demonstrate that global health impact assessment is a useful tool to quantify the health impacts of air pollution and potential benefits of its mitigation, but major improvements are needed to enhance the quality and credibility of the methodology. Figure 5.1 shows the cascade of uncertainties permeating these case studies and global health impact assessment in general. Some sources of uncertainty are related to simulation of O_3 and $PM_{2.5}$ concentrations, including uncertainty in emissions inventories, the chemical and physical processes parameterized in global atmospheric models, and the horizontal and vertical resolution at which the atmospheric chemistry model is run. While regional scale health impact assessments are increasingly approaching the fine spatial scales at which humans are exposed to air pollution in reality (Hubbell et al. 2009), due to computing power constraints, global CTMs are often run at a horizontal resolution of about 2°x2°, translating to grid cells approximately 170 km per side. These grid cells are too coarse to capture the fine spatial gradients in concentration, and since the health impact assessment is performed on the same resolution as the simulated concentrations, population gradients are also diluted into the large grid area. Coarse grid resolution may cause oversimulation of O_3 concentrations but undersimulation of $PM_{2.5}$ concentrations (Anenberg et al. 2010).

The importance of uncertainty from coarse grid resolution on estimated changes in mortality can be explored using global CTMs. For example, one approach to explore is distributing concentrations of some species that have a very short atmospheric lifetime, such as carbonaceous aerosols, on a much finer grid within each grid cell according to population. Another option would be to compare coarsely resolved simulated concentrations of both O_3 and $PM_{2.5}$ with observations from surface monitors or with concentrations simulated by a more highly resolved regional model to build sub-grid scale concentration gradients. A third option would be to utilize fine-scale satellite observations in coordination with meteorological information to derive more finely resolved surface concentrations, as has been demonstrated by van Donkelaar et al. (2010). The disadvantage of using satellite information is the inability to distinguish between $PM_{2.5}$ components, though aerosol optical depth could potentially be used to differentiate absorbing and reflective components. Finally, a fourth option would be a more complex task of running a global CTM with finer resolution grids nested within the coarse global grid, where the nested grids would be implemented over highly populated regions. These approaches should all be considered for their potential value and effect on estimated deaths.

Other sources of uncertainty are associated with the concentration-response relationship, which is derived from epidemiology studies that relate O_3 and $PM_{2.5}$ concentrations with mortality. While short-term epidemiology studies performed around the world generally find consistent associations between acute O_3 and $PM_{2.5}$ exposure and daily mortality (Anderson et al. 2004; Health Effects Institute Scientific Oversight Committee 2004; Health Effects Institute 2010; Atkinson et al. 2011), the body of long-

term epidemiology cohort studies, which are more resource-intensive, is limited to a few studies in the US and Europe. To date, all global health impact assessments of $PM_{2.5}$ have extrapolated concentration-response relationships for chronic exposure found in the US and Europe to the rest of the world, despite differences in populations, lifestyles, age structure, medical care, and, perhaps most importantly, concentration levels.

While evidence from studies of exposure levels experienced by smokers and indoor air pollution concentrations, which tend to be much higher than ambient concentrations in the developing world, suggests that the marginal effect of a unit increase in $PM_{2.5}$ concentration is smaller at higher concentrations (Pope et al. 2009; Smith and Peel 2010), the lack of epidemiology studies examining cohorts exposed to high ambient concentrations prevents conclusive determination of this relationship. Currently, there are several methods of extrapolating concentration-response relationships from low to high concentrations, with some studies assuming a linear extrapolation and others assuming a log function which flattens at high concentrations. While both assumptions may be justified given the lack of data at high concentrations, the assumed shape of the function has a substantial impact on estimated deaths, both in terms of the global total and the regional distribution.

Finally, $PM_{2.5}$ composition is non-uniform and varies widely around the world depending on proximal emission sources and other factors. Epidemiology studies examining differential toxicity of $PM_{2.5}$ mixtures are limited, and despite short-term and toxicology studies suggesting otherwise (e.g. Ostro et al. 2007; Ostro et al. 2008; Bell et al. 2009; Peng et al. 2009; Wilker et al. 2010), all health impact assessments, global as well as domestic, assume all $PM_{2.5}$ components and mixtures are equally toxic. Air

pollution epidemiology studies are increasingly moving from single pollutant studies to multi-pollutant studies (e.g. Dominici et al. 2010; Greenbaum et al. 2010) to support growing interest in multi-pollutant air quality management (e.g. Wesson et al. 2010), but there is no consensus yet on health impacts of different air pollution mixtures, or even how multi-pollutant epidemiology studies should be designed (Vedal and Kaufman, 2011). Understanding of the differential toxicity of air pollution mixtures is therefore unlikely to be achieved in the near term. In the meantime, research is needed to examine the assumption that all $PM_{2.5}$ components and mixtures are equally toxic and the effect of that assumption on estimated deaths.

In summary, the uncertainties associated with global health impact assessment are not well studied and are very difficult to quantify. Prioritization of research needs can be achieved by analyzing the value of information for narrowing the uncertainty around each parameter. Specifically, the above parameters that feed into the health impact function should be examined for the magnitude of their uncertainties, whether their uncertainties are symmetric around the mean, whether improvements to each source of uncertainty will likely narrow the uncertainty bands, whether narrowing the uncertainty bands will likely narrow the uncertainty on the mortality estimate, and whether narrowing the uncertainty on the mortality estimate will likely influence decisions on potential mitigation strategies. Evaluating these questions will help indicate the health impact function parameters and assumptions that should be prioritized for future research. Results will to lead to additional research targeted at reducing uncertainty associated with the highest priority health impact function parameters.

5.3. Conclusion

This dissertation examined several aspects of the global health impacts of air pollution, finding that air pollution remains a substantial problem for global public health and is driven both by concentrations and by the demographics of the exposed populations. In addition, while the impacts of black carbon largely occur within the source region, secondarily formed pollutants such as O_3 and sulfate affect air quality and health on larger spatial scales. These results suggest that international cooperation may be needed to complement local control efforts in mitigating local air pollution-related mortality and to mitigate air pollution and climate change in a coordinated way. Finally, this work demonstrates that global health impact assessment is a useful tool to quantify the health impacts of air pollution and potential benefits of its mitigation, but improvements are needed to enhance the quality and credibility of the methodology. Future research should incorporate future demographic shifts, evaluate the impacts of realistic mitigation strategies, and assess the influence of various sources of uncertainty in global health impact assessment.

5.4. Tables and figures

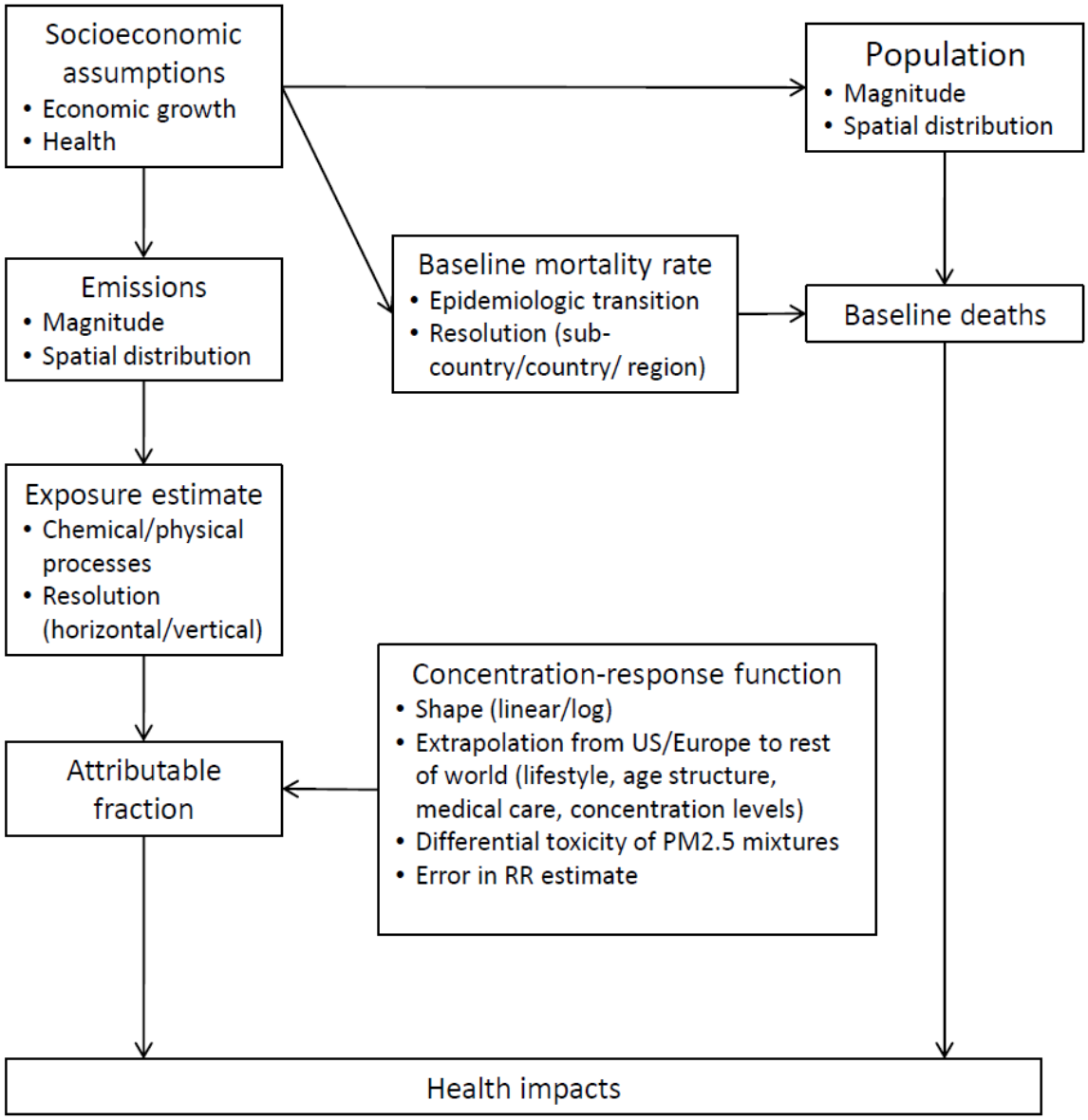

Figure 5.1. Cascade of uncertainties in global health impact assessment.

Appendix A. An estimate of the global burden of anthropogenic ozone and fine particulate matter on premature human mortality using atmospheric modeling: Supporting material

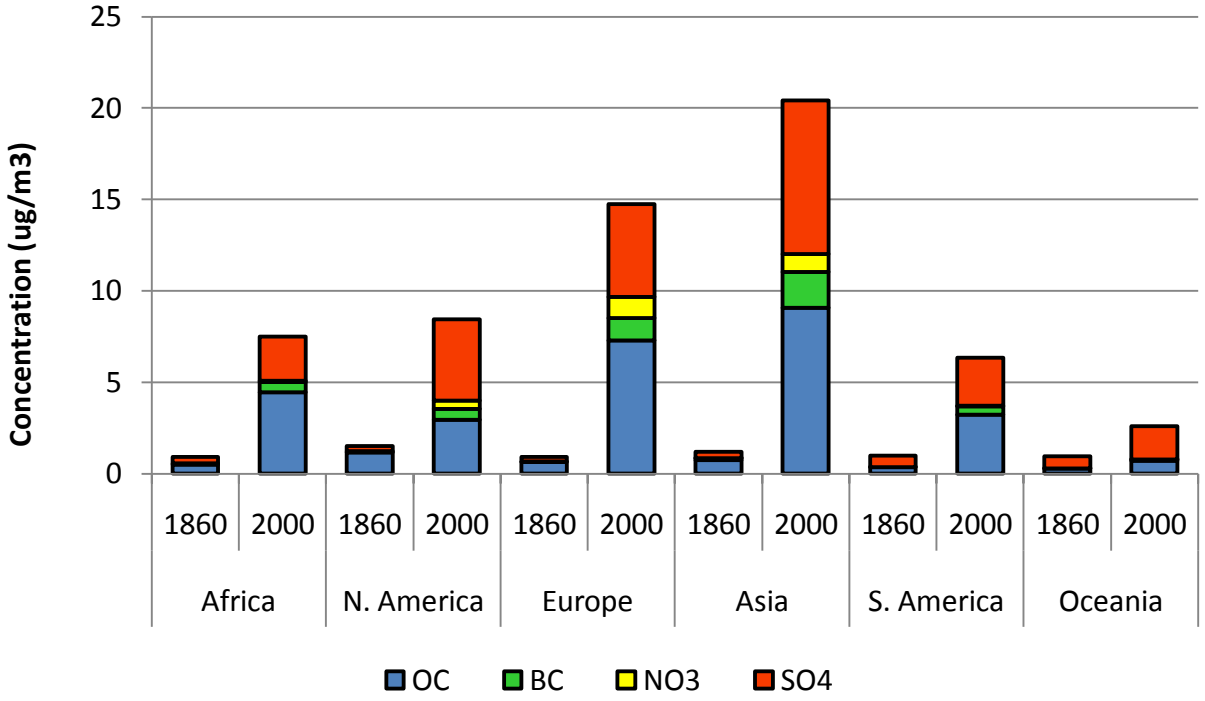

Figure A.1. Population-weighted annual average $PM_{2.5}$ component concentrations from MOZART-2 simulations of the preindustrial (1860) and present (2000) (Horowitz 2006). NH_4 is included in the values for NO_3 and SO_4, as all SO_4 and NO_3 are assumed to exist as $(NH_4)_2SO_4$ and NH_4NO_3, following Ginoux et al. (2006).

Modeled Surface Ozone Comparison with Observations

We compare monthly mean surface ozone concentrations modeled with the Model of Ozone and Related Chemical Tracers, version 2 (MOZART-2) for the present day (2000) (Horowitz 2006) with observations from three non-urban networks, the Clean Air Status and Trends Network (CASTNet) for the US (Figure A.2), the European Monitoring and Evaluation Programme (EMEP) for Europe (Figure A.3), and the Acid Deposition Monitoring Network in East Asia (EANET) for Japan (Figure A.4). We also compare surface ozone with the Climate Monitoring and Diagnostics Laboratory (CMDL) monitoring network for remote locations around the world (Figure A.5). CASTNet and EMEP observations are from 2000, EANET observations are from 2001, and CMDL observations are from 1998-2004, depending on data availability. Overall mean bias is 2.9 ppb for CASTNet, -0.2 ppb for EMEP, 0.4 for EANET, and 2.5 ppb for CMDL. Since mean bias is within 3 ppb for all networks, we do not apply a bias correction for the main results, but examine the sensitivity to a concentration change of 25% in both directions. Mortality results change about proportionally with concentration.

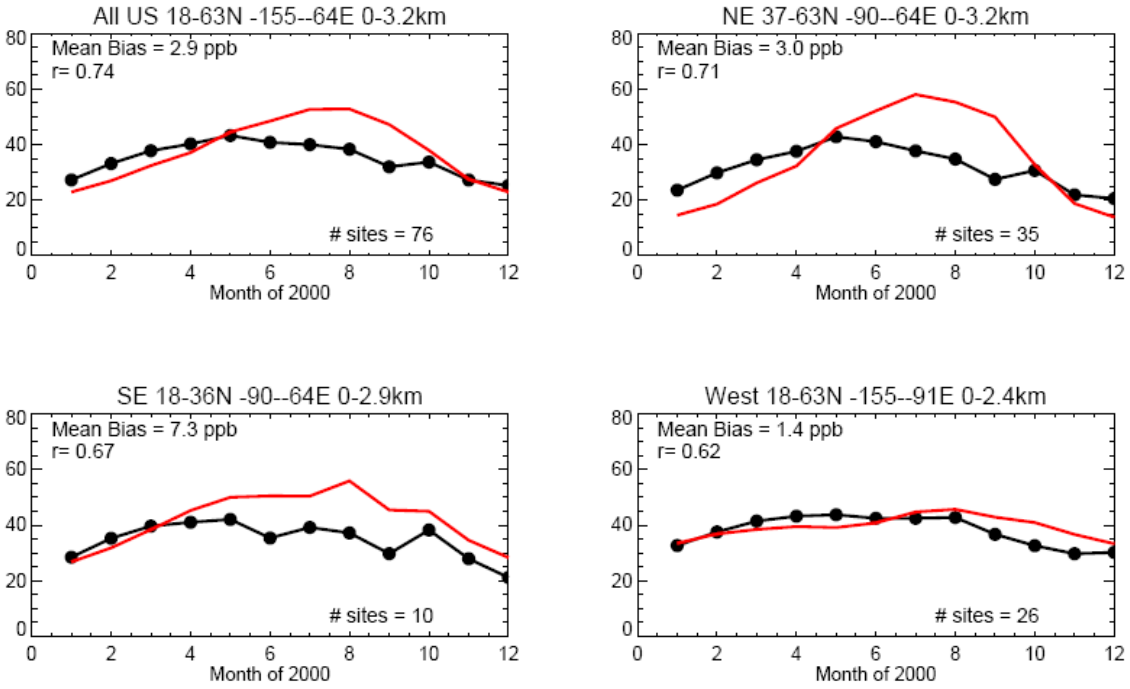

Figure A.2. Comparison of simulated monthly mean surface ozone concentrations (2000) with CASTNet monitored concentrations (2000) for the entire US and three subregions.

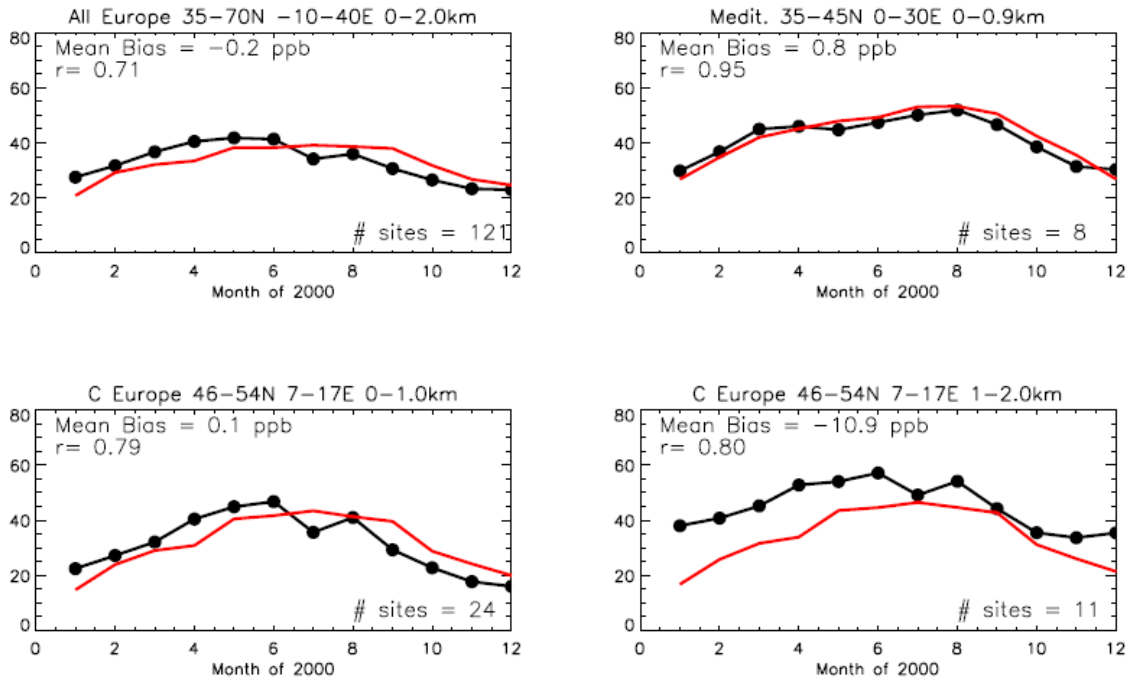

Figure A.3. Comparison of simulated monthly mean surface ozone concentrations (2000) with EMEP monitored concentrations (2000) for all of Europe and three subregions.

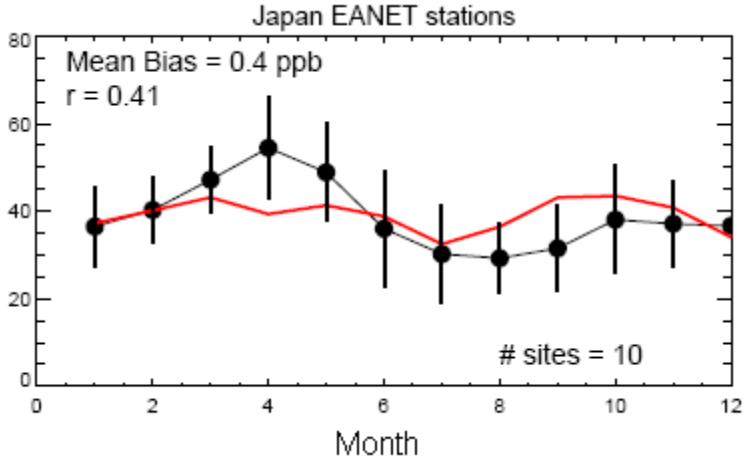

Figure A.4. Comparison of simulated monthly mean surface ozone concentrations (2000) with EANET monitored concentrations (2001) for Japan.

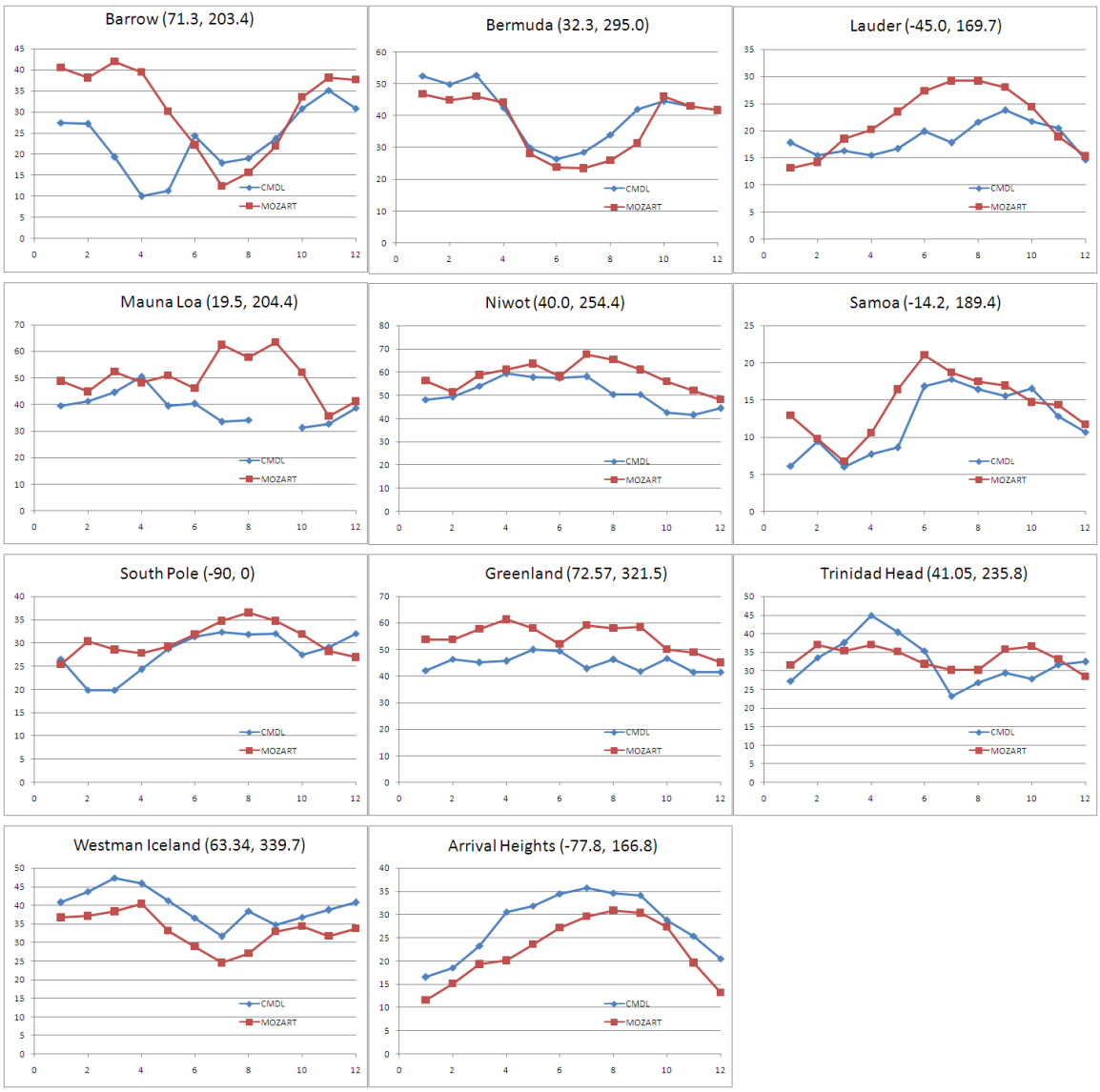

Figure A.5. Comparison of simulated monthly mean surface ozone concentrations for 2000, in ppb (Horowitz 2006), with CMDL monitored concentrations (1998-2004) for remote locations.

Health Impact Function Input Parameters

Population

We use 2006 population from the Landscan database (Oak Ridge National Laboratory 2008), which apportions population to very fine resolution grid cells (30”x30”) based on nighttime lights, proximity to roads, and other indicators (Figure A.6). We also use the fraction of the population aged 30 and older for 14 world regions (World Health Organization 2004) to determine the exposed population consistent with Pope et al. (2002) for $PM_{2.5}$ mortality estimates (Figure A.6 and Figure A.7).

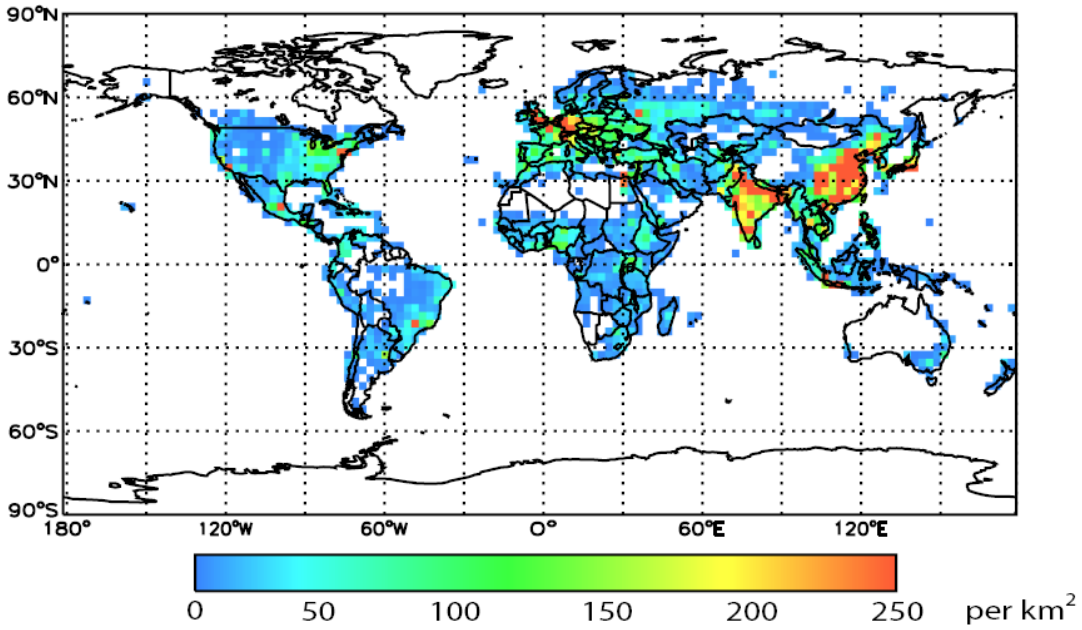

Figure A.6. Population aged 30 and older mapped on the MOZART-2 grid.

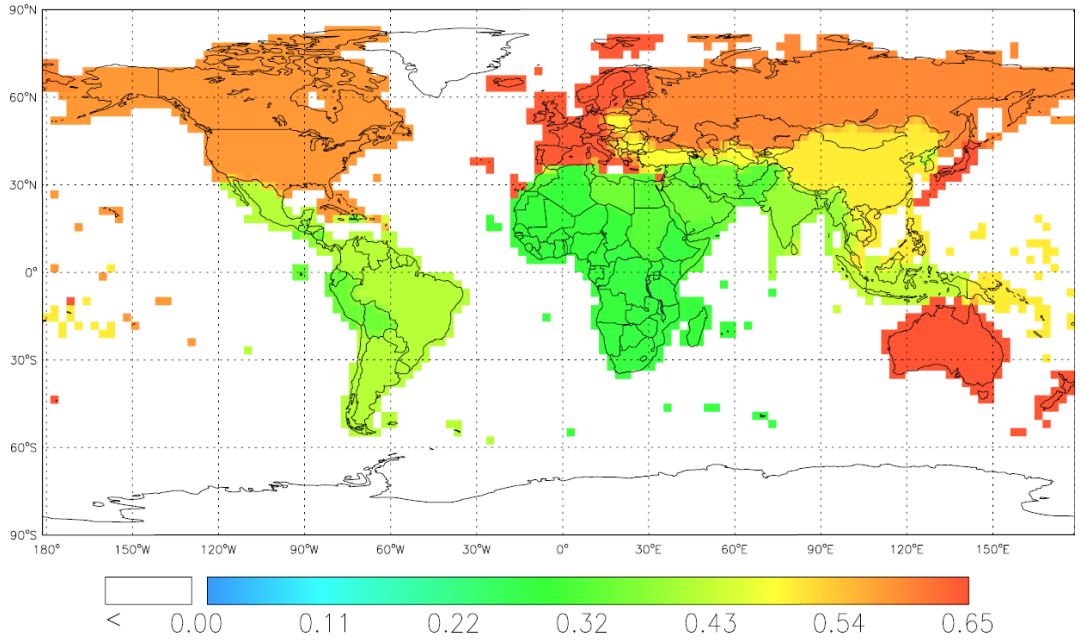

Figure A.7. Fraction of the population aged 30 and older (World Health Organization 2004) mapped onto MOZART-2 grid.

Baseline Mortality Rates

Baseline all-cause, non-accidental, cardiopulmonary, and lung cancer mortality rates for the population aged 30 and older for 66 countries and 14 world regions are from the World Health Organization (2004; 2008b) and are mapped onto the MOZART-2 grid (Figure A.8-Figure A.11). Where country-specific data are unavailable, we back-calculate mortality rates from regional rates. When a grid cell contains portions of more than one country within it, we calculate an area-weighted average mortality rate using a Geographic Information System (GIS).

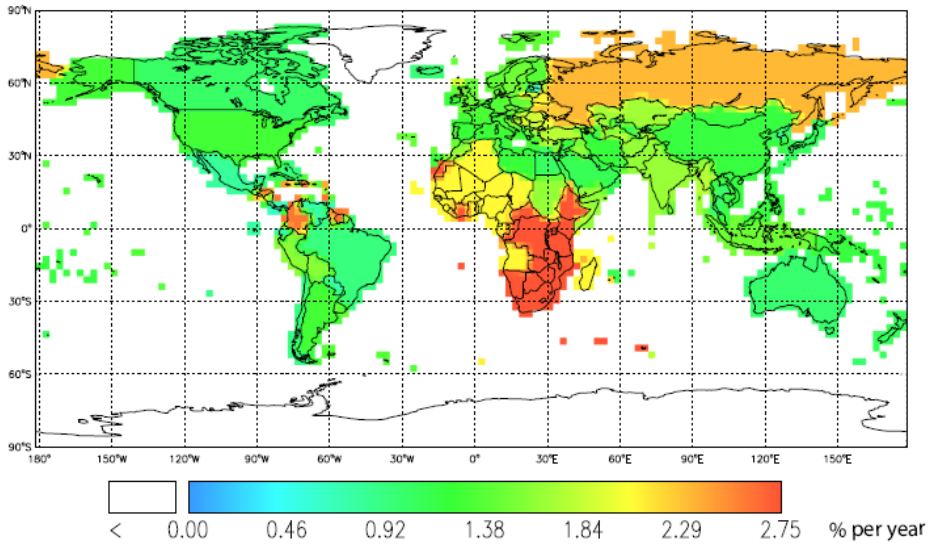

Figure A.8. Baseline all-cause mortality rates for the population aged 30 and older mapped on MOZART-2 grid.

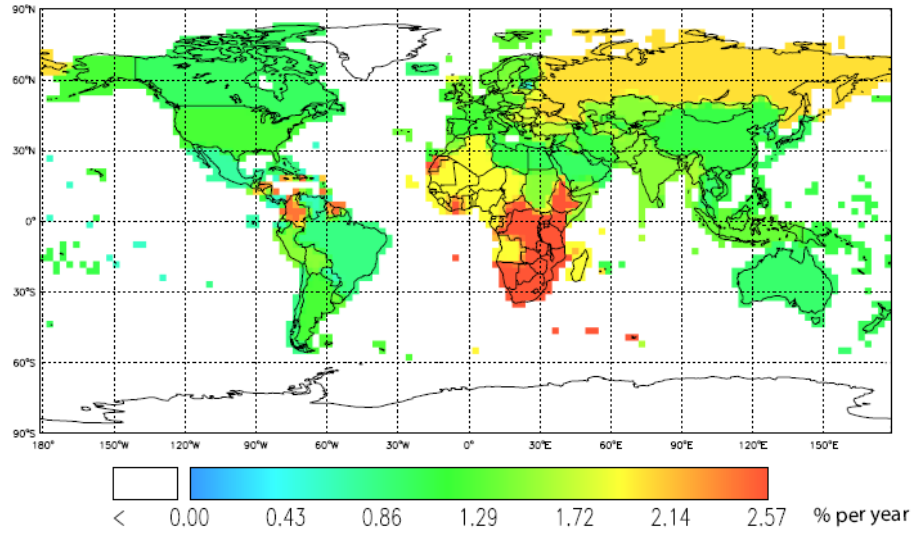

Figure A.9. Baseline non-accidental mortality rates for the population aged 30 and older mapped onto MOZART-2 grid.

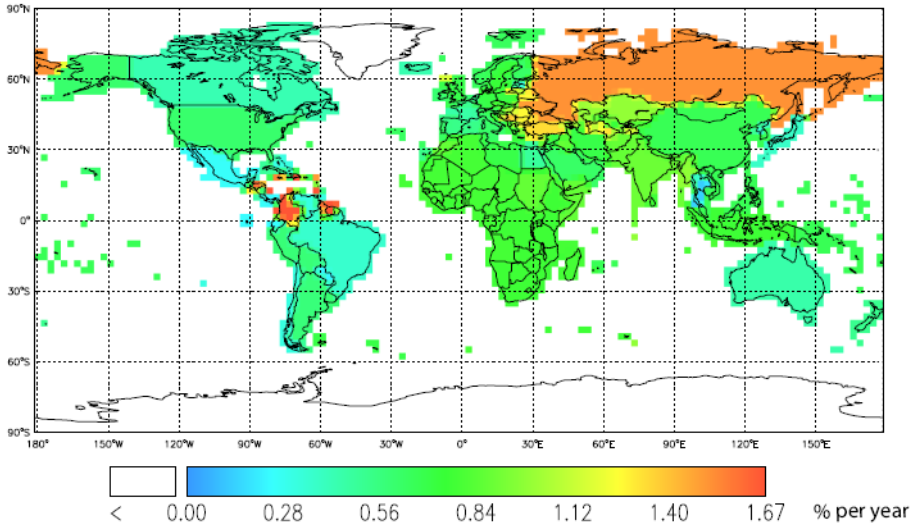

Figure A.10. Baseline cardiopulmonary mortality rates for the population aged 30 and older mapped onto MOZART-2 grid.

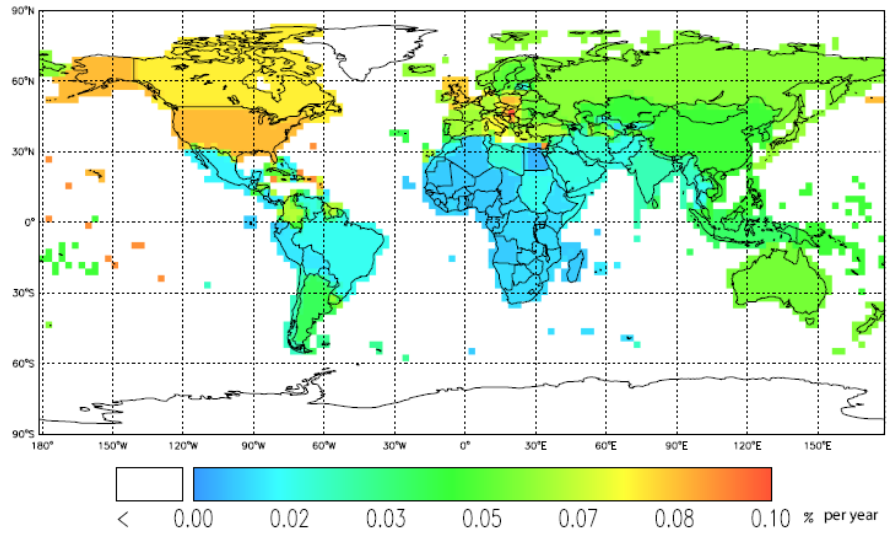

Figure A.11. Baseline lung cancer mortality rates for the population aged 30 and older mapped onto MOZART-2 grid.

Table A.1. Years of life lost per death, using 3% discount rate and age-weighting (World Health Organization 2008a)

	Cardiopulmonary Disease	Respiratory Disease	Lung Cancer
Africa	11.00	14.30	13.43
North America	6.48	8.13	8.92
Europe	7.40	5.93	10.04
Asia	7.98	7.96	10.49
South America	7.61	7.59	9.62
Oceania	5.54	6.97	8.46
World	7.89	8.93	9.77

Table A.2. As in Table 2.5.

		All-Cause (000s)	Cardiopulmonary (000s)	Lung Cancer (000s)
Krewski et al. (2009)		3381 ± 986	3499 ± 864	222 ± 80
	LCT=5.8 μg/m^3	2378 ± 876 (-29.7%)	2506 ± 816 (-28.4%)	164 ± 68 (-26.1%)
	LCT=7.5 μg/m^3	2077 ± 822 (-38.6%)	2201 ± 780 (-37.1%)	146 ± 64 (-34.2%)
	HCT=30 μg/m^3	3059 ± 774 (-9.5%)	3205 ± 676 (-8.4%)	201 ± 68 (-9.5%)
	HCT=50 μg/m^3	3338 ± 940 (-1.3%)	3464 ± 826 (-1.0%)	219 ± 78 (-1.4%)
Pope et al. (2002) avg.[a]		3378 ± 1516 (-0.0%)	2563 ± 1088 (-26.8%)	221 ± 86 (-0.5%)
	LCT=5.8 μg/m^3	2375 ± 1209 (-29.8%)	1835 ± 886 (-47.6%)	164 ± 73 (-26.1%)
	LCT=7.5 μg/m^3	2075 ± 1104 (-38.6%)	1612 ± 815 (-53.9%)	145 ± 68 (-34.7%)
	HCT=30 μg/m^3	3062 ± 1303 (-9.4%)	2332 ± 944 (-33.4%)	201 ± 75 (-9.5%)
	HCT=50 μg/m^3	3336 ± 1476 (-1.3%)	2534 ± 1062 (-27.6%)	219 ± 84 (-1.4%)
Pope et al. (2002) 79-83[a]		2333 ± 1196 (-31.0%)	1800 ± 742 (-48.6%)	139 ± 72 (-37.4%)
	LCT=5.8 μg/m^3	1641 ± 935 (-51.5%)	1289 ± 609 (-63.2%)	103 ± 58 (-53.6%)
	LCT=7.5 μg/m^3	1433 ± 848 (-57.6%)	1132 ± 562 (-67.6%)	91 ± 54 (-59.0%)
	HCT=30 μg/m^3	2103 ± 1027 (-37.8%)	1624 ± 627 (-53.6%)	124 ± 62 (-44.1%)
	HCT=50 μg/m^3	2301 ± 1163 (-31.9%)	1777 ± 720 (-49.2%)	137 ± 71 (-38.3%)
Laden et al. (2006)[b]		7714 ± 2736 (+128.2%)	4549 ± 1439 (+30.0%)	336 ± 198 (+51.4%)
	LCT=5.8 μg/m^3	5420 ± 2276 (+60.3%)	3208 ± 1236 (-8.3%)	249 ± 156 (+12.2%)
	LCT=7.5 μg/m^3	4732 ± 2102 (+40.0%)	2796 ± 1151 (-20.1%)	221 ± 142 (-0.5%)
	HCT=30 μg/m^3	7150 ± 2430 (+111.5%)	4308 ± 1331 (+23.1%)	316 ± 185 (+42.3%)
	HCT=50 μg/m^3	7651 ± 2685 (+126.3%)	4526 ± 1424 (+29.4%)	334 ± 196 (+50.5%)

[a] Pope et al. (2002) reported relative risk estimates for two time periods (1979-1983 and 1999-2000) and for the integrated average of both. The relative risk estimates for 1979-1983 were more conservative than those from 1999-2000 and the integrated average.

[b] Laden et al. (2006) extended the follow-up of the Harvard Six Cities adult cohort study for eight years, finding significantly higher relative risk estimates for overall mortality than the original study and Krewski et al. (2009)

Appendix B. Intercontinental impacts of ozone pollution on human mortality: Supporting material

Methods

Table B.1. List of models and contact persons and the scenarios for which they were run

Model	Resolution (lon x lat x layers)	Institution	Model Contact	SR2	SR6
CAMCHEM-3311m13	2.5°x2°x30	NCAR, USA	Peter Hess	Y	Y
EMEP-rv26 (NH only)	1°x1°x20	EMEP, Norway	Jan Eiof Jonson	Y	Y
FRSGC/UCI-v01	2.81°x2.81°x37	Lancaster University, UK	Oliver Wild	Y	Y
GEMAQ-v1p0	4°x4°x28	York University, Canada	Alexandru Lupu	Y	Y
GEOSChem-v07	2.5°x2°x30	Harvard University, USA	Rokjin Park	Y	Y
GEOSChemv07-res4x5	5°x4°x30	CIEMAT, Spain	Marta Garcia Vivanco	Y	N
GISS-PUCCINI-modelE	5°x4°x23	NASA GISS, USA	Drew Shindell	Y	Y
GMI-v02f	2.5°x2°x42	NASA GSFC, USA	Bryan Duncan	Y	Y
LMDz3-INCA1	3.75°x2.5°x19	LSCE, France	Sophie Szopa	Y	Y
LLNL-IMPACT-T5a	2.5°x2°x48	LLNL, USA	Daniel Bergmann	Y	Y
MOZARTGFDL-v2	1.88°x1.88°x28	GFDL, USA	Arlene Fiore	Y	Y
MOZECH-v16	2.81°x2.81°x31	FZ Julich, Germany	Martin Schultz	Y	Y
OsloCTM2	2.81°x2.81°x40	University of Oslo, Norway	Michael Gauss	Y	N
STOC-HadAM3-v01	5°x5°x19	University of Edinburgh, UK	Ian MacKenzie	Y	Y
STOCHEM-HadGEM	3.72°x2.5°x20	Met Office, Hadley Centre, UK	Michael Sanderson	Y	N
TM5-JRC-cy2-ipcc-v1	1°x1°x25	JRC, Italy	Frank Dentener Elina Marmer	Y	Y
UM-CAM-v01	3.72°x2.5°x19	University of Cambridge, UK	Guang Zeng	Y	Y

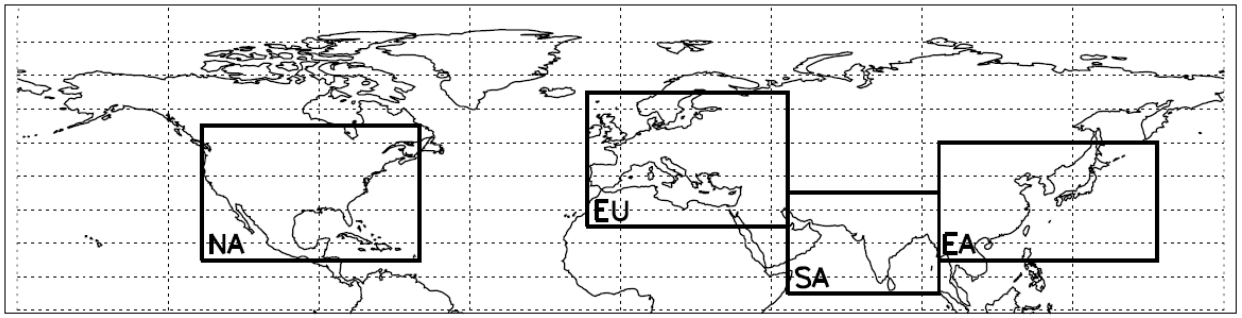

Figure B.1. Map of source-receptor regions

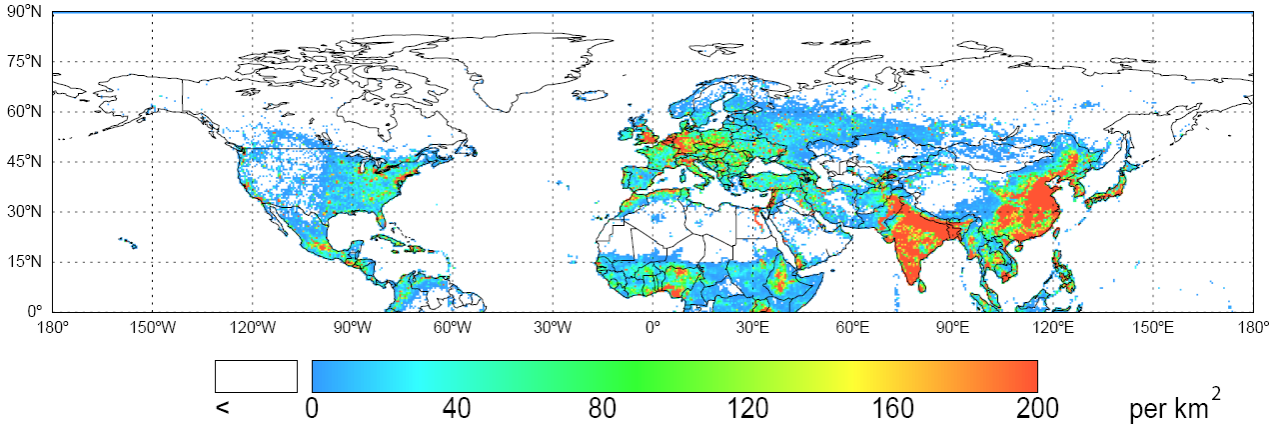

Figure B.2. Population (year 2006) per km^2 mapped to 0.5 x 0.5 degree grid (Oak Ridge National Laboratory 2008)

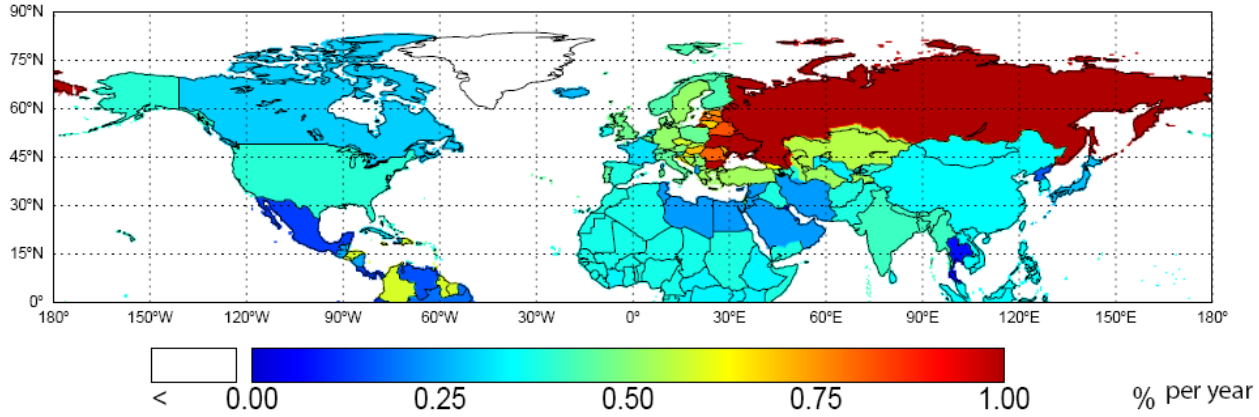

Figure B.3. Baseline cardiopulmonary mortality rates mapped to 0.5 x 0.5 degree grid (World Health Organization 2004; 2008b)

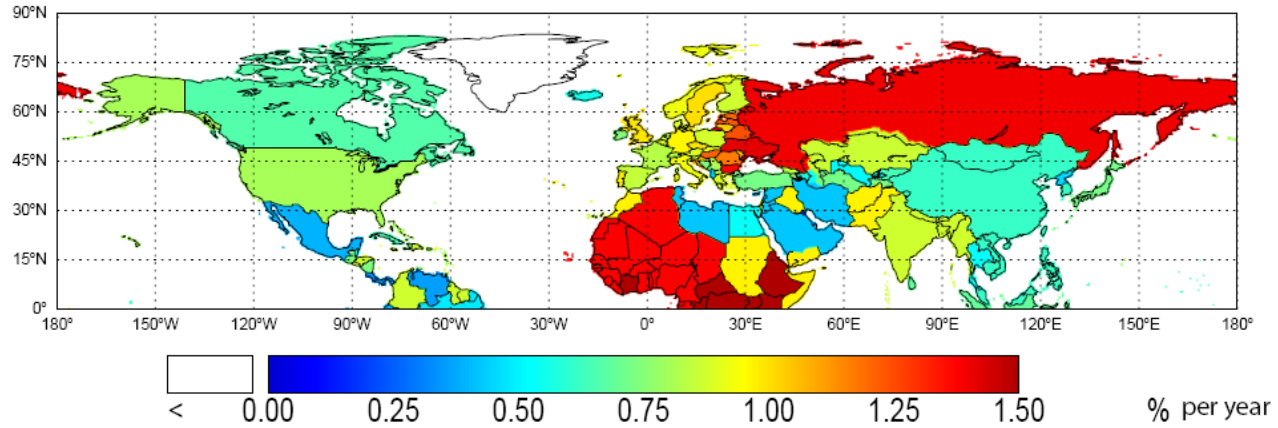

Figure B.4. Baseline non-accidental mortality rates mapped to 0.5 x 0.5 degree grid (World Health Organization 2004; 2008b)

Table B.2. As Table 3.2, but for non-accidental mortalities.

Source Region	Receptor Region				
	NA	**EA**	**SA**	**EU**	**NH**
NA	16 (8 - 23) *16 (8 - 24)*	10 (5 - 15) *6 (3 - 10)*	10 (5 - 15) *10 (5 - 14)*	17 (9 - 25) *9 (5 - 14)*	60 (31 - 89) *45 (24 - 67)*
EA	3 (2 - 5) *2 (1 - 3)*	65 (30 - 96) *60 (31 - 89)*	10 (5 - 15) *9 (4 - 13)*	8 (4 - 12) *4 (2 - 6)*	93 (48 - 137) *77 (40 - 114)*
SA	1 (1 - 2) *1 (0 - 1)*	6 (3 - 9) *4 (2 - 6)*	132 (70 - 196) *115 (60 - 170)*	3 (2 - 4) *2 (1 - 2)*	148 (77 - 218) *123 (64 - 182)*
EU	3 (1 - 4) *2 (1 - 2)*	12 (6 - 18) *8 (4 - 13)*	11 (6 - 17) *10 (5 - 15)*	25 (13 - 37) *37 (19 - 54)*	60 (31 - 89) *62 (32 - 92)*

Table B.3. Sensitivity of the annual avoided non-accidental mortalities (hundreds) from 20% NO_x, NMVOC, and CO emission reductions in each region and the NH to changing parameters, assuming no concentration threshold. For Case 1, confidence intervals (68%) are ±1 standard deviation of the model ensemble's ozone perturbation in each grid cell (Fiore et al. 2009) and do not reflect uncertainty in the CRF (Bell et al. 2004). For Case 2, we use the mean and confidence intervals (95%) of the CRFs from three meta-analyses of O_3 mortality (Bell et al. 2005; Ito et al. 2005; Levy et al. 2005). Confidence limits for Case 2 reflect uncertainty in the CRF only. We convert the results reported by Ito et al. (2005) and Levy et al. (2005) for 1-hr. maximum O_3 concentrations to 24-hr. mean O_3 concentrations using a ratio of 1-hr. maximum to 24-hr. mean equal to 2 (Levy et al. 2005).

Source Region	Case	Receptor Region				
		NA	EA	SA	EU	NH
NA	1	16 (1 - 30)	10 (5 - 15)	10 (6 - 15)	17 (9 - 25)	60 (27 - 94)
	2	25 (17 - 32)	16 (11 - 21)	16 (11 - 21)	27 (18 - 35)	96 (66 - 124)
EA	1	3 (2 - 5)	65 (15 - 116)	10 (5 - 16)	8 (5 - 11)	93 (26 - 157)
	2	5 (4 - 7)	103 (71 - 134)	16 (11 - 21)	13 (9 - 17)	175 (101 - 192)
SA	1	1 (0 - 2)	6 (2 - 10)	132 (83 - 182)	3 (1 - 5)	148 (89 - 210)
	2	2 (1 - 2)	10 (7 - 13)	210 (144 - 273)	5 (3 - 6)	234 (161 - 304)
EU	1	3 (2 - 4)	12 (6 - 18)	11 (6 - 17)	25 (-9 - 58)	60 (9 - 111)
	2	4 (3 - 6)	19 (13 - 25)	18 (12 - 23)	39 (27 - 51)	96 (66 - 124)

Comparison of results with a previous health impact assessment using a regional-scale model

To understand the impact of the coarse grid resolution of the global model used here on our results, we compare our results for NA with a previous estimate of 415 excess non-accidental mortalities in the US due to a population-weighted O_3 increase of 0.72 ppb, assuming a low-concentration threshold of 35 ppb (Jacobson 2008). We estimate that O_3 precursor emission reductions in NA reduce O_3 by 0.96 ppb domestically (Table 3.1), resulting in about 1600 avoided premature mortalities in NA, assuming a threshold of 25 ppb (Table B.2). While we use similar baseline mortality rates and concentration-response factors, our results are expected to be higher due to the difference in population-weighted O_3 change (0.96 ppb vs. 0.72 ppb) and the population of NA vs. the US [481 million (Table 3.1) vs. about 300 million]. In addition, Jacobson (2008) calculates mortalities only for the population exposed to four month average O_3 concentrations (July – November) above the 35 ppb threshold (184.8 million), while we include the population exposed each month to monthly average O_3 concentrations above the 25 ppb threshold. Taking these differences into account, our results are similar to those calculated by Jacobson (2008), suggesting that the coarse resolution of the global model used here impacts results less than other assumptions, including thresholds and exposed populations.

Method of inferring regional CH_4 contributions to CH_4 mixing ratio reduction

Following the methods used by Fiore et al. (2009), we infer the contribution of 20% anthropogenic CH_4 emission reductions in each region to the O_3 response, from the simulation where the global CH_4 mixing ratio was decreased by 20% (SR2 vs. SR1). Accounting for the feedback of CH_4 on its own lifetime and assuming that 60% of total global CH_4 emissions are anthropogenic, a 20% reduction in the CH_4 mixing ratio corresponds to an estimated 25.7% decrease in global anthropogenic CH_4 emissions. Based on the percentage of global anthropogenic emissions occurring in each region, 20% reductions of anthropogenic emissions in NA, EA, SA, and EU are estimated to produce 12.9%, 14.8%, 13.4%, and 12.5% of the O_3 decrease from the SR1 to SR2 scenario. We scale the O_3 decrease (SR2 minus SR1) by these percentages to calculate the annual avoided mortalities from 20% regional reductions in anthropogenic CH_4 emissions within the four regions.

Table B.4. As

Table 3.3, but with a low-concentration threshold of 35 ppb.

Receptor Region	Avoided Cardiopulmonary Mortalities (hundreds)	Avoided Non-accidental Mortalities (hundreds)
NA	7 (3 – 10)	11 (6 – 17)
EA	27 (13 – 41)	41 (21 – 60)
SA	40 (19 – 61)	70 (37 – 104)
EU	23 (11 – 35)	35 (18 – 51)
NH	105 (51 – 161)	177 (92 – 262)

Table B.5. As Table 3.4, but with a low-concentration threshold of 35 ppb.

Source Region	Avoided Cardiopulmonary Mortalities (hundreds)	Avoided Non-accidental Mortalities (hundreds)
NA	14 (7 - 21)	23 (12 - 35)
EA	16 (8 - 24)	27 (14 - 40)
SA	14 (7 - 22)	24 (13 - 36)
EU	13 (7 - 21)	23 (12 - 34)

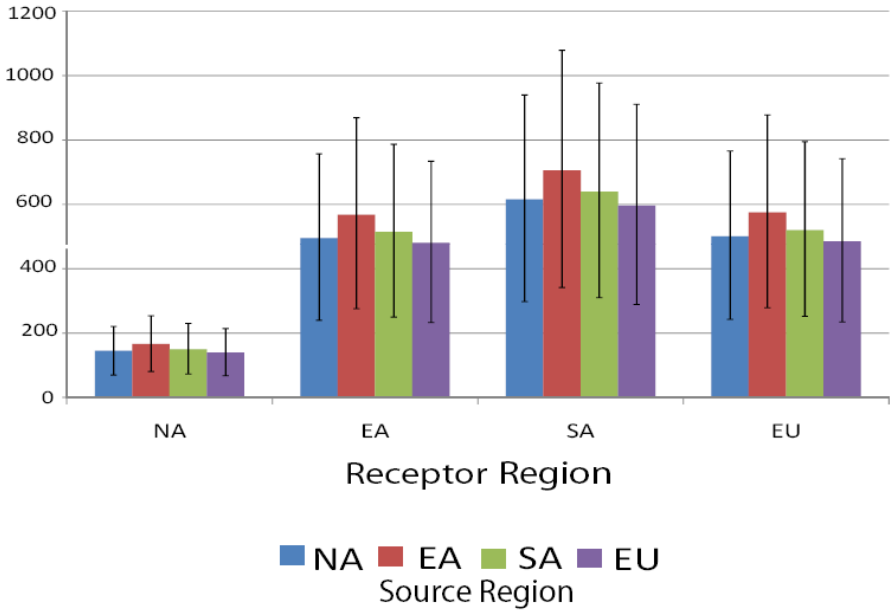

Figure B.5. Annual avoided cardiopulmonary mortalities from regional 20% anthropogenic CH_4 emissions reductions for each source-receptor pair assuming no threshold, estimated as described in the text. Vertical black lines represent the 95% confidence interval in the CRF only (Bell et al. 2004).

Seasonality of foreign and domestic impacts in NA

In NA, reducing O_3 precursor emissions has the largest effect on domestic cardiopulmonary mortalities in the summer, when the impact of foreign emissions is smallest (Figure B.6). Domestic emission reductions increase wintertime mortality in NA, due to the wintertime increase in O_3 following NO_x emission reductions (Fiore et al. 2009). Foreign precursor emission reductions impact mortality in NA the most during spring and least from July through September (Figure B.6), reflecting the seasonality of long-range transport (Fiore et al. 2009). Owing to data limitations, we do not include

seasonal changes in baseline mortality rates, nor possible seasonal changes in the CRF which are not well understood but may occur (National Academy of Sciences 2008).

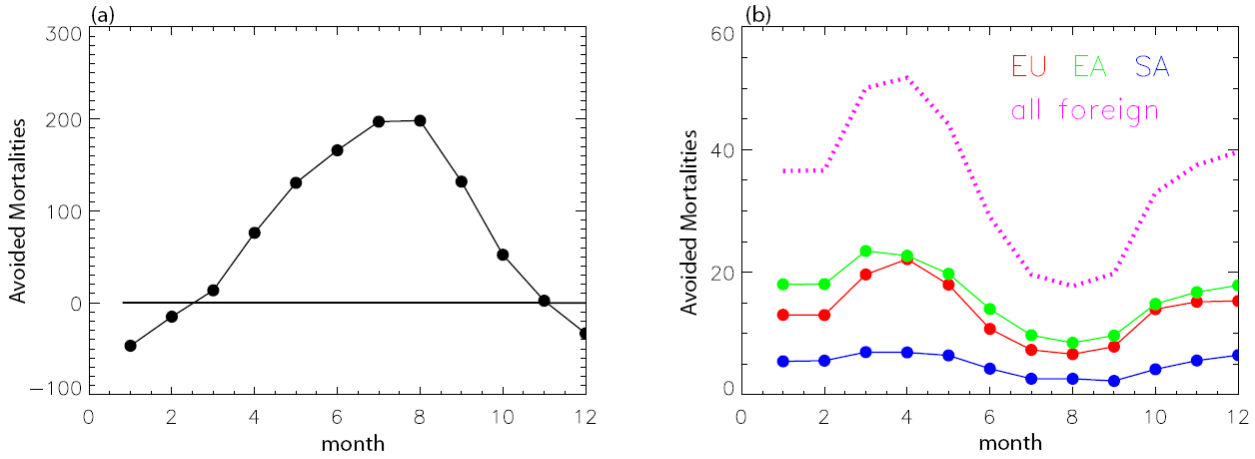

Figure B.6. Seasonality of avoided cardiopulmonary mortalities in NA due to (a) simultaneous 20% reductions in anthropogenic emissions of NO_x, NMVOC, and CO within NA and (b) simultaneous 20% reductions in anthropogenic emissions of NO_x, NMVOC, and CO within the three foreign regions (EA, SA, and EU) individually and summed together, assuming no threshold.

Appendix C. Impacts of global, regional, and sectoral black carbon emission reductions on surface air quality and human mortality: Supporting material

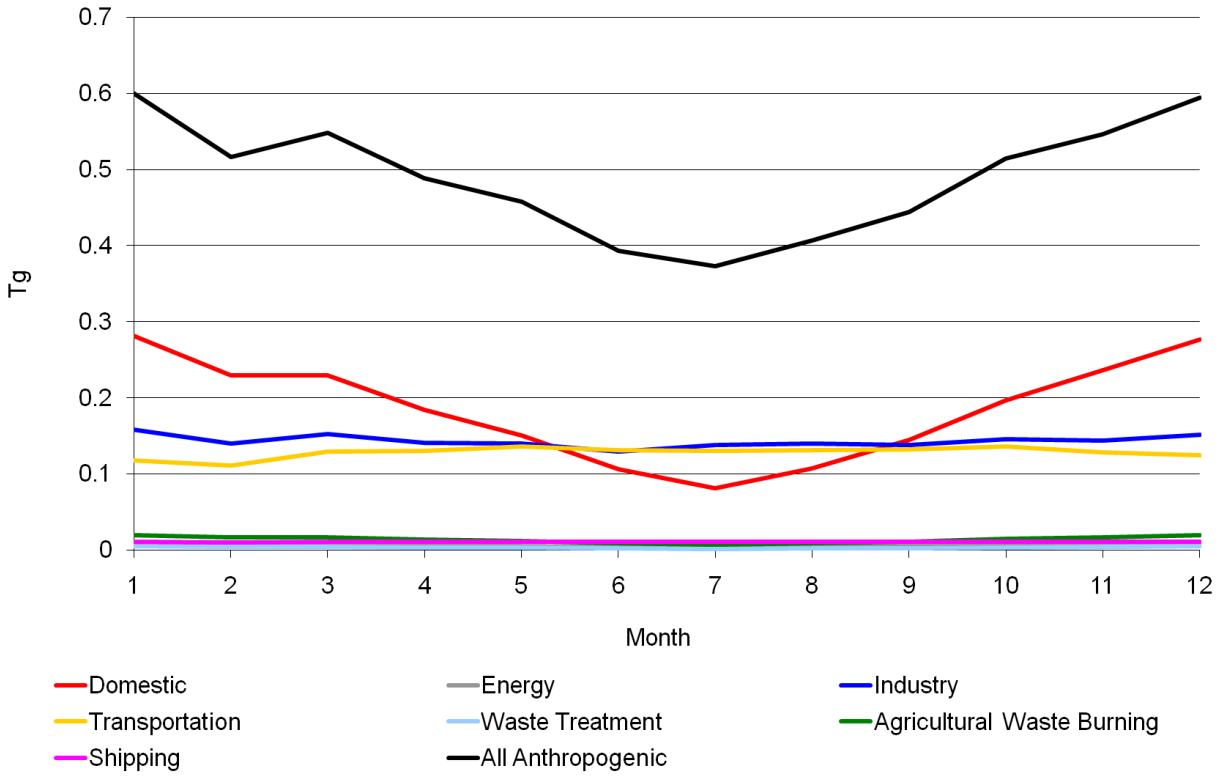

Figure C.1. Monthly variation of global BC emissions by sector, according to seasonal variation of CO from RETRO inventory.

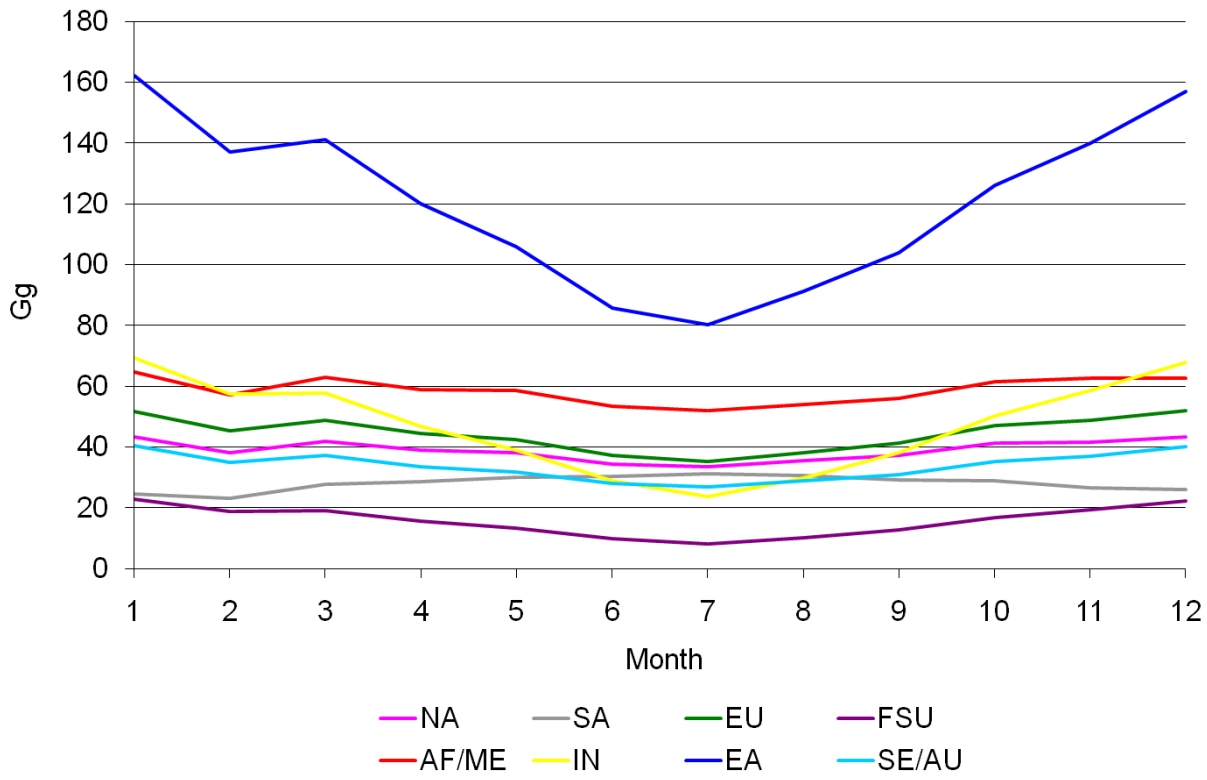

Figure C.2. Monthly anthropogenic BC emissions by region, according to seasonal variation of CO from RETRO inventory.

Table C.1. Total global emissions of relevant species for base case year 2002, in Tg(species)/year. NO_x ($NO+NO_2$) emissions are reported as NO.

Species	Emissions
BC	8.6
OC	41.2
NO_x	93.6
SO_2	149.5

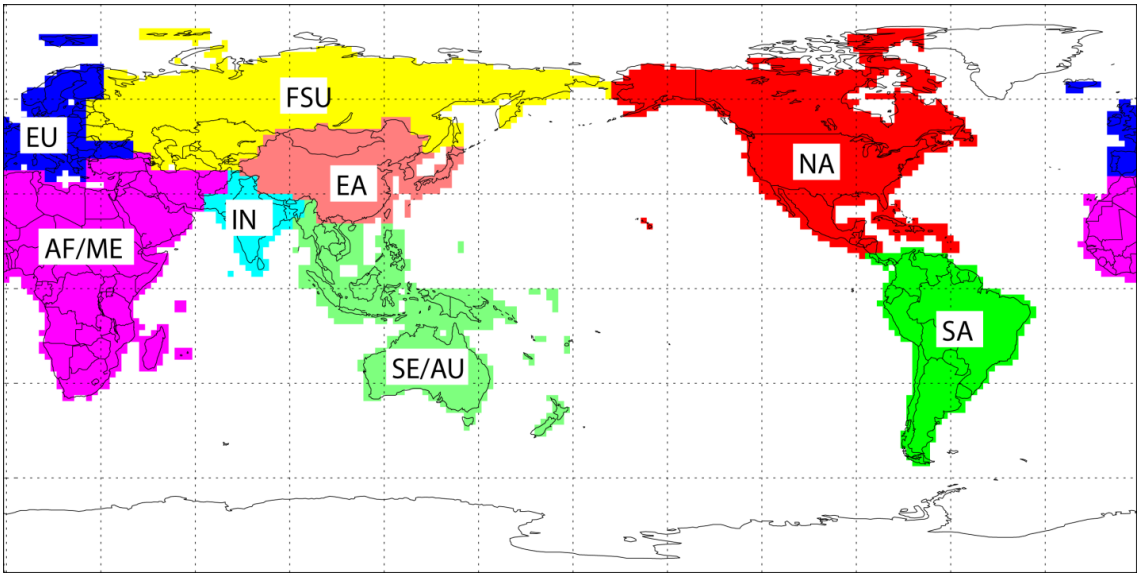

Figure C.3. Regional definitions, gridded to MOZART-4 grid.

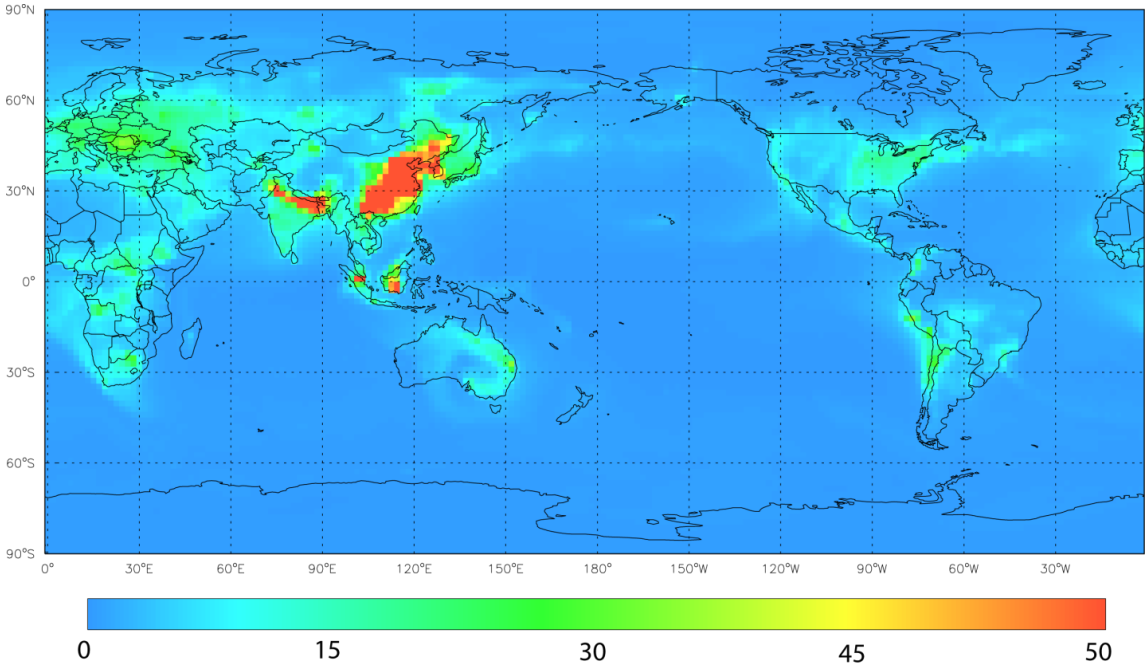

Figure C.4. Annual average concentration (µg/m^3) of total $PM_{2.5}$ for the 2002 base case

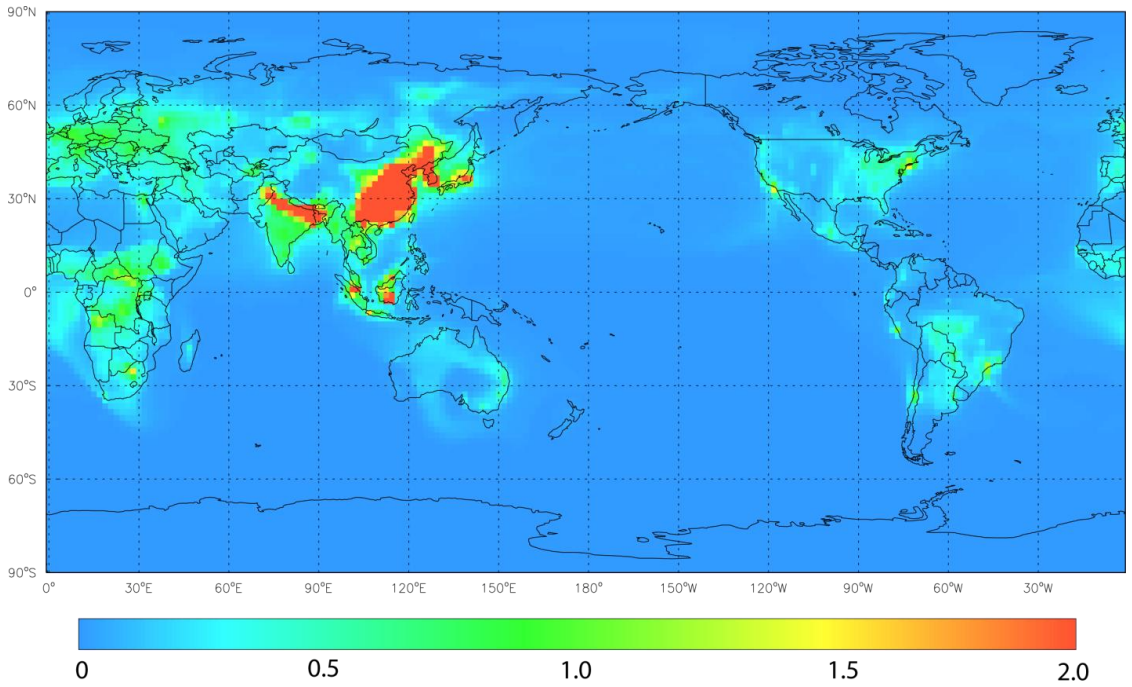

Figure C.5. As Figure C.4, but for BC

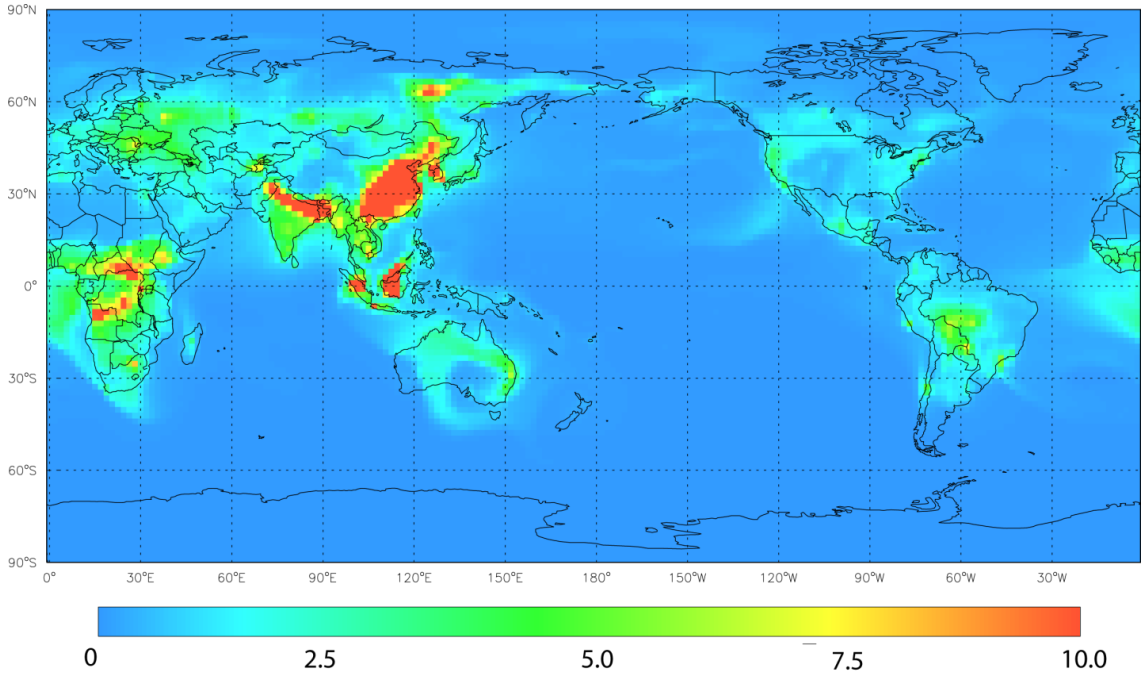

Figure C.6. As Figure C.4, but for OM (includes SOA)

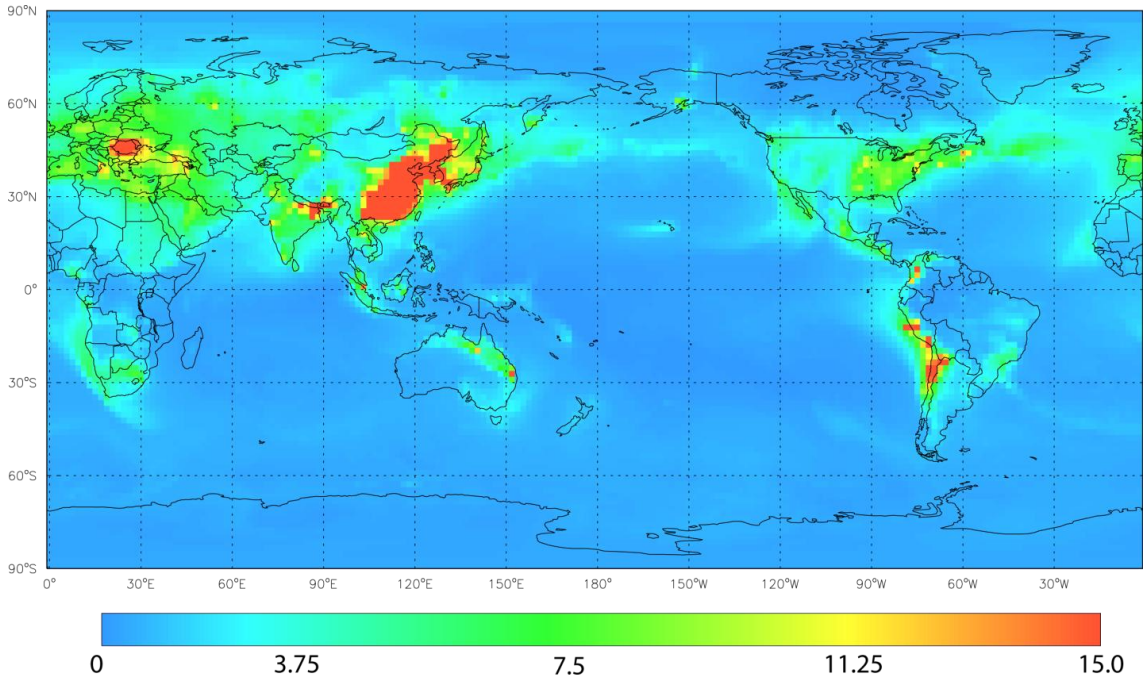

Figure C.7. As Figure C.4, but for SO_4

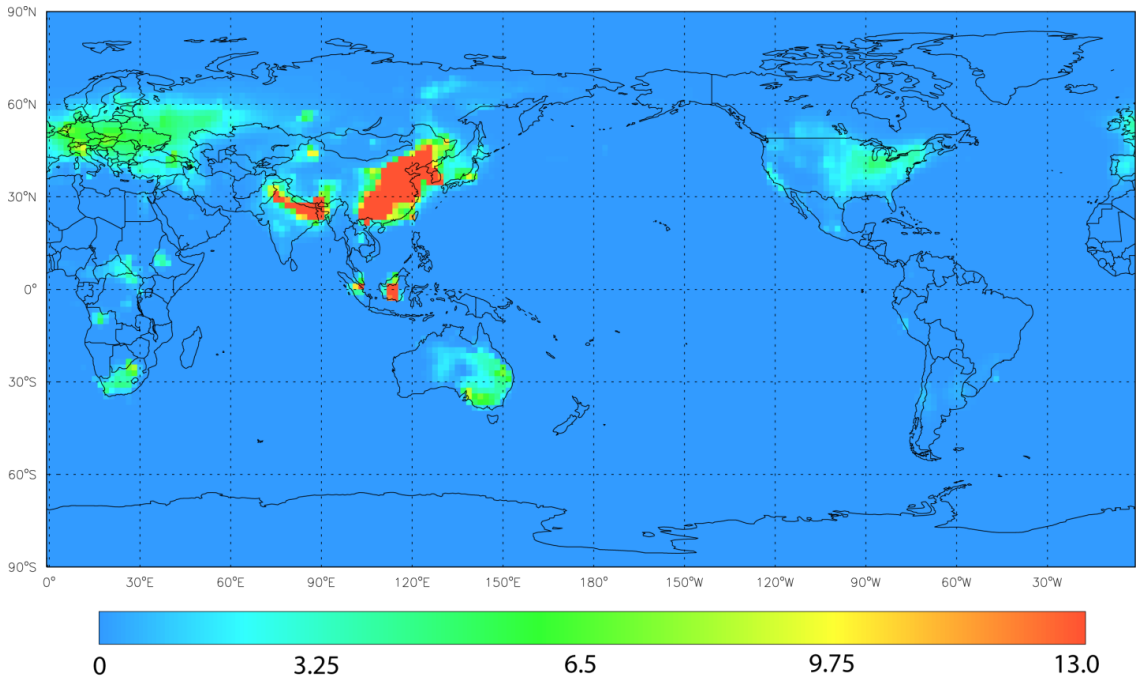

Figure C.8. As Figure C.4 but for NO_3

Table C.2. Simulated simple and population-weighted regional average base case concentrations of BC, OM, SO_4, and NO_3 ($\mu g/m^3$).

	BC		OM		SO_4		NO_3	
Region	Simple Average	Population-weighted Average	Simple Average	Population-weighted Average	Simple Average	Population-weighted Average	Simple Average	Population-weighted Average
NA	0.11	0.36	0.76	1.54	2.26	5.07	0.41	1.32
SA	0.15	0.31	1.36	1.75	2.28	3.84	0.05	0.13
EU	0.36	0.54	1.41	1.86	5.86	7.20	2.14	3.79
FSU	0.17	0.45	1.64	3.27	3.31	6.11	0.74	2.47
AF/ME	0.26	0.39	2.09	2.99	2.68	3.31	0.30	0.53
IN	0.99	1.75	6.33	11.32	5.66	8.08	6.31	15.14
EA	1.28	3.46	5.61	14.35	10.45	21.70	10.65	30.64
SE/AU	0.23	0.66	2.19	4.81	1.62	3.06	0.78	1.02
World	0.10	1.46	0.68	7.42	1.52	9.39	0.45	11.43

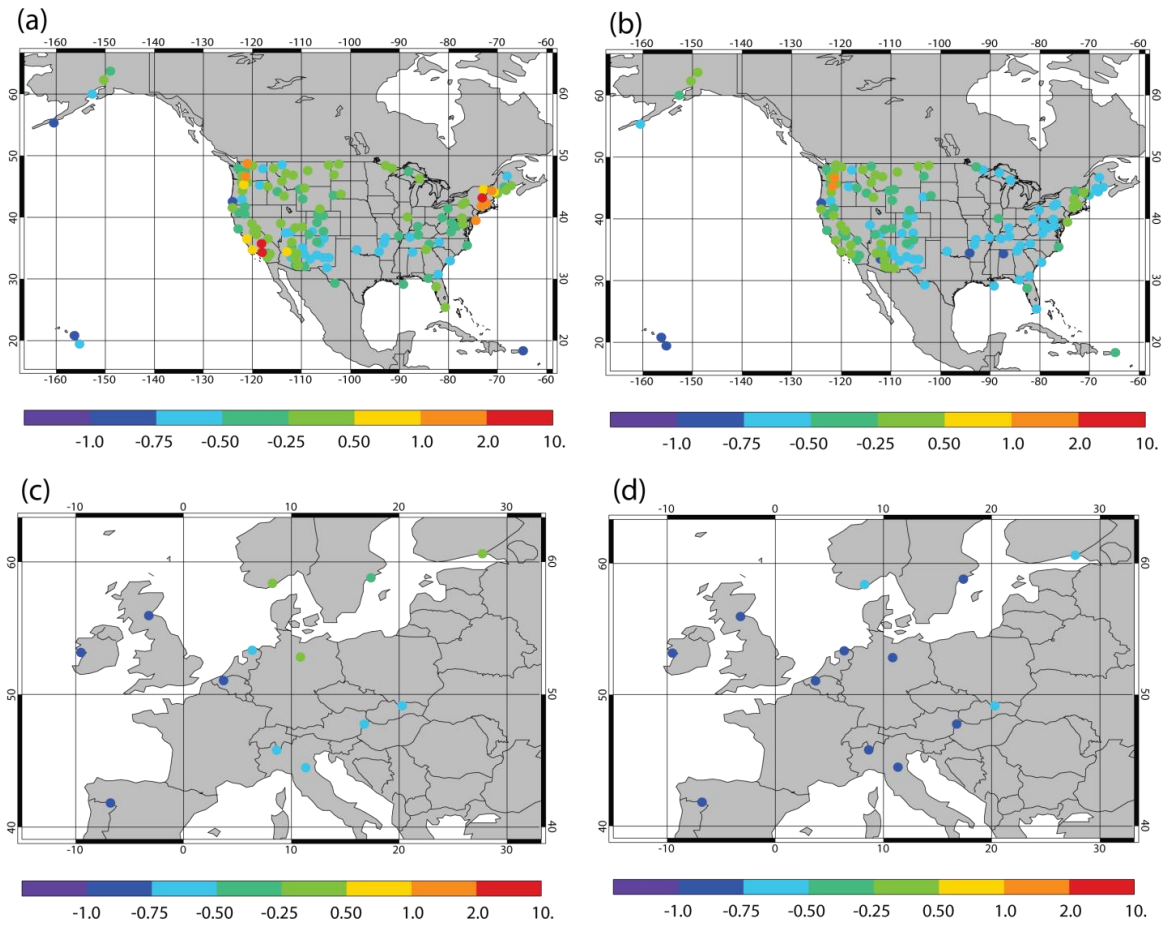

Figure C.9. As Figure 4.3, but plotted on a spatial map to show a comparison of modeled and measured concentrations [(modeled-observed)/observed] in µg/m^3.

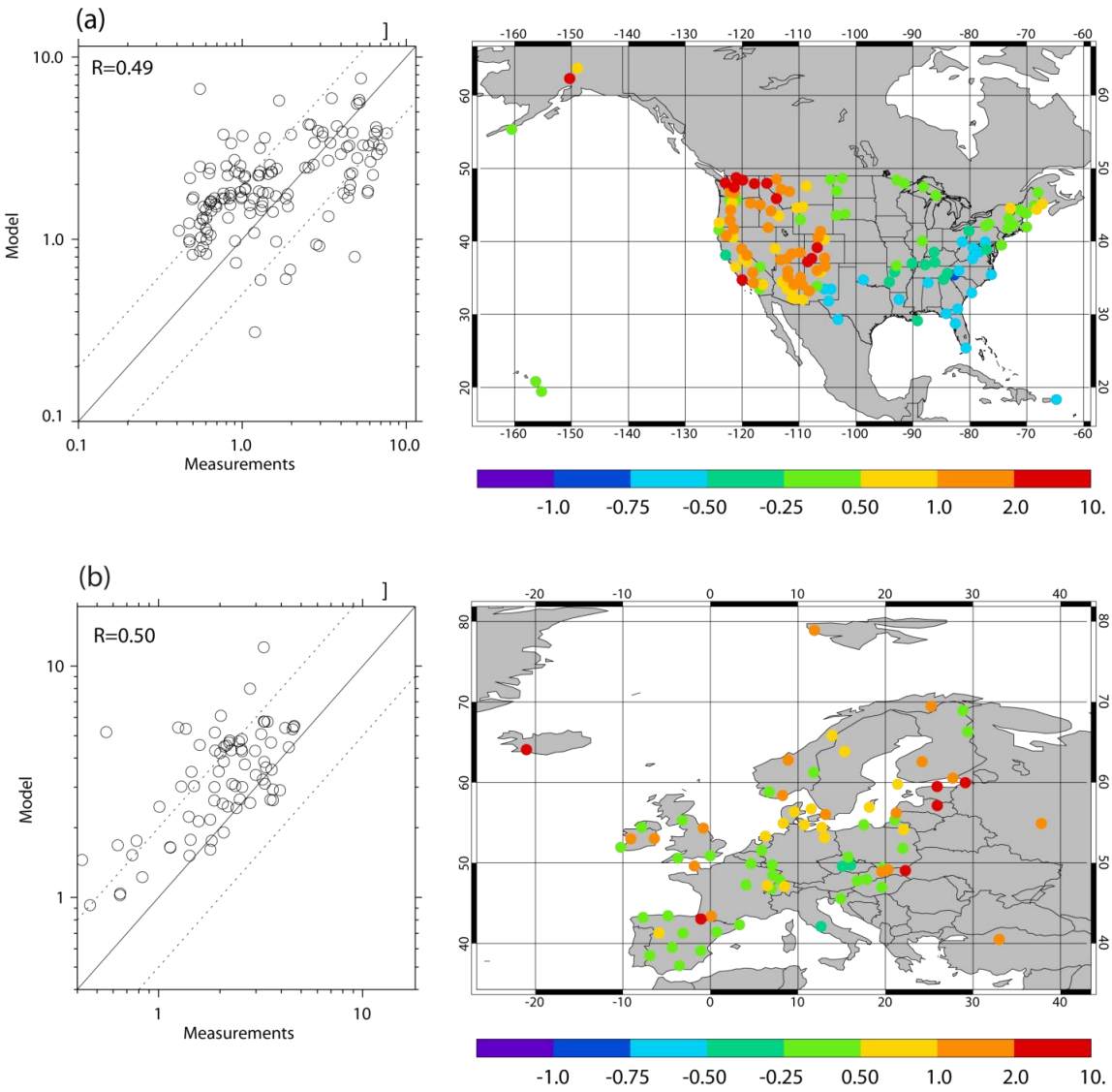

Figure C.10. Comparison of simulated annual average surface SO_4 concentrations with the IMPROVE surface monitoring network for remote locations in the United States and with the EMEP surface monitoring network for Europe (average 2002-2003). The panels on the right show a comparison of modeled and measured concentrations [(modeled-observed)/observed] in $\mu g/m^3$.

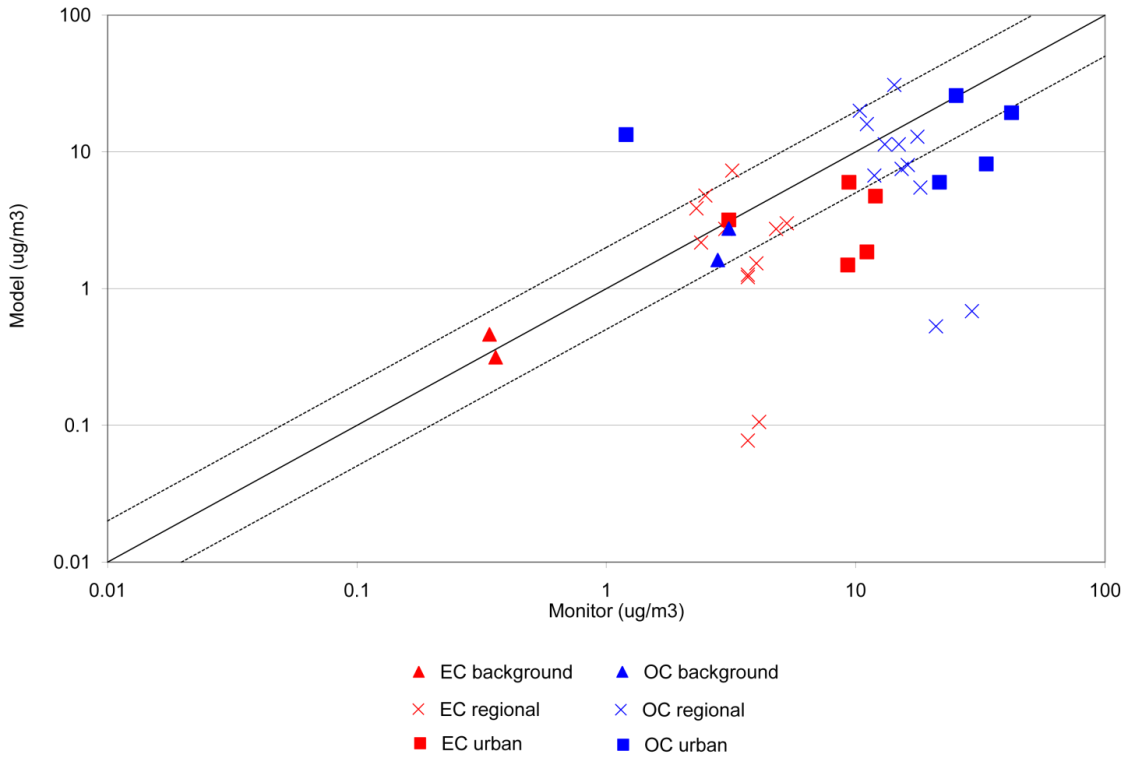

Figure C.11. Comparison of modeled annual average (2002) BC and OC with observed annual average EC and OC at 15 sites in China in 2006 (Zhang et al. 2008).

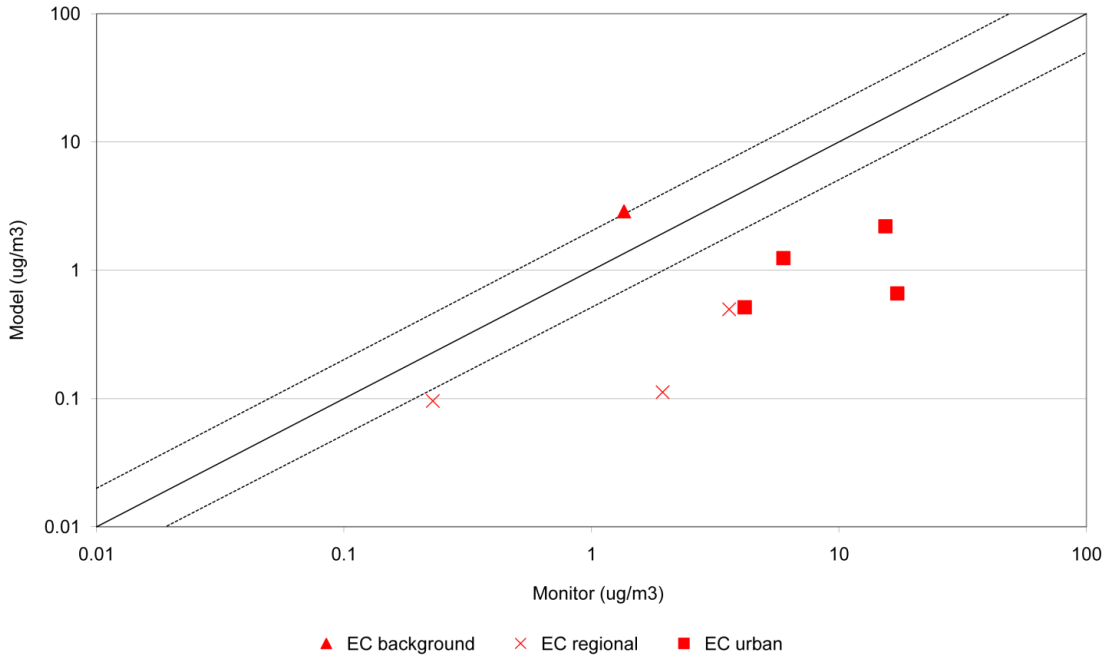

Figure C.12. Comparison of modeled annual average BC (2002) with observed EC in India for the pre-monsoon season (average January-May) at eight sites in India in 2006 (Beegum et al. 2009).

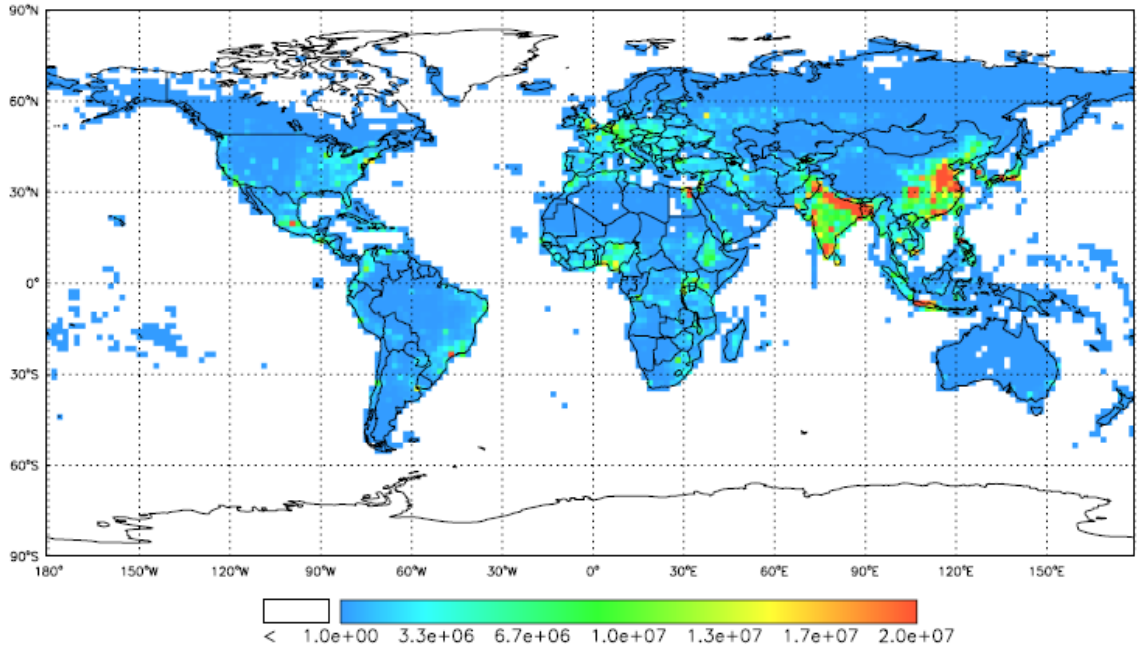

Figure C.13. 2006 population from Landscan database (Oak Ridge National Laboratory 2008) aggregated to MOZART-4 grid.

Table C.3. Population aged 30 and older, baseline total (for all population), cardiopulmonary (for the population ≥30), and lung cancer (for the population ≥30) mortality rates, and simulated simple and population-weighted average $PM_{2.5}$ concentrations ($\mu g/m^3$) for the 2002 base case, for each region.

Region	Population 30+	Baseline Mortality Rates (% per year) All-cause	Cardio-pulmonary (30+)	Lung Cancer (30+)	Base Case $PM_{2.5}$ Concentration Range ($\mu g/m^3$)
NA	2.70E+08	0.723	0.488	0.072	0.32 - 17.82
SA	1.50E+08	0.615	0.500	0.024	0.64 - 28.63
EU	3.46E+08	1.000	0.735	0.061	1.08 - 29.87
FSU	1.66E+08	1.514	1.421	0.055	0.57 - 27.49
AF/ME	3.59E+08	1.206	0.746	0.014	0.40 - 23.71
IN	5.87E+08	0.919	0.835	0.026	1.69 - 185.36
EA	8.03E+08	0.741	0.679	0.046	2.26 - 233.65
SE/AU	2.61E+08	0.599	0.490	0.040	0.11 - 86.89
World	2.94E+09	0.858	0.676	0.038	0.10 - 233.65

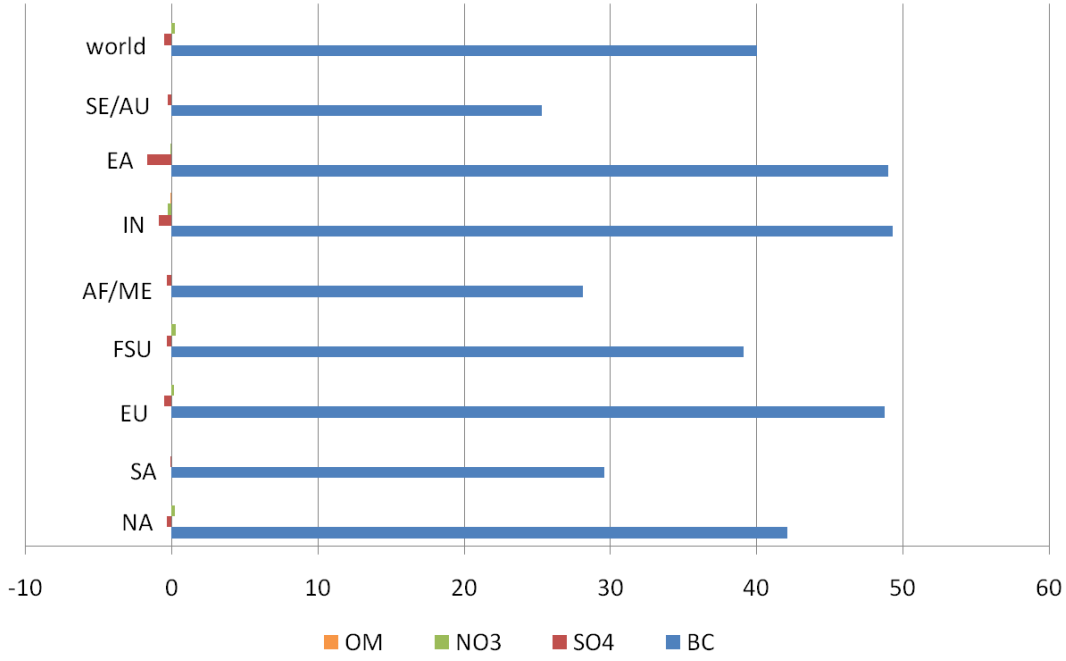

Figure C.14. Percentage reduction in annual average concentrations (ng/m^3) of $PM_{2.5}$ species for halving global anthropogenic BC emissions relative to the base case.

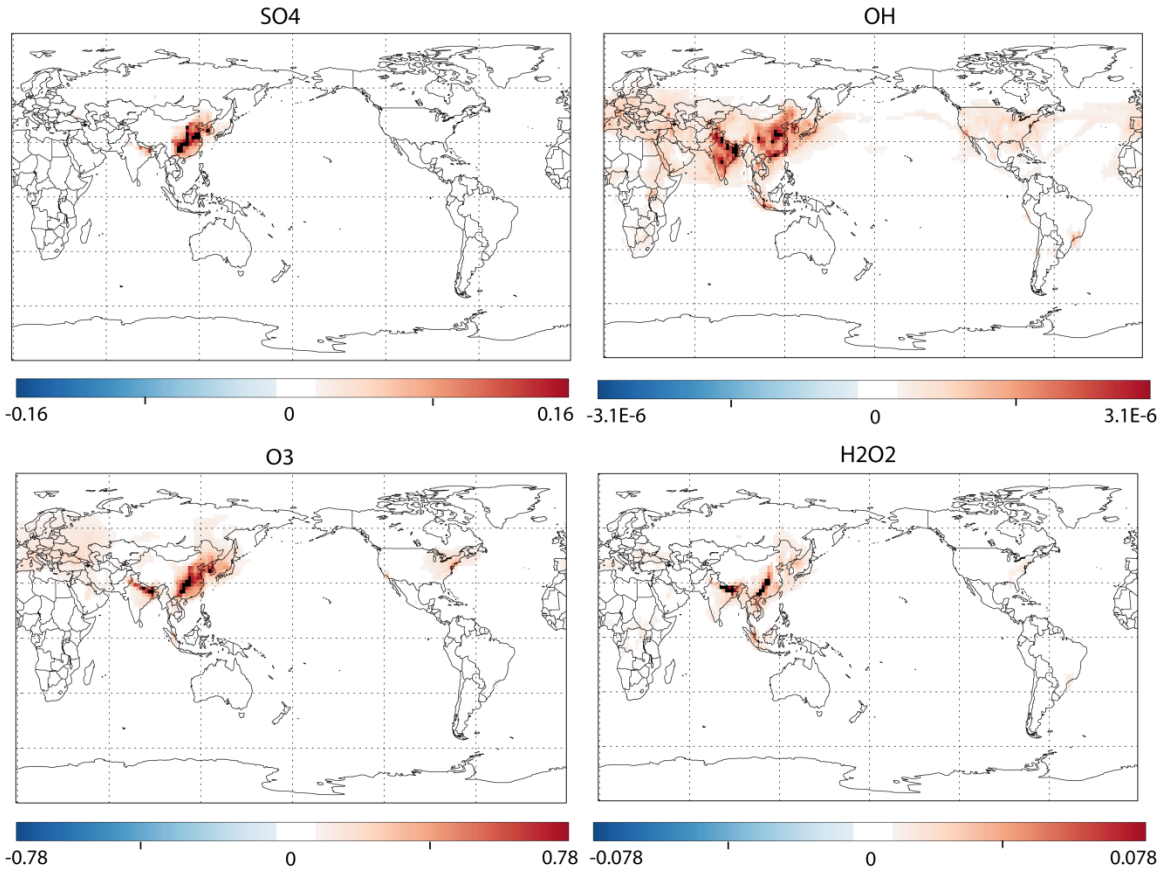

Figure C.15. Change in annual average surface SO_4, OH, O_3, and H_2O_2 concentrations (ppb) for halving global anthropogenic BC emissions relative to the base case.

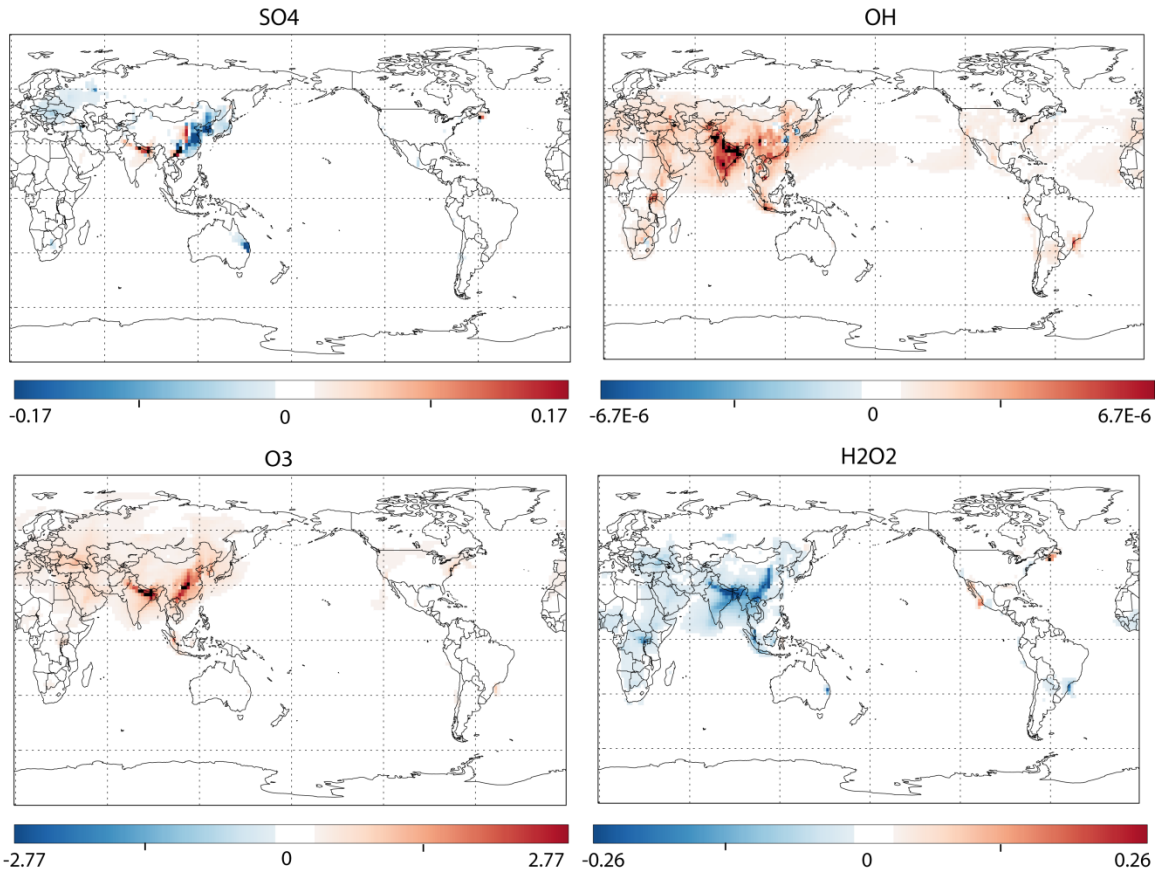

Figure C.16. As Figure C.15 but for halving global anthropogenic BC+OC emissions.

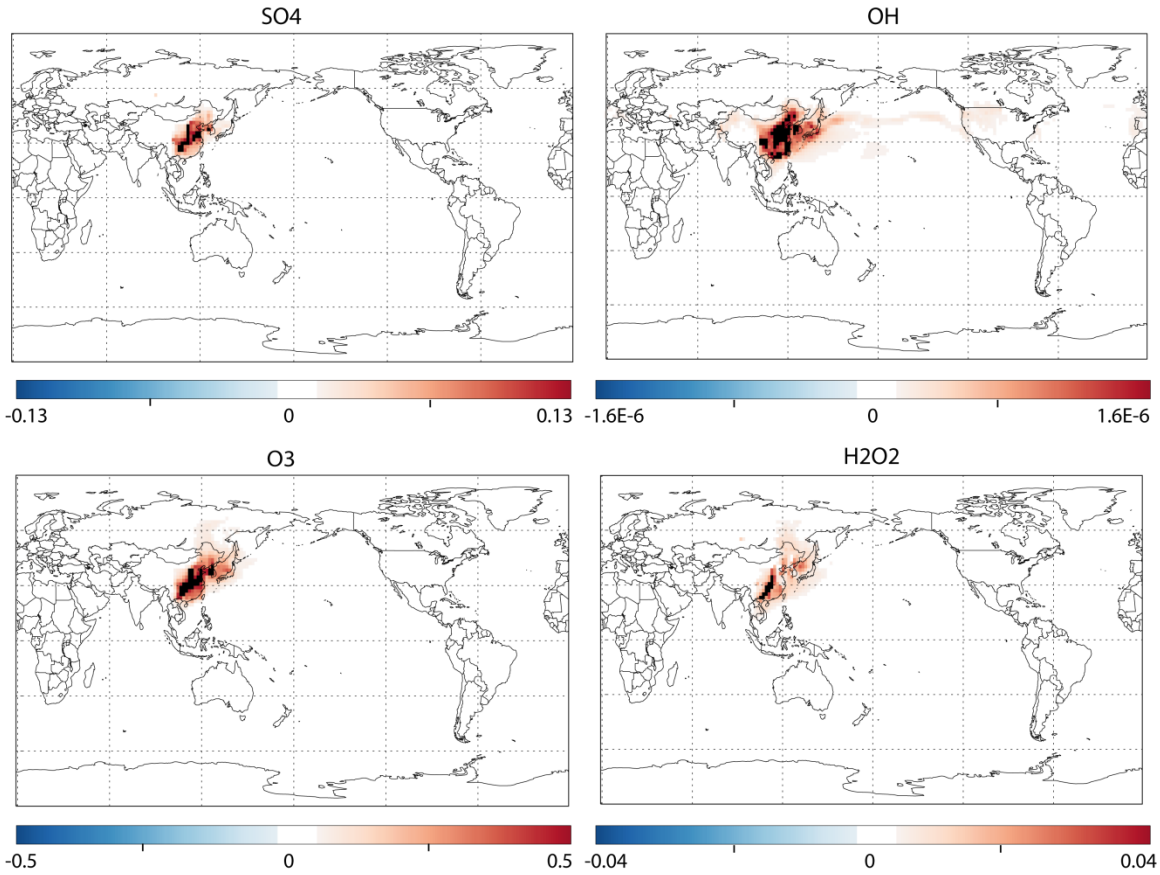

Figure C.17. As Figure C.15 but for halving anthropogenic BC emissions in EA only.

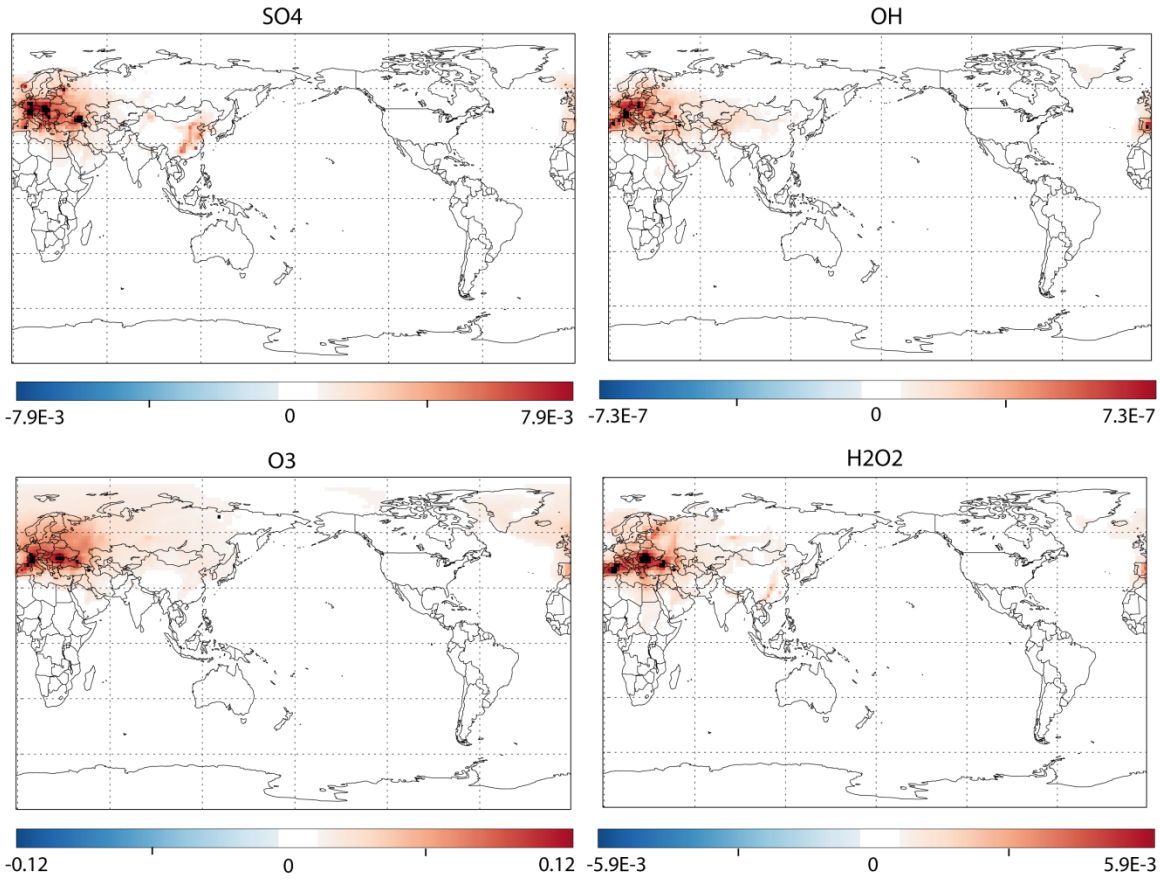

Figure C.18. As Figure C.15 but for halving anthropogenic BC emissions in EU only.

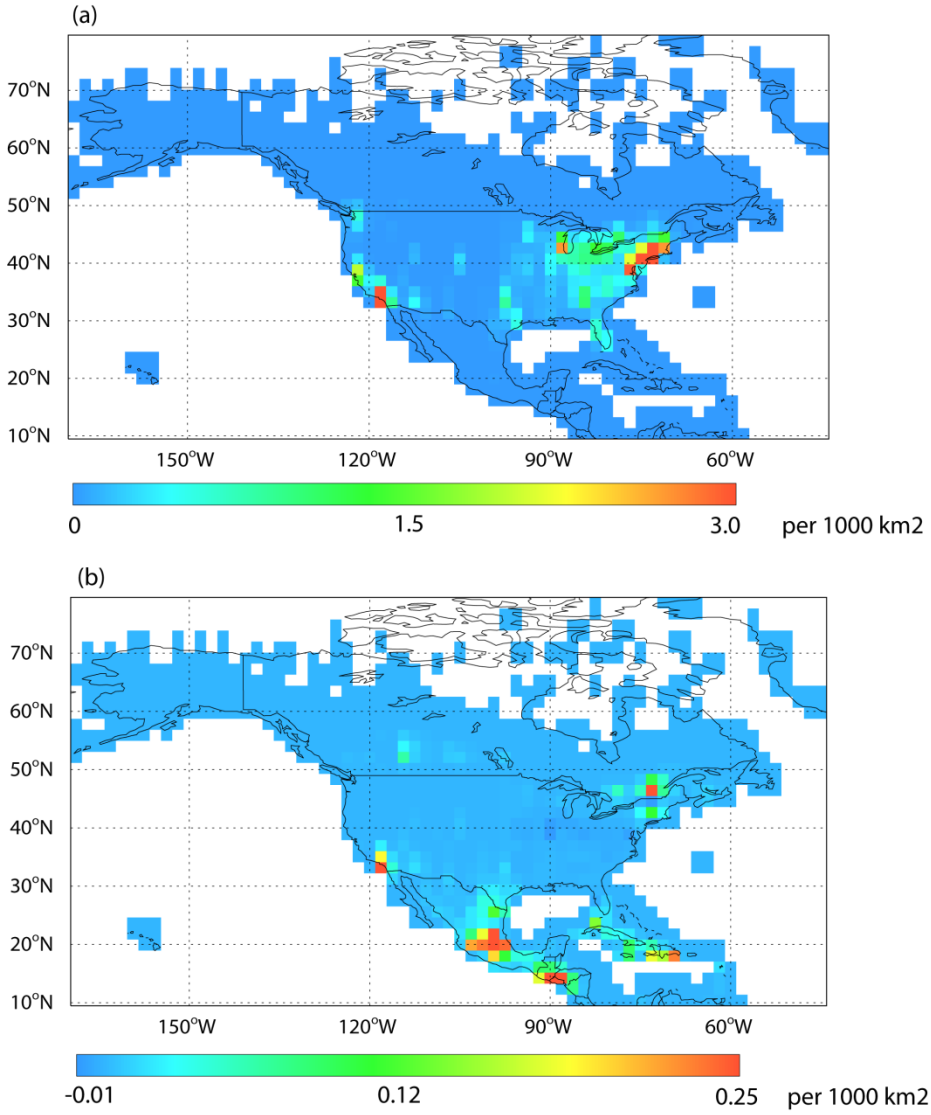

Figure C.19. (a) Avoided premature deaths from halving US anthropogenic BC emissions relative to the base case, and (b) difference in avoided deaths from halving BC emissions in NA vs. the US only (NA reduction minus US reduction).

Appendix D. Guide to running MOZART-4 on UNC's Kure cluster

Running MOZART-4 requires three steps: compiling the pre-processor, compiling the model, and running the model. Compiling the pre-processor and model takes 10-15 minutes and must only be done once for each model configuration. Running the model takes much longer and must be performed for each experimental setup. For example, if you change a chemical mechanism, you must re-compile the pre-processor and model. However, if you are only changing emissions inputs, you can run the model many times with different emissions after compiling the pre-processor and model only once.

First create MOZART-4 directory hierarchy:

/largefs/[onyen]/mz4.6/

- proc/
- model/
- run/

Compiling the pre-processor

You should have six directories within the proc/ directory – bin/; bkend/; inputs/; output/; procfiles/; src/; tmp/

In the inputs/ directory, you should have a symbolic link to the mozpp executable in the proc/bin/ directory and a .inp input file. To compile the pre-processor, issue the following command in the inputs/ directory:

- ./mozpp mz4.test.inp

If the pre-processor compiled successfully, you will have new files in the proc/output/ directory:

- moz.mat.F90
- moz.mods.F90
- mozpp.subs.tar
- moz.subs.F90
- mz4.test.dat
- mz4.test.doc
- params.h

Ignore each of these files except the .tar file, which you will need to compile the model, the .dat file, which you will need to run the model, and the .doc file which contains the specified run parameters.

Compiling the model

You should have several directories within the model/ directory:

- Base
- bin
- chem

- OBJ
- pp

And several files:

- Makefile
- make_test

Open the Makefile and redirect it to point to your netcdf library.

Create a directory called “pp_test/” and copy the .tar file you created in the proc step into this new directory. Un-tar the .tar file you just copied over.

- tar –xvf mozpp.subs.tar

Edit make_test to point to the new pp_test/ directory (instead of pp/ (set ppdir=”$pwd/pp_test”). Check the name of the output executable listed in the make file. This will be the name of the file created in the bin/ directory.

To compile the model, issue the following command:

- ./make_test

If the model compiles successfully, you will have a new executable in the model/bin/ directory with the name you specified in make_test. Each time you create a new model configuration, create a new pp_XXXX/ directory, modify the make file to point to that pp_XXXX/ directory, and change the name of the output file to reflect the new configuration.

Running the model

A new directory should be created for each model run. The name of the run directory should be logical and should refer to the unique parameters of that run.

1) Create a directory named run_test/. You will need several files in this directory: mz4.nml, run_mz4_openmp, runScript, sim.params.nml. In addition, copy the .doc and .dat files from the proc/output/ directory into this directory. Create hist/ and rest/ directories.

The mz4.6/mozart_data/ directory includes all the input files needed for MOZART to run, including meteorological data, emissions, boundary conditions, initial conditions, etc.

2) Change into the mozart_data directory. Go into each directory and look at the header of several of the netcdf files by issuing the following command:

- ncdump –h filename | less

Piping the ncdump –h command through the less command displays the resulting information one page at a time. You can scroll through the pages using Page Up and Page Down. This header information tells you what variables are contained within the file, as well as some information on the source of the data and the years to which the data correspond.

Some data, such as meteorology, changes daily. You may want to check to see the dates to which each file corresponds. To see the dates to which the meteorology files correspond, issue the following command:

- ncdump –v date ncepfilename

Now the header information will be followed by a listing of the dates contained within the netcdf file. The dates correspond to the format YYYYMMDD.

3) Edit the namelist file (mz4.nml) to specify how long to run, how often to write output and restart files, and file locations for meteorology, emissions, initial conditions, boundary conditions, etc. The namelist file should be edited for each model run.

Typical output frequencies are monthly, daily, and hourly output files and monthly restart files. If for some reason, your model crashes while running, restart files allow you to restart the model at some mid-point, saving time and computing resources. To run the model in restart mode, copy the mz4.nml file to mz4.nml_restart. Change the "sim_type" from "INITIAL" to "RESTART." Make sure you also change your run_mz4 file to point to this new .nml file (or you can create a new run_mz4_restart file that points to the new .nml file – just make sure to submit run_mz4_restart to the queue instead of run_mz4).

4) Edit the run scripts to point to the namelist file and the executable created in the model step:

- run_mz4_openmp
- runScript

5) Run the model by invoking the following command:

- bsub < run_mz4_openmp

The job has now been submitted to the default "week" queue on Kure.

6) Check to see that the job is running by issuing the following command:

- bjobs

Your job should be listed with a status denoting PEND or RUN. When the job finishes, it will write out a log file, mz4.test.log. If your run was successful, you will see a series of files in the hist/ directory named h0001.nc, ha0001.nc, hb0001.nc, hc0001.nc, hd0001.nc

Useful rules to remember

- The computing resources requested to run MOZART-4 are dependent on your choice of model resolution.
    - The number of CPUs requested must evenly divide into the number of latitudes.
    - There must be four latitudes at a minimum per MPI process

      For example, with 96 latitudes, the maximum number of CPUs that can be requested is 24.
- The temporal resolution of restart files should match the temporal resolution of the history output files with the longest averaging time. For instance, if you are writing out history output files with monthly, daily, and hourly output files, you should write out monthly (or multiples of monthly) restart files. Restarting from the middle of the month may cause averaging errors in the monthly history output file.
- All output variables must be specified in the "input" file, except for aerosol optical depth variables, which must be specified in the .nml file.
- UNC specific:
    - Running on Emerald requires a workaround to read the .nml file; Running on Kure does not.

- Running in hybrid MPI+OpenMP requires two run scripts on Kure, but only one on Emerald (examples below).
- At least on Emerald, output files specified in the “input” file must be separated into several smaller files. Otherwise, not enough memory.

Sample runscript on Emerald

run_mz4:

```
#!/bin/csh –f

rm –f mz4.log

#BSUB –n 16

#BSUB –o mz4.log

#BSUB –J mz4_run

setenv LSF_PAM_HOSTLIST_USE unique

setenv OMP_NUM_THREADS 4

setenv KMP_STACKSIZE 96m

setenv NL  mz4.nml

setenv EXEC ../model/bin/mz4.6_mpi

time mpirun.lsf –pam “-n 4” $EXEC $NL
```

Sample runscripts on Kure

run_mz4_openmp:

```
#!/bin/csh –f
rm –f mz4.test.log
#BSUB –n 32
#BSUB –o mz4.test.log
#BSUB –J mz4_test
#BSUB –q week
setenv LSF_PAM_HOSTLIST_USE unique
mpirun.lsf –pam “-n 8” ./runScript
```

runScript:

```
#!/bin/csh –f
setenv OMP_NUM_THREADS 4
setenv KMP_STACKSIZE 96m
setenv NL mz4.nml
setenv EXEC ../model/bin/mz4.6_test
$EXEC $NL
```

MOZART resources

MOZART-4 wiki, maintained by Louisa Emmons at NCAR:

https://wiki.ucar.edu/display/mozart4/Home

NCAR MOZART-4 page: http://www.acd.ucar.edu/gctm/mozart/

Emmons et al. 2010 - Paper describing MOZART-4 published in Geoscientific Model Development: http://www.geosci-model-dev.net/3/43/2010/gmd-3-43-2010.html

Larry Horowitz's (GFDL) MOZART webpage for info on earlier versions:

http://www.gfdl.noaa.gov/mozart

MOZART on Wikipedia: http://en.wikipedia.org/wiki/MOZART_%28model%29

Tie et al. 2005 – Paper describing aerosol scheme used in MOZART-4 published in G. Geophys. Res.: http://www.agu.org/pubs/crossref/2005/2004JD005359.shtml

REFERENCES

Akimoto, H. (2003). Global air quality and pollution. Science 302, 1716-1719.

Anderson, H. R., Atkinson, R. W., Peacock, J. L., Marston, L., and Konstantinou, K. (2004). Meta-analysis of time-series studies and panel studies of particulate matter (PM) and ozone (O3). Report of a WHO Task Group. Copenhagen: World Health Organization, 1-68.

Anenberg, S. C., Talgo, K., Dolwick, P., Jang, C., Arunachalam, S., and West, J. J. Impacts of global, regional, and sectoral black carbon emission reductions on surface air quality and human mortality. Atmospheric Chemistry and Physics.

Anenberg, S. C., Horowitz, L. W., Tong, D. Q., and West, J. J. (2010). An estimate of the global burden of anthropogenic ozone and fine particulate matter on premature human mortality using atmospheric modeling. Environmental Health Perspectives 118, 1189-1195.

Anenberg, S. C., Horowitz, L. W., Tong, D. Q., and West, J. J. (2011). The global burden of outdoor air pollution on mortality: Anenberg et al. respond. Environmental Health Perspectives.

Anenberg, S. C. et al. (2009). Intercontinental impacts of ozone pollution on human mortality. Environmental Science & Technology 43, 6482–6487.

Atkinson, R. W., Cohen, A., Mehta, S., and Anderson, H. R. (2011). Systematic review and meta-analysis of epidemiological time-series studies on outdoor air pollution and health in Asia. Air Quality, Atmosphere & Health, 1–9.

Balkanski, Y., Myhre, G., Gauss, M., Radel, G., Highwood, E. J., and Shine, K. P. (2010). Direct radiative effect of aerosols emitted by transport: from road, shipping and aviation. Atmospheric Chemistry and Physics 10, 4477-4489.

Barrett, S. R. H., Britter, R. E., and Waitz, I. A. (2010). Global mortality attributable to aircraft cruise emissions. Environmental Science & Technology 44, 325–346.

Beegum, S., Moorthy, K., Babu, S., Satheesh, S., Vinoj, V., Badarinath, K., Safai, P., Devara, P., and Singh, S. (2009). Spatial distribution of aerosol black carbon over India during pre-monsoon season. Atmospheric Environment 43, 1071-1078.

Bell, M. L., and Davis, D. L. (2001). Reassessment of the lethal London fog of 1952: novel indicators of acute and chronic consequences of acute exposure to air pollution. Environmental Health Perspectives 109, 389-394.

Bell, M. L., Dominici, F., and Samet, J. M. (2005). A meta-analysis of time-series studies of ozone and mortality with comparison to the national morbidity, mortality, and air pollution study. Epidemiology 16, 436-445.

Bell, M. L., and Ebisu, K. (2010). Community-level spatial heterogeneity of chemical constituent levels of fine particulates and implications for epidemiological research. Journal of Exposure Science and Environmental Epidemiology.

Bell, M. L., Ebisu, K., Peng, R. D., Samet, J. M., and Dominici, F. (2009). Hospital admissions and chemical composition of fine particle air pollution. American Journal of Respiratory and Critical Care Medicine 179, 1115-1120.

Bell, M. L., McDermott, A., Zeger, S. L., Samet, J. M., and Dominici, F. (2004). Ozone and short-term mortality in 95 US urban communities, 1987-2000. Journal of the American Medical Association 292, 2372-2378.

Bloomer, B. J., Stehr, J. W., Piety, C. A., Salawitch, R. J., and Dickerson, R. R. (2009). Observed relationship of ozone air pollution with temperature and emissions. Geophysical Research Letters 36, 1-5.

Bollen, J., Hers, S., and Zwaan, B. van der (2010). An integrated assessment of climate change, air pollution, and energy security policy. Energy Policy 38, 4021-4030.

Bond, T. C., Bhardwaj, E., Dong, R., Jogani, R., Jung, S., Roden, C., Streets, D. G., and Trautmann, N. M. (2007). Historical emissions of black and organic carbon aerosol from energy-related combustion, 1850-2000. Global Biogeochemical Cycles 21, 1-16.

Bond, T. C., Streets, D. G., Yarber, K. F., Nelson, S. M., Woo, J.-H., and Klimont, Z. (2004). A technology-based global inventory of black and organic carbon emissions from combustion. Journal of Geophysical Research 109, D14203.

Bond, T. C., and Sun, H. (2005). Can reducing black carbon emissions counteract global warming? Environmental Science & Technology 39, 5921–5926.

Brunekreef, B. (2009). Effects of Long-term Exposure to Traffic-related Air Pollution on Respiratory Cardiovascular Mortality in the Netherlands: The NLCS-AIR Study. Research Report Health Effects Institute, 5-71; discussion 73-89.

Castro, T., Madronich, S., Rivale, S., Muhlia, A., and Mar, B. (2001). The influence of aerosols on photochemical smog in Mexico City. Atmospheric Environment 35, 1765-1772.

Cohen, A. J. et al. (2004). Urban air pollution. In Comparative Quantification of Health Risks M. Ezzati, A. D. Lopez, A. Rodgers, and C. J. L. Murray, eds. (Geneva: World Health Organization), pp. 1353-1434.

Cooke, R. M., Wilson, A. M., Tuomisto, J. T., Morales, O., Tainio, M., and Evans, J. S. (2007). A Probabilistic Characterization of the Relationship between Fine Particulate Matter and Mortality: Elicitation of European Experts. Environmental Science & Technology 41, 6598-6605.

Cooke, W. F., Liousse, C., Cachier, H., and Feichter, J. (1999). Construction of a 1° × 1° fossil fuel emission data set for carbonaceous aerosol and implementation and radiative impact in the ECHAM4 model. Journal of Geophysical Research 104, 22137-22162.

Corbett, J. J., Winebrake, J. J., Green, E. H., Kasibhatla, P., Eyring, V., and Lauer, A. (2007). Mortality from ship emissions: A global assessment. Environmental Science & Technology 41, 8512-8518.

Dentener, F. et al., others (2006). Emissions of primary aerosol and precursor gases in the years 2000 and 1750 prescribed data-sets for AeroCom. Atmospheric Chemistry and Physics 6, 4321–4344.

Dickerson, R. R., Andreae, M. O., Campos, T., Mayol-Bracero, O. L., Neusuess, C., and Streets, D. G. (2002). Analysis of black carbon and carbon monoxide observed over the Indian Ocean: Implications for emissions and photochemistry. Journal of Geophysical Research 107, 8017.

Dickerson, R. R., Kondragunta, S., Stenchikov, G., Civerolo, K. L., Doddridge, B. G., and Holben, B. N. (1997). The impact of aerosols on solar ultraviolet radiation and photochemical smog. Science 278, 827-830.

Dockery, D. W., Pope, C. A., Xu, X., Spengler, J. D., Ware, J. H., Fay, M. E., Ferris, B. G., and Speizer, F. E. (1993). An association between Air pollution and mortality in six U.S. cities. The New England Journal of Medicine 329, 1753-1759.

Dominici, F., Peng, R. D., Barr, C. D., and Bell, M. L. (2010). Protecting human health from air pollution: Shifting from a single-pollutant to a multipollutant approach. Epidemiology 21, 187-194.

Donkelaar, A. van, Martin, R., Brauer, M., Kahn, R., Levy, R., Verduzco, C., and Villeneuve, P. (2010). Global estimates of ambient fine particulate matter concentrations from satellite-based aerosol optical depth: Development and applciation. Environmental Health Perspectives 118, 847-855.

Duncan, B. N., West, J. J., Yoshida, Y., Fiore, A. M., and Ziemke, J. R. (2008). The influence of European pollution on ozone in the Near East and northern Africa. Atmospheric Chemistry and Physics 8, 2267-2283.

Dunlea, E. J. et al. (2009). Evolution of Asian aerosols during transpacific transport in INTEX-B. Atmospheric Chemistry and Physics 9, 7257-7287.

Emmons, L. K. et al. (2010a). Impact of Mexico City emissions on regional air quality from MOZART-4 simulations. Atmospheric Chemistry and Physics 10, 6195-6212.

Emmons, L. K. et al. (2010b). Description and evaluation of the Model for Ozone and Related chemical Tracers, version 4 (MOZART-4). Geosci. Model Dev 3, 43–67.

Ezzati, M., Hoorn, S. V., Lopez, A. D., Rodgers, A., Mathers, C. D., and L, C. J. (1999). Comparative Quantification of Mortality and Burden of Disease Attributable to Selected Risk Factors. In Global Burden of Disease and Risk Factors, pp. 241-396.

Fann, N., and Risley, D. (2011). The public health context for PM2.5 and ozone air quality trends. Air Quality, Atmosphere & Health, 1-11.

Fiore, A. M. et al. (2009). Multimodel estimates of intercontinental source-receptor relationships for ozone pollution. Journal of Geophysical Research 114, 1-21.

Fiore, A. M., West, J. J., Horowitz, L. W., Naik, V., and Schwarzkopf, M. D. (2008). Characterizing the tropospheric ozone response to methane emission controls and the benefits to climate and air quality. Journal of Geophysical Research 113, 1-16.

Franklin, M., Koutrakis, P., and Schwartz, J. (2008). The role of particle composition on the association between PM2. 5 and mortality. Epidemiology 19, 680-689.

Fuglestvedt, J. S., Shine, K. P., Berntsen, T., Cook, J., Lee, D. S., Stenke, A., Skeie, R. B., Velders, G. J. M., and Waitz, I. a (2009). Transport impacts on atmosphere and climate: Metrics. Atmospheric Environment, 1-30.

Gilardoni, S., Vignati, E., and Wilson, J. (2011). Using measurements for evaluating black carbon modeling. Atmospheric Chemistry & Physics 11, 439-455.

Ginoux, P., Horowitz, L. W., Ramaswamy, V., Geogdzhayev, I. V., Holben, B. N., Stenchikov, G., and Tie, X. (2006). Evaluation of aerosol distribution and optical depth in the Geophysical Fluid Dynamics Laboratory coupled model CM2. 1 for present climate. Journal of Geophysical Research 111, D22210.

Global Atmospheric Pollution Forum (2010). Discussion Paper: Atmospheric Pollution: Developing a Global Approach.

Granier, C. et al. (2005). POET, a database of surface emissions of ozone precursors.

Greenbaum, D., and Shaikh, R. (2010). First steps toward multipollutant science for air quality decisions. Epidemiology 21, 195-197.

Haines, A. et al. (2010). Public health benefits of strategies to reduce greenhouse-gas emissions: overview and implications for policy makers. The Lancet 374, 2104–2114.

Hansen, J., Sato, M., Ruedy, R., Lacis, A., and Oinas, V. (2000). Global warming in the twenty-first century: an alternative scenario. Proceedings of the National Academy of Sciences of the United States of America 97, 9875-80.

Hansen, J., and Nazarenko, L. (2004). Soot climate forcing via snow and ice albedos. Proceedings of the National Academy of Sciences 101, 423-428.

He, S., and Carmichael, G. R. (1999). Sensitivity of photolysis rates and ozone production in the troposphere to aerosol properties. J. Geophys. Res 104, 26307-26324.

Health Effects Institute (2010). Public Health and Air Pollution in Asia (PAPA): Coordinated Studies of Short-Term Exposure to Air Pollution and Daily Mortality in Four Cities (Boston, MA).

Health Effects Institute Scientific Oversight Committee (2004). Health Effects of Outdoor Air Pollution in Developing Countries of Asia : A Literature Review (Boston, MA).

Hoek, G., Brunekreef, B., Goldbohm, S., Fischer, P., and Brandt, P. A. van den (2002). Association between mortality and indicators of traffic-related air pollution in the Netherlands: a cohort study. The Lancet 360, 1203–1209.

Holland, M., Hunt, A., Hurley, F., Navrud, S., and Watkiss, P. (2005). Methodology for the Cost-Benefit analysis for CAFE : Volume 1 : Overview of Methodology February 2005.

Holloway, T., Fiore, A., and Hastings, M. G. (2003). Intercontinental transport of air pollution: will emerging science lead to a new hemispheric treaty? Evironmental Science & Technology 37, 4535–4542.

Horowitz, L. W. (2006). Past, present, and future concentrations of tropospheric ozone and aerosols: Methodology, ozone evaluation, and sensitivity to aerosol wet removal. Journal of Geophysical Research 111, D22211.

Horowitz, L. W. et al. (2003). A global simulation of tropospheric ozone and related tracers: Description and evaluation of MOZART, version 2. Journal of Geophysical Research 108, 4784.

Horvath, H. (1993). Atmospheric light absorption—A review. Atmospheric Environment. Part A. General Topics 27, 293-317.

Hubbell, B., Fann, N., and Levy, J. I. (2009). Methodological considerations in developing local-scale health impact assessments: balancing national, regional, and local data. Air Quality, Atmosphere & Health 2, 99-110.

Hubbell, B. J., Hallberg, A., McCubbin, D. R., and Post, E. (2004). Health-related benefits of attaining the 8-hr ozone standard. Environmental Health Perspectives 113, 73-82.

Ito, K., De Leon, S. F., and Lippmann, M. (2005). Associations between ozone and daily mortality - Analysis and meta-analysis. Epidemiology 16, 446-457.

Jacob, D., and Winner, D. (2009). Effect of climate change on air quality. Atmospheric Environment 43, 51-63.

Jacobson, M. Z. (1998). Studying the effects of aerosols on vertical photolysis rate coefficient and temperature profiles over an urban airshed. Journal of Geophysical Research 103, 10593-10604.

Jacobson, M. Z. (2002). Control of fossil-fuel particulate black carbon and organic matter, possibly the most effective method of slowing global warming. Journal of Geophysical Research 107, 4410.

Jacobson, M. Z. (2008). On the causal link between carbon dioxide and air pollution mortality. Geophysical Research Letters 35, 1-5.

Jacobson, M. Z. (2010). Short-term effects of controlling fossil-fuel soot, biofuel soot and gases, and methane on climate, Arctic ice, and air pollution health. Journal of Geophysical Research 115, D14209.

Jerrett, M., Burnett, R., Pope, C. A., Ito, K., Thurston, G., Krewski, D., Shi, Y., Calle, E., and Thun, M. (2009). Long-term ozone exposure and mortality. The New England journal of medicine 360, 1085-95.

Jerrett, M., Burnett, R. T., Pope, C. A., Ito, K., Thurston, G., Krewski, D., Shi, Y., Calle, E., and Thun, M. (2009). Long-term ozone exposure and mortality. The New England Journal of Medicine 360, 1085-1095.

Junker, C., and Liousse, C. (2008). A global emission inventory of carbonaceous aerosol from historic records of fossil fuel and biofuel consumption for the period 1860-1997. Atmospheric Chemistry and Physics 8, 1-13.

Kalnay, E. C. et al. (1996). The NCEP/NCAR 40-year reanalysis project. Bulletin of the American Meteorological Society 77, 437–471.

Keating, T. J., West, J. J., and Farrell, A. E. (2004). Prospects for international management of intercontinental air pollution transport. In Intercontinental Transport of Air Pollution A. Stohl, ed. (Berlin: Springer), p. 295–320.

Kim, C. S. et al. (2011). Lung function and inflammatory responses in healthy young adults exposed to 0.06 ppm ozone for 6.6 hours. American Journal of Respiratory and Critical Care Medicine.

Kistler, R. et al. (2001). NCEP-NCAR 50-year reanalysis: monthly mean CD rom and documentation. Bull. Amer. Meteor. Soc. 82, 247 - 267.

Koch, D., Bond, T. C., Streets, D., Unger, N., and Werf, G. R. van der (2007). Global impacts of aerosols from particular source regions and sectors. Journal of Geophysical Research 112, 1-24.

Koch, D., and Del Genio, A. D. (2010). Black carbon semi-direct effects on cloud cover: review and synthesis. Atmospheric Chemistry and Physics 10, 7685-7696.

Koch, D. et al. (2009). Evaluation of black carbon estimations in global aerosol models. Atmospheric Chemistry and Physics 9, 9001–9026.

Kopp, R. E., and Mauzerall, D. L. (2010). Assessing the climatic benefits of black carbon mitigation. Proceedings of the National Academy of Sciences of the United States of America 107, 11703-11708.

Krewski, D., Burnett, R., Goldberg, M., Siemiatycki, J., Jerrett, M., Abramowicz, M., and White, W. (2000). Reanalysis of the Harvard Six Cities Study and the American Cancer Society Study of Particulate Air Pollution and Mortality.

Krewski, D. et al. (2009). Extended follow-up and spatial analysis of the American Cancer Society study linking particulate air pollution and mortality (Boston, MA: Health Effects Institute).

Laden, F., Schwartz, J., Speizer, F. E., and Dockery, D. W. (2006). Reduction in fine particulate air pollution and mortality: extended follow-up of the Harvard Six Cities study. American Journal of Respiratory and Critical Care Medicine 173, 667-672.

Lamarque, J.-F. et al. (2010). Historical (1850–2000) gridded anthropogenic and biomass burning emissions of reactive gases and aerosols: methodology and application. Atmospheric Chemistry and Physics 10, 7017-7039.

Levy, H., Schwarzkopf, M. D., Horowitz, L., Ramaswamy, V., and Findell, K. L. (2008). Strong sensitivity of late 21st century climate to projected changes in short-lived air pollutants. Journal of Geophysical Research 113, D06102.

Levy, J. I., Chemerynski, S. M., and Sarnat, J. A. (2005). Ozone exposure and mortality: an empiric bayes metaregression analysis. Epidemiology 16, 458-468.

Li, G., Zhang, R., Fan, J., and Tie, X. (2005). Impacts of black carbon aerosol on photolysis and ozone. J. Geophys. Res 110, D23206.

Liao, H., Yung, Y. L., and Seinfeld, J. H. (1999). Effects of aerosols on tropospheric photolysis rates in clear and cloudy atmospheres. J. Geophys. Res 104, 23697-23707.

Liu, J., Mauzerall, D. L., and Horowitz, L. W. (2009). Evaluating inter-continental transport of fine aerosols:(2) Global health impact. Atmospheric Environment 43, 4339-4347.

Liu, J., Mauzerall, D. L., Horowitz, L. W., Ginoux, P., and Fiore, A. M. (2009). Evaluating inter-continental transport of fine aerosols: (1) Methodology, global aerosol distribution and optical depth. Atmospheric Environment 43, 4327-4338.

Martin, R. M., Jacob, D. J., Yantosca, R. M., Chin, M., and Ginoux, P. (2003). Global and regional decreases in tropospheric oxidants from photochemical effects of aerosols. J. Geophys. Res. 108, doi:10.1029/2002JD002622.

Ming, Y., Ramaswamy, V., Ginoux, P., and Horowitz, L. (2005). Direct radiative forcing of anthropogenic organic aerosol. Journal of Geophysical Research 110, D20208.

Murray, C., and Lopez, A. (1997). Alternative projections of mortality and disability by cause 1990-2020: Global Burden of Disease Study. The Lancet 349, 1498-1504.

National Academy of Sciences (2008). Estimating Mortality Risk Reduction and Economic Benefits from Controlling Ozone Air Pollution (Washington, DC).

Nemet, G. F., Holloway, T., and Meier, P. (2010). Implications of incorporating air-quality co-benefits into climate change policymaking. Environmental Research Letters 5, 014007.

Novakov, T., Menon, S., Kirchstetter, T. W., Koch, D., and Hansen, J. E. (2005). Aerosol organic carbon to black carbon ratios: Analysis of published data and implications for climate forcing. Journal of Geophysical Research 110, D21205.

Oak Ridge National Laboratory (2008). LandScan Global Population Database 2006.

Ohara, T., Akimoto, H., Kurokawa, J., Horii, N., Yamaji, K., Yan, X., and Hayasaka, T. (2007). An Asian emission inventory of anthropogenic emission sources for the period 1980? 2020. Atmospheric Chemistry and Physics 7, 4419-4444.

Olivier, J., Peters, J., Granier, C., Petron, G., Muller, J.-F., and Wallens, S. (2003). Present and future surface emissions of atmospheric compounds, POET Report #2, EU project EVK2-1999-00011.

Ostro, B., Feng, W.-Y., Broadwin, R., Green, S., and Lipsett, M. (2007). The effects of components of fine particulate air pollution on mortality in california: results from CALFINE. Environmental Health Perspectives 115, 13-19.

Ostro, B. D., Feng, W.-Y., Broadwin, R., Malig, B. J., Green, R. S., and Lipsett, M. J. (2008). The impact of components of fine particulate matter on cardiovascular mortality in susceptible subpopulations. Occupational and Environmental Medicine 65, 750-756.

Ostro, B. D., Tran, H., and Levy, J. I. (2006). The health benefits of reduced tropospheric ozone in California. Journal of the Air & Waste Management Association 56, 1007-1021.

Park, R. J., Jacob, D. J., Field, B. D., Yantosca, R. M., and Chin, M. (2004). Natural and transboundary pollution influences on sulfate-nitrate-ammonium aerosols in the United States: Implications for policy. Journal of Geophysical Research 109, D15204.

Peng, R. D., Bell, M. L., Geyh, A. S., McDermott, A., Zeger, S. L., Samet, J. M., and Dominici, F. (2009). Emergency admissions for cardiovascular and respiratory diseases and the chemical composition of fine particle air pollution. Environmental Health Perspectives 117, 957-963.

Pope III, C. A., Burnett, R. T., Krewski, D., Jerrett, M., Shi, Y., Calle, E. E., and Thun, M. J. (2009). Cardiovascular mortality and exposure to airborne fine particulate matter and cigarette smoke: shape of the exposure-response relationship. Circulation 120, 941-948.

Pope III, C. A., Burnett, R. T., Thun, M. J., Calle, E., Krewski, D., Ito, K., and Thurston, G. (2002). Lung cancer, cardiopulmonary mortality, and long-term exposure to fine particulate air pollution. Journal of the American Medical Association 287, 1132-1141.

Pope III, C. A., and Dockery, D. W. (2006). Health effects of fine particulate air pollution: lines that connect. Journal of the Air & Waste Management Association 56, 709–742.

Ramanathan, V., and Carmichael, G. (2008). Global and regional climate changes due to black carbon. Nature Geoscience 1, 221-227.

Reddy, M. S., and Boucher, O. (2007). Climate impact of black carbon emitted from energy consumption in the world□ s regions. Geophysical Research Letters 34, L11802.

Ren, C., Williams, G. M., Mengersen, K., Morawska, L., and Tong, S. (2008). Does temperature modify short-term effects of ozone on total mortality in 60 large eastern US communities? An assessment using the NMMAPS data. Environment International 34, 451-458.

Ren, C., Williams, G. M., Mengersen, K., Morawska, L., and Tong, S. (2009). Temperature enhanced effects of ozone on cardiovascular mortality in 95 large US communities, 1987-2000: Assessment using the NMMAPS data. Archives of Environmental & Occupational Health 64, 177-184.

Reynolds, C. C. O., and Kandlikar, M. (2008). Climate Impacts of Air Quality Policy: Switching to a Natural Gas-Fueled Public Transportation System in New Delhi. Environmental Science & Technology 42, 5860-5865.

Roman, H. A., Walker, K. D., Walsh, T. L., Conner, L., Richmond, H. M., Hubbell, B. J., and Kinney, P. L. (2008). Expert judgment assessment of the mortality impact of changes in ambient fine particulate matter in the US. Environmental science & technology 42, 2268–2274.

Schulz, M. et al. (2006). Radiative forcing by aerosols as derived from the AeroCom present-day and pre-industrial simulations. Atmospheric Chemistry and Physics 6, 5225-5246.

Schwartz, J., and Zanobetti, A. (2000). Using meta-smoothing to estimate dose-response trends across multiple studies, with application to air pollution and daily death. Epidemiology 11, 666-672.

Selin, N. E., Wu, S., Nam, K. M., Reilly, J. M., Paltsev, S., Prinn, R. G., and Webster, M. D. (2009). Global health and economic impacts of future ozone pollution. Environmental Research Letters 4, 044014.

Shindell, D., Faluvegi, G., Walsh, M., Anenberg, S. C., Van Dingenen, R., Muller, N. Z., Austin, J., Koch, D., and Milly, G. Climate, health, agricultural and economic impacts of tighter on-road vehicle emissions standards. Nature Climate Change.

Shindell, D. T., Levy, H., Schwarzkopf, M. D., Horowitz, L. W., Lamarque, J. F., and Faluvegi, G. (2008). Multimodel projections of climate change from short-lived emissions due to human activities. Journal of Geophysical Research 113, D11109.

Smith, K. R. et al. (2009). Public health benefits of strategies to reduce greenhouse-gas emissions: health implications of short-lived greenhouse pollutants. The Lancet 374, 2091-2103.

Smith, K. R., and Peel, J. L. (2010). Mind the Gap. Environmental Health Perspectives 118.

Staehelin, J., Harris, N. R. P., Appenzeller, C., and Eberhard, J. (2001). Ozone trends: A review. Reviews of Geophysics 39, 231-290.

Swall, J., and Foley, K. (2009). The impact of spatial correlation and incommensurability on model evaluation. Atmospheric Environment 43, 1204-1217.

Task Force on Hemispheric Transport of Air Pollution (TF HTAP) (2007). Hemispheric Transport of Air Pollution 2007. In Air Pollution Studies (New York and Geneva: United Nations Economic Commission for Europe).

Task Force on Hemispheric Transport of Air Pollution (TF HTAP) (2010). Hemispheric Transport of Air Pollution 2010. In Air Pollution Studies (New York and Geneva: United Nations Economic Commission for Europe).

Tie, X., Brasseur, G., Emmons, L., Horowitz, L., and Kinnison, D. (2001). Effects of aerosols on tropospheric oxidants: A global model study. Journal of Geophysical Research 106, 22931-22964.

Tie, X., Madronich, S., Walters, S., Edwards, D. P., Ginoux, P., Mahowald, N., Zhang, R. Y., Lou, C., and Brasseur, G. (2005). Assessment of the global impact of aerosols on tropospheric oxidants. Journal of Geophysical Research 110, D03204.

Unger, N., Bond, T. C., Wang, J. S., Koch, D. M., Menon, S., Shindell, D. T., and Bauer, S. (2010). Attribution of climate forcing to economic sectors. Proceedings of the National Academy of Sciences 107, 3382-3387.

United Nations Environment Programme (UNEP) Opportunities to limit near-term climate change: An integrated assessment of black carbon and tropospheric ozone and its precursors.

US Environmental Protection Agency (US EPA) (2008a). EPA/600/R-08/139 - Integrated Science Assessment for Particulate Matter (External Draft Review).

US Environmental Protection Agency (US EPA) (2010). Integrated Science Assessment for Particulate Matter EPA/600/R-08/139F.

US Environmental Protection Agency (US EPA) (2007). Latest findings on national air quality: Status and trends through 2006 (Research Triangle Park, NC).

US Environmental Protection Agency (US EPA) (2008b). National Air Quality - Status and Trends through 2007 (Research Triangle Park, NC).

US Environmental Protection Agency (US EPA) (2009). Risk Assessment to Support the Review of the PM Primary National Ambient Air Quality Standards (External Review Draft). EPA 450/P-09-006. (Research Triangle Park, NC).

Van der Werf, G. R., Randerson, J. T., Giglio, L., Collatz, G. J., Kasibhatla, P. S., and Arellano Jr, A. F. (2006). Interannual variability of global biomass burning emissions from 1997 to 2004. Atmospheric Chemistry and Physics 6, 3423-3341.

Vedal, S., and Kaufman, J. D. (2011). What does multi-pollutant air pollution research mean? American Journal of Respiratory and Critical Care Medicine 183, 4-6.

Vignati, E., Karl, M., Krol, M., Wilson, J., Stier, P., and Cavalli, F. (2010). Sources of uncertainties in modelling black carbon at the global scale. Atmospheric Chemistry and Physics 10, 2595-2611.

Vingarzan, R. (2004). A review of surface ozone background levels and trends. Atmospheric Environment 38, 3431-3442.

Volz, A., and Kley, D. (1988). Evaluation of the Montsouris series of ozone measurements made in the nineteenth century. Nature 332, 240-243.

Wesson, K., Fann, N., Morris, M., Fox, T., and Hubbell, B. (2010). A multi-pollutant, risk-based approach to air quality management: Case study for Detroit. Atmospheric Pollution Research 1, 296-304.

West, J. J., Fiore, A. M., Horowitz, L. W., and Mauzerall, D. L. (2006). Global health benefits of mitigating ozone pollution with methane emission controls. Proceedings of the National Academy of Sciences 103, 3988-3993.

West, J. J., Naik, V., Horowitz, L. W., and Fiore, A. M. (2009a). Effect of regional precursor emission controls on long-range ozone transport- Part 1: Short-term changes in ozone air quality. Atmospheric Chemistry and Physics 9, 6077–6093.

West, J. J., Naik, V., Horowitz, L. W., and Fiore, A. M. (2009b). Effect of regional precursor emission controls on long-range ozone transport- Part 2: Steady-state changes in ozone air quality and impacts on human mortality. Atmospheric Chemistry and Physics 9, 6095–6107.

West, J. J., Osnaya, P., Laguna, I., Martinez, J., and Fernandez, A. (2004). Co-control of urban air pollutants and greenhouse gases in Mexico City. Environmental Science & Technology 38, 3474-3481.

West, J. J., Szopa, S., and Hauglustaine, D. A. (2007). Human mortality effects of future concentrations of tropospheric ozone. Comptes Rendus Geosciences 339, 775–783.

Wild, O., and Prather, M. J. (2006). Global tropospheric ozone modelling: Quantifying errors due to grid resolution. Journal of Geophysical Research 111, D11305.

Wild, O., Prather, M. J., and Akimoto, H. (2001). Indirect long-term global cooling from NOx emissions. Geophysical Research Letters 28, 1719-1722.

Wilker, E. H., Baccarelli, A., Suh, H., Vokonas, P., Wright, R. O., and Schwartz, J. (2010). Black carbon exposures, blood pressure and interactions with SNPs in MicroRNA processing genes. Environmental Health Perspectives, 943-948.

World Health Organization (2008a). The global burden of disease: 2004 update (Geneva).

World Health Organization (2004). The World Health Report 2004: Changing History (Geneva).

World Health Organization (2008b). WHO Mortality Database: Tables (Geneva).

Zanobetti, A., Schwartz, J., and Gold, D. (2000). Are there sensitive subgroups for the effects of airborne particles? Environmental Health Perspectives 108, 841-845.

Zhang, X. Y., Wang, Y. Q., Zhang, X. C., Guo, W., and Gong, S. L. (2008). Carbonaceous aerosol composition over various regions of China during 2006. Journal of Geophysical Research 113, 1-10.